

**ENHANCED SENSING SENSITIVITY OF LONG PERIOD FIBER
GRATING BY SELF-ASSEMBLED POLYELECTROLYTE MULTI-
LAYERS**

NG FOONG MUN

**A project report submitted in partial fulfilment of the
requirements for the award of the degree of
Bachelor of Engineering (Hons) Electronic Engineering**

**Faculty of Engineering and Green Technology
Universiti Tunku Abdul Rahman**

SEPTEMBER 2015

DECLARATION

I hereby declare that this project report is based on my original work except for citations and quotations which have been duly acknowledged. I also declare that it has not been previously and concurrently submitted for any other degree or award at UTAR or other institutions.

Signature : _____

Name : _____

ID No. : _____

Date : _____

APPROVAL FOR SUBMISSION

I certify that this project report entitled “**Enhanced Sensing Sensitivity of Long Period Fiber Grating by Self-Assembled Polyelectrolyte Multi-layers** ” was prepared by **Ng Foong Mun** has met the required standard for submission in partial fulfilment of the requirements for the award of Bachelor of Engineering (Hons) Electronic Engineering at Universiti Tunku Abdul Rahman.

Approved by,

Signature : _____

Supervisor: Mr. Yong Yun Thung

Date : _____

The copyright of this report belongs to the author under the terms of the copyright Act 1987 as qualified by Intellectual Property Policy of Universiti Tunku Abdul Rahman. Due acknowledgement shall always be made of the use of any material contained in, or derived from, this report.

© 2015, NG FOONG MUN of candidate. All right reserved.

Specially dedicated to
my beloved grandmother, mother and father

ACKNOWLEDGEMENTS

I would like to thank everyone who had contributed to the successful completion of this project. I would like to express my gratitude to my research supervisor, Mr. Yong Yun Thung for his guidance, encouragement and contribution for this project. He gave me useful advices, motivates me when I encountered problems and willingly shares knowledge regarding this project. I am really thankful for his full support for the time along. He impressed me very much by his responsibility and strict attitude in training students.

In addition, I want to thank to University Tunku Abdul Rahman (UTAR) to further my study in bachelor of engineering degree and give me a chance to complete my final year project, UTAR provided many help in terms of opportunity and advantages for the technology and equipment in order to lead my project to a success. Also a lot of knowledge and experiences lecturer and master student who's ready to help when there is problem arise. I am sure all this experiences and knowledge will be useful in the real engineering world.

Thank you very much my lovely friends that helps me a lot for the success of this final year report they shared their knowledge and gave me a big help in this project. Not forgotten, special thanks to my family that keep on supporting and encourage me to finish the project although it would some problems arise during this project. Finally with the helps, spirits and courage they gave me, I had overcome all the difficulties and problems I faced. Last but not least, I wish to thank everyone who has involved in helping me, directly or indirectly, throughout my project.

**ENHANCED SENSING SENSITIVITY OF LONG PERIOD FIBER
GRATING BY SELF-ASSEMBLED POLYELECTROLYTE MULTI-
LAYERS**

ABSTRACT

Coating technique is one of the common methods used to enhance the sensing capability on Long Period Fiber Grating (LPFG) fiber sensor. The main drawback of coating technique like layer by layer (LBL) is time consuming for establishing the layer by layer coating on fiber sensor. It showed that the optimal sucrose sensitivity can be improved by 20 to 25% when applying 100 bilayers of poly(allylamine hydrochloride) (PAH)/poly(sodium-p-styrenesulfonate) (PSS) coating on LPFG by Qiushun Li et al. In this project, we proposed a new method to reduce the number of bilayers using double-pass configuration which has showed significant improved in terms of power referenced sensing. The coating materials was done by using positive charged PDDA (poly-diallyldimethylammonium chloride) and negative charged PSS (poly-sodium styrene sulfonate) to form the multiple layers coating on the LPFG. The sensitivity performance was verified by the various concentration of sucrose solutions. From the experiment result, it showed that the increment of concentration of sucrose solution caused the LPFG transmission spectra gradually moving toward the short wavelength side. The comparison of single pass LBL and double pass LBL indicated that significant improvement of sucrose sensing in terms of power referenced for double pass as compared to single pass with LBL at certain range of sucrose concentration. In conclusion, it is achievable to reduce the number of coating layers using double pass to get comparable sucrose sensitivity sensing result.

TABLE OF CONTENTS

DECLARATION	1
APPROVAL FOR SUBMISSION	2
ACKNOWLEDGEMENTS	5
ABSTRACT	6
TABLE OF CONTENTS	7
LIST OF TABLES	10
LIST OF FIGURES	11
LIST OF SYMBOLS / ABBREVIATIONS	19
LIST OF APPENDICES	Error! Bookmark not defined.

CHAPTER

1	INTRODUCTION	20
	1.1 Background	20
	1.2 Problem Statements	21
	1.3 Aims and Objectives	21
2	LITERATURE REVIEW	23
	2.1 Introduction of Long Period Fiber Grating	23
	2.2 Long Period Fiber Grating Fabrication Techniques	24
	2.2.1 Long period fiber grating fabrication with femtosecond pulse radiation at different wavelengths.	24
	2.2.2 Fabrication and Mode Identification of Compact Long Period Grating Written by CO ₂ Laser	25

2.2.3	Corrugated long period gratings as band-rejection filters	27
2.2.4	Flexible Fabrication of Long Period Fiber Gratings	28
2.2.5	Summary of Fabrication Techniques	29
2.3	Application of Other Optical Fiber Sensor on the Sucrose Sensing	29
2.3.1	Application of an Optical Fiber Sensor on the Determination on Sucrose and Ethanol Concentration in Process Streams and Effluents of Sugarcane Bio-ethanol Industry	29
2.3.2	Characteristics Analysis of Chemical Concentration Sensor Based on Three Layer FBG	31
2.3.3	Fiber Optic Sucrose Sensor Based on Mode-Filtered Light Detection	32
2.4	Application of Long Period Fiber Grating on the Sucrose Sensing	33
2.4.1	Enhanced sucrose sensing sensitivity of long period fiber grating by self-assembled polyelectrolyte multi-layers	33
2.4.2	Optical Glucose Sensor Based on a Fiber Bragg Grating Concatenated with a long period Grating	35
2.4.3	Summary Application of an Optical Fiber Sensor on the Determination on Sucrose	38
3	METHODOLOGY	39
3.1	Introduction	39
3.2	Project Flow Chart	41
3.2.1	Fabrication of Long Period Fiber Grating	42
3.2.2	Material Preparation	44
3.2.3	Instrument Preparation	46
3.2.4	Setup Techniques of Single Pass and Double Pass	47
4	RESULTS AND DISCUSSIONS	50

4.1	Result of Sucrose Solution Test	50
4.2	Single Pass Test Result	53
4.2.1	Single Pass with Uncoated Normal Test	53
4.2.2	Single Pass with Layer by Layer Test	58
4.2.3	Compared Between Single Pass with Uncoated Test and Single Pass with LBL Test	63
4.3	Double Pass Test Result	67
4.3.1	Double Pass with Uncoated Normal Test	67
4.3.2	Double Pass with Layer-by-Layer Test	72
4.3.3	Compare Between Double Pass with Uncoated Normal Test and Double Pass with LBL Test	77
4.4	Comparison of Air between Single Pass and Double Pass	80
4.4.1	Single Pass	80
4.4.2	Double Pass	82
4.5	Compare Same Grating between Single Pass and Double Pass	84
4.6	Discussion	89
5	CONCLUSION AND RECOMMENDATIONS	91
5.1	Conclusion	91
5.2	Recommendations	91
	REFERENCES	93

LIST OF TABLES

TABLE	TITLE	PAGE
	Table 1: Summary of optical fabrication techniques	29
	Table 2: Summary of optic fiber for sucrose sensing	38
	Table 3: Refractive indices of sucrose solutions	44
	Table 4: List instrument	46

LIST OF FIGURES

FIGURE	TITLE	PAGE
Figure 2.1:	A.M.Vengsarkar et al, J Lightwave Technol, 14 (1996) 58	24
Figure 2.2:	Transmission spectrum of LPFG inscribed at 264nm and 400nm in FORC fiber (70 grooves) (Kryukov and Larionov, 2003).	25
Figure 2.3:	CO ₂ laser LPFG fabrication process (Chan and Alhassen, 2008).	25
Figure 2.4:	transmission spectres of LPFG (Chan and Alhassen, 2008)	26
Figure 2.5:	the transmission spectra of LPFG with λ range from 555 to 605 μ m (Chan and Alhassen, 2008).	26
Figure 2.6:	schematic diagram of an LPFG by using corrugated fabrication (Lim and Wang, 2000).	27
Figure 2.7:	(a) transmission spectra of the LPFG when adopted the strains and 2.7 (b) is adopted the twists (Lim and Wang, 2008).	28
Figure 2.8:	Creating LPFG the experimental setup (Everall and Fallon, 1998)	28
Figure 2.9:	Using the optical fiber reflectometr to measurement of liquid solution (Fujiwara and Suzuki, 2012).	29
Figure 2.10:	is shown the sucrose solution in 1550nm Fujiwara and Suzuki, 2012	30
Figure 2.11:	shown the experiment setup (Zhaoxia Wu and Xinyan Yu, 2013)	31
Figure 2-12:	(a) differences solution of the concentration and refractive index of the correlation and 2.12(b) the	

relationship between the wavelength and the concentration of the differences solution (Zhaoxia Wu and Xinyan Yu, 2013).	31
Figure 2.13: mode optical instrument schematic (Jun Zhang and Wenping Cheng, 2013)	32
Figure 2-14: filter response mode sensor for different concentrations of sucrose (Jun Zhang and Wenping Cheng, 2013)	33
Figure 2.15: the impact of overlay on the effective refractive index of different cladding modes in aqueous solution (Qiushun Li and Xu-lin Zhang, 2010).	34
Figure 2-16: (a) relationship between of film thickness and bi-layer number. 2.16 (b) the relations between of attenuation band and number of PEM central wavelength (Qiushun Li and Xu-lin Zhang, 2010).	34
Figure 2.17: experiment results of LPFGs transmission spectra at different sucrose solution 2.17 (a) pure LPFGs 0-60%, 2.17 (c) 100 bi-layers 20-25% and 2.17 (e) 115 bi-layers 0-5% (Qiushun Li and Xu-lin Zhang, 2010).	35
Figure 2.18: Modular fiber grating structure diagrams (Ming-Yue Fu and Hung-Ying Chang, 2014).	36
Figure 2.19: transmission spectra of a FBG-LPFG (Ming-Yue Fu and Hung-Ying Chang, 2014)	36
Figure 2.20: (a) and (b) is relationship of different of power transmission between concentration of glucose solution and temperature (Ming-Yue Fu and Hung-Ying Chang, 2014).	37
Figure 3.1: Project flow chart.	41
Figure 3.2: an electric arcing fabrication system for LPFG	42
Figure 3.3: periodic perturbation crated by electric arcing along the optical fiber (Yun-Thung Yong, 2014).	42
Figure 3.4: transmission spectra of an arc- induced LPFG 260315-650-1-18-26-D-04	43
Figure 3.5: (a) and (b) Scheme of multilayer fabrication process and basic principle.	45

Figure 3.6: LPFG single pass configuration	47
Figure 3.7: LPFG double pass configuration	48
Figure 3.8: Refractive index testing setup	48
Figure 4.1: The relationship between sucrose solution and refractive index	50
Figure 4.2: principle of Snell's Law	51
Figure 4.3: fiber structure	51
Figure 4.4: (a) Total internal reflection	52
Figure 4.5: Grating 35-Transmission spectra at different sucrose solution (0-70%) using single pass with uncoated technique	53
Figure 4.6: Grating 35-Resonance wavelength shift of LPFG with different refractive index	54
Figure 4.7: Grating 35-Power transmission shift of LPFG with different sucrose using single pass with uncoated technique	54
Figure 4.8: Grating 38-Transmission spectra at different sucrose solution (0-70%) using single pass with uncoated technique	55
Figure 4.9: Grating 38-Resonance wavelength shift of LPFG with different refractive index using single pass with uncoated	55
Figure 4.10: Grating 38-Power transmission shift of LPFG with different sucrose solution using single pass with uncoated technique	56
Figure 4.11: Grating 39-Transmission spectra at different sucrose solution (0-70%) using single pass with uncoated technique	56
Figure 4.12: Grating 39-Wavelength shift of LPFG with different refractive index using single pass with uncoated technique	57
Figure 4.13: Grating 39-Power transmission shift of LPFG with different sucrose solution using single pass with uncoated	57

Figure 4.14: Grating 35-Transmission spectra at different sucrose solution (0-70%) using single pass with layer by layer technique	58
Figure 4.15: Grating 35-Wavelength shift of LPFG with different refractive index using single pass with layer by layer technique	59
Figure 4.16: Grating 35-Power transmission shift of LPFG with different sucrose solution using single pass with layer by layer technique	59
Figure 4.17: Grating 38-Transmission spectra at different sucrose solution (0-70%) using single pass with layer by layer technique	60
Figure 4.18: Grating 38-Wavelength shift of LPFG with different refractive index using single pass with layer by layer technique	60
Figure 4.19: Grating 38-Power transmission shift of LPFG with different sucrose solution using single pass with layer by layer technique	61
Figure 4.20: Grating 39-Transmission spectra at different sucrose solution (0-70%) using single pass with layer by layer technique	61
Figure 4.21: Grating 39-Wavelength shift of LPFG with different refractive index using single pass with layer by layer technique	62
Figure 4.22: Grating 39-Power transmission shift of LPFG with different sucrose solution using single pass with layer by layer technique	62
Figure 4.23: Grating 35-Different wavelength shift between singlepass uncoater and layer by layer techniques.	63
Figure 4.24: Grating 35-Different power transmission shift between singlepass uncoater and layer by layer techniques.	64
Figure 4.25: Grating 38- Different wavelength shift between singlepass uncoater and layer by layer techniques.	64
Figure 4.26: Grating 38-Different power transmission shift between singlepass uncoater and layer by layer techniques.	65

Figure 4.27: Grating 39- Different wavelength shift between singlepass uncoater and layer by layer techniques.	65
Figure 4.28: Grating 39-Differrent power transmission shift between singlepass uncoater and layer by layer techniques.	66
Figure 4.29: Grating 33-Transmission spectra at different sucrose solution (0-70%) using double pass with uncoated technique	67
Figure 4.30: Grating 33-Wavelength shift of LPFG with different refractie index using double pass with uncoated technique	67
Figure 4.31: Grating 33-Power transmission shift of LPFG with different sucrose using double pass with uncoated technique	68
Figure 4.32: Grating 35-Transmission spectra at different sucrose solution (0-70%) using double pass with uncoated technique	68
Figure 4.33: Grating 35-Wavelength shift of LPFG with different refractie index using double pass with uncoated technique	69
Figure 4.34: Grating 35-Power transmission shift of LPFG with different sucrose using double pass with uncoated technique	69
Figure 4.35: Grating 38-Transmission spectra at different sucrose solution (0-70%) using double pass with uncoated technique	70
Figure 4.36: Grating 38-Wavelength shift of LPFG with different refractie index using double pass with uncoated technique	70
Figure 4.37: Grating 38-Power transmission shift of LPFG with different sucrose using double pass with uncoated technique	71
Figure 4.38: Grating 33-Transmission spectra at different sucrose solution (0-70%) using double pass with coated technique	72
Figure 4.39: Grating 33-Wavelength shift of LPFG with different refractie index using double pass with coated technique	72

Figure 4.40: Grating 33-Power transmission shift of LPFG with different sucrose using double pass with coated technique	73
Figure 4.41: Grating 35-Transmission spectra at different sucrose solution (0-70%) using double pass with coated technique	73
Figure 4.42: Grating 35-Wavelength shift of LPFG with different refractive index using double pass with coated technique	74
Figure 4.43: Grating 35-Power transmission shift of LPFG with different sucrose using double pass with coated technique	74
Figure 4.44: Grating 38-Transmission spectra at different sucrose solution (0-70%) using double pass with coated technique	75
Figure 4.45: Grating 38-Wavelength shift of LPFG with different refractive index using double pass with coated technique	75
Figure 4.46: Grating 38-Power transmission shift of LPFG with different sucrose using double pass with coated technique	76
Figure 4.47: Grating 33- Different wavelength shift between double pass uncoater and layer by layer techniques.	77
Figure 4.48: Grating 33- Different power transmission shift between double pass uncoater and layer by layer techniques.	77
Figure 4.49: Grating 35- Different wavelength shift between double pass uncoater and layer by layer techniques.	78
Figure 4.50: Grating 35- Different power transmission shift between double pass uncoater and layer by layer techniques.	78
Figure 4.51: Grating 38- Different wavelength shift between double pass uncoater and layer by layer techniques.	79

Figure 4.52: Grating 38- Different power transmission shift between double pass uncoater and layer by layer techniques.	79
Figure 4.53: Grating 35- Different air wavelength shift between single pass uncoated and layer by layer test	80
Figure 4.54: Grating 38- Different air wavelength shift between single pass uncoated and layer by layer test	81
Figure 4.55: Grating 39- Different air wavelength shift between single pass uncoated and layer by layer test	82
Figure 4.56: Grating 33-Different air wavelength shift between double pass uncoated and layer by layer test	82
Figure 4.57: Grating 35-Different air wavelength shift between double pass uncoated and layer by layer test	83
Figure 4.58: Grating 38-Different air wavelength shift between double pass uncoated and layer by layer test	83
Figure 4.59: Grating 35-Different wavelength shift between single pass with uncoater and double pass with uncoated techniques	84
Figure 4.60: Grating 35- Different wavelength shift between single pass with layer by layer and double pass with layer by layer techniques	85
Figure 4.61: Grating 35- Different power transmission shift between single pass with uncoater and double pass with uncoated techniques	85
Figure 4.62: Grating 35- Different power transmission between single pass with layer by layer and double pass with layer by layer techniques	86
Figure 4.63: Grating 38- Different wavelength shift between single pass with uncoater and double pass with uncoated techniques	87
Figure 4.64: Grating 38- Different wavelength shift between single pass with layer by layer and double pass with layer by layer techniques	87
Figure 4.65: Grating 38- Different power transmission shift between single pass with uncoater and double pass with uncoated techniques	88

Figure 4.66: Grating 38- Different power transmission between single pass with layer by layer and double pass with layer by layer techniques

LIST OF SYMBOLS / ABBREVIATIONS

Λ	Grating period
λ_{BL}	Bragg Wavelength
$\Delta\lambda$	Wavelength shift
ΔP	Power change
n	Refractive index
LPFG	Long Period Fiber Grating
PDDS	poly-diallyldimethylammonium chloride
PSS	poly-sodium styrene sulfonate
PEM	polyelectrolyte multilayer
PHA	allylamine hydrochloride

CHAPTER 1

INTRODUCTION

1.1 Background

In recent years, fiber optic sensing technology has been getting considerable attention by researchers as refractive index sensor. The fiber has a small, material light, anti-electromagnetic interference, the signal transmission and sensing concentrated in one and it had anti-corrosion and more resistant to high temperatures. Other than that transmission light with low interference and loss, bandwidth had high stability so that it can combined with security detection or monitoring system to develop new application.

Besides that, fiber optic sensing technology more valuable because nowadays there have been many successful development related researchers and optoelectronic fiber optic sensing technology to mature stage. The application of fiber optic sensing system can be used to measure small changes in refractive index. The title of my final year project is Enhanced Sensing Sensitivity of Long Period Fiber Grating by Self Assemble Polyelectrolyte Multi-layers.

This project is used to measure the optimal sensitivity of 60-70% sucrose concentration solutions and will use the operating principle of long period fiber grating. Based on long period fiber grating sensor is suitable for stress, load, bending and pressure sensing measurements. Long period grating has a refractive index of the

external environment is based on different performance sensitive environments have different refractive indices sensitive capabilities.

It operate as band rejection filters in optic fibers which is useful for sensing and signal shaping applications. Long period grating has sensitivity can be achieved through a surface coated with a multilayer PDDA (poly-diallyldimethylammonium chloride) and negative charged PSS (poly-sodium styrene sulfonate); approach to improve. Long period grating sensor compared with a conventional electrical sensor which are high sensitivity, corrosion resistance and high reliability. Therefore, the refractive index sensor based on long period fiber grating is one of the effective methods for measuring the concentration of the sucrose solutions.

1.2 Problem Statements

Sucrose solution is one of the most important parameters characterizing of numerous chemical and biochemical such as refine sugar, food industry, pharmacy and another. Some of the existing technologies are sensitive to the detection of food samples sucrose. For example methods of the analysis of sucrose solution the limitation is accurate for sucrose or empirical calibration required. Multiple layers are promising to enhance the refractive index sensing but require huge number of layers with time consuming. In order to overcome this problem, a double pass configuration is proposed to reduce the number of layers due to the optical power sensing is more sensitive when using double pass as compared single pass.

1.3 Aims and Objectives

The objectives of the thesis are shown as following:

- i) To study and understand the concept of long period fiber grating.
- ii) To study and fabricate LPFG at the desired wavelength.
- iii) To perform multi-layers coating on LPFG using polyelectrolyte material to improve the sensing capability.

- iv) To compare the double pass technique and other technique performance on the coated LPFG for optimization on number of polyelectrolyte layers.

CHAPTER 2

LITERATURE REVIEW

2.1 Introduction of Long Period Fiber Grating

Fiber grating is using the ultraviolet quartz fiber sensing properties of structural to change in the refractive index of the period to make an optic device. It was developed in the 1990s a new type of optic devices that is one hottest areas of research. Fiber grating have different period so that can be divided two types as short period fiber (fiber Bragg) and long period fiber grating.

LPFG is a transmission grating in an optical fiber or waveguide to achieve light coupling between the propagation core mode and co-propagation cladding mode. The long period fiber grating (LPFG) has a period typical in the range from $100\mu\text{m}$ to $1000\mu\text{m}$. LPFG's history dates back to 1996, Ashish Vengsarkar who was used LPFG (as show below figure 2.1) to achieve an in communication system for gain equalization and erbium doped amplifiers. After, Turan Erdogan depended on the mode coupling theory to analysis of the spectral characteristics of an LPFG, laid the theoretical foundation of an LPFG.

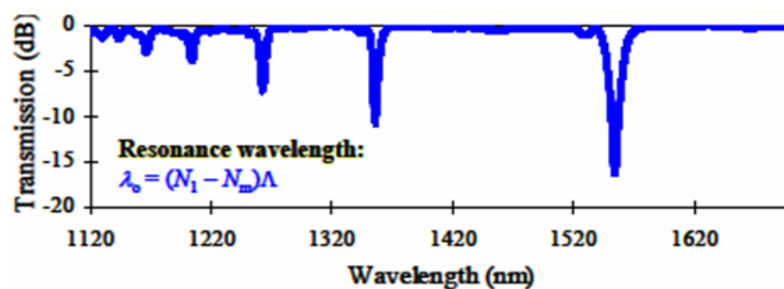


Figure 2.1:A.M.Vengsarkar et al, J Lightwave Technol, 14 (1996) 58

LPFG is a good reliability of fiber optic sensors for example it have pressure interference ability, simple structure suitable for a variety of application, environment ruggedness and anti-electromagnetic interference. This feature makes LPFG resonant wavelength and the resonance intensity is very sensitive to the external environment, with more than FBG with good temperature, stress, bending, and twisting, lateral load refractive index sensitivity so LPFG sensor has better application development potential.

2.2 Long Period Fiber Grating Fabrication Techniques

2.2.1 Long period fiber grating fabrication with femtosecond pulse radiation at different wavelengths.

In the paper proposed by Kryukov and Larionov (2003) the standard communication coated fibers using an infrared femtosecond laser step by step inscription. When the fiber core receives by higher than a certain intensity of femtosecond laser irradiation than the refractive index in the axial direction will change to periodically since the photon density (10^{12} - 10^{15}) femtosecond laser pulses much higher than other laser sources.

The fabrication of an LPFG use the UV femtosecond laser (800nm, 60fs pulse from a Ti: sapphire laser and repetition rate of 82MHz) then in the cladding and core will produced the grating and thermal stability up to 500°C. Beside, the LPFG has a strong peak attenuation (greater than 20dB) can induced in the H2-

loaded Ge-doped optical fiber by second harmonic using femtosecond Titanium germanium hydrogen loaded fiber without using an amplifier (400nm and 70fs) and enlarger fourth harmonic pulse from a Neodymium glass laser (264nm and 220fs). In figure 2.2 above as can be seen the formation of radiation induced loss peak intensity of high quality fiber gratings. Due to Ti: sapphire laser is a higher average power and LPFG is almost equal to the two lasers.

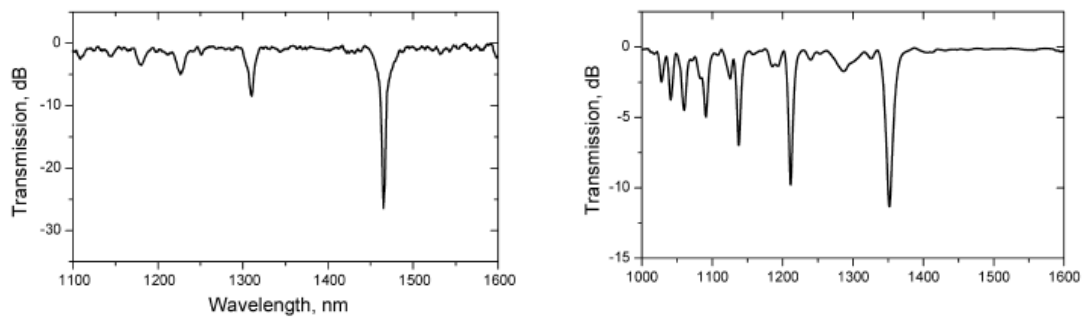


Figure 2.2: Transmission spectrum of LPFG inscribed at 264nm and 400nm in FORC fiber (70 grooves) (Kryukov and Larionov, 2003).

2.2.2 Fabrication and Mode Identification of Compact Long Period Grating Written by CO₂ Laser

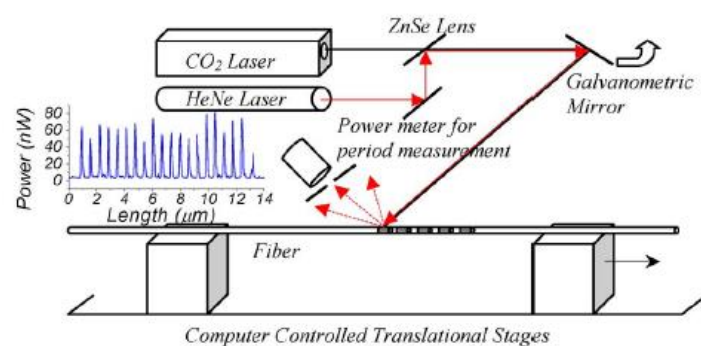


Figure 2.3: CO₂ laser LPFG fabrication process (Chan and Alhassen, 2008).

In the paper proposed by Chan and Alhassen (2008) a conventional single-mode fiber stripped of plastic sheath than to install on two computers; first computer is fix another computer is control of the moving distance at a constant speed. The fiber is made to hold the stage vacuum force. A SYNRAD J48-1 CO₂ laser is focused

with a lens having a 200mm focal length ZnSe fiber 450 μm for a fairly large spot. In the CO₂ laser fiber is then scanned across the galvanometer mirror by a computer-controlled. The power density in the fiber was estimated to be 0.94 kW/cm². If the CO₂ laser softening fibers, the pulling action of the translation stage provides the necessary tension and deformation of the fiber. Creating a periodic refractive index variation of optical fibers, than to dither the laser beam sinusoidal (by controlling the galvanomirror) at a fixed angular frequency, because it is scanned at a constant linear velocity (linear scan) along the fiber.

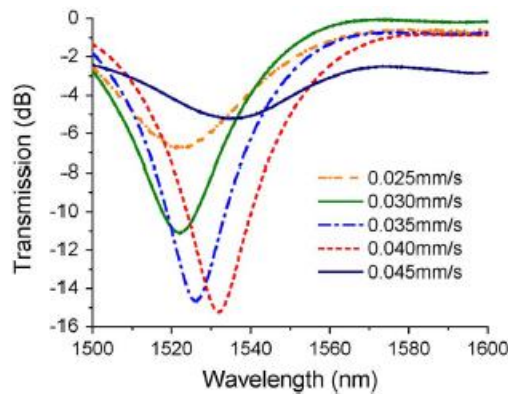


Figure 2.4: transmission spectres of LPFG (Chan and Alhassen, 2008)

In figure 2.4 above show the transmission spectres versus pulling speed of LPFG and show the coupling maximum are pulling speed of 0.045mm/s. In this technique that can see the coupling strength, the insertion loss is increased monotonically with the deformation due to the tension applied.

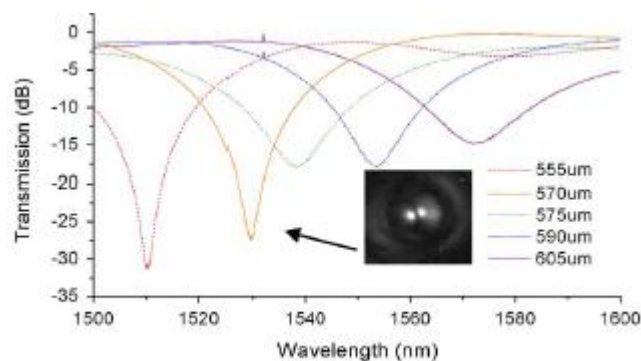


Figure 2.5: the transmission spectra of LPFG with Δ range from 555 to 605 μm (Chan and Alhassen, 2008).

The figure 2.5 shown five grating with 20 period it can seen the large notch is -30dB and a low insertion loss is lower than 0.25dB. In the fabrication, it can found no substantial difference between the scanning beam method and point by point method, if the control parameters are optimized separately for each method.

2.2.3 Corrugated long period gratings as band-rejection filters

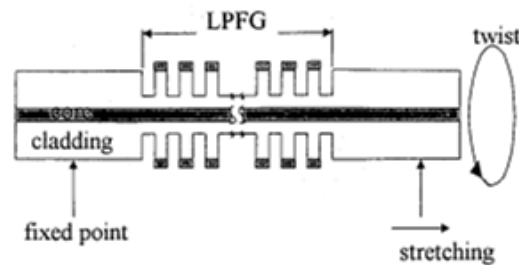


Figure 2.6: schematic diagram of an LPFG by using corrugated fabrication (Lim and Wang, 2000).

Lim and Wang (2008) proposed the cladding diameter 125 μm release coating of the fiber than the surface will treated to flat and fixed in axially spaced uniformly metalized thin layer a certain width. Next, the optical fiber is placed in hydrofluoric acid solution which is etching of the fiber material properties will uncoated fiber surface of the metal layer is etched to form circumferential axially symmetric periodic structure that means a reduced diameter as shown in figure 2.6. This modulation is very small unless the part is etched close to the core. Thus the coupling efficiency between the core and cladding modes is very small. However, when a stress is applied, a more powerful induced refractive index change in the corrugated

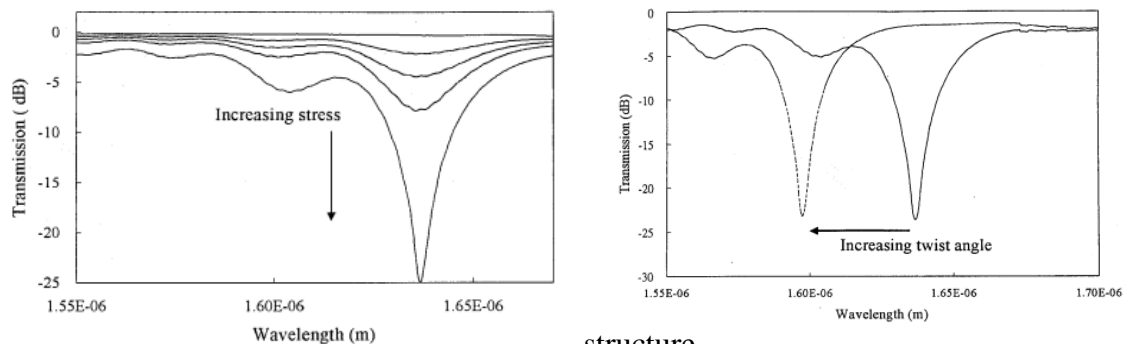


Figure 2.7: (a) transmission spectra of the LPFG when adopted the strains and 2.7 (b) is adopted the twists (Lim and Wang, 2008).

The transmission spectral of long period fiber grating had different stress are shown in Figure 2.7(a). As can be seen, increase in transmission loss and pressure in the resonance peak because the refractive index difference in etching and undetected region becomes large so the maximum loss of up to- 25dB. Figure 2.7(b) is shows the resonance peak wavelength can be tuned by twisting the long period fiber grating.

2.2.4 Flexible Fabrication of Long Period Fiber Gratings

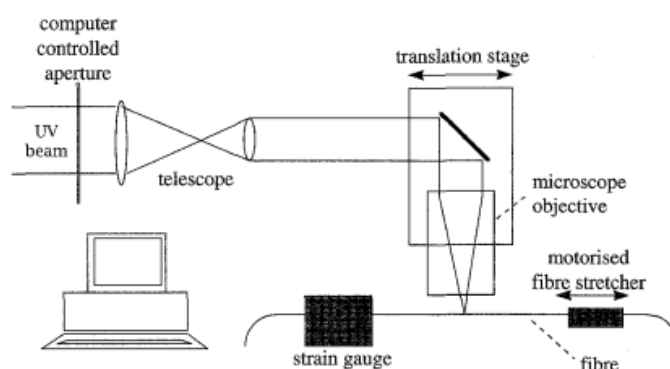


Figure 2.8: Creating LPFG the experimental setup (Everall and Fallon, 1998)

Everall and Fallon (1998) proposed this approach extends the point by point write technology and does not require additional costs can be written in any form LPFG. Experimental apparatus shown in Figure 2.8, UV light beam through the microscope objective lens to the optical fiber, the role of the microscope objective lens is focused by the beam and size can reduce less than $30\mu\text{m}$. To move the translation stage enables UV beam is scanned along the fiber direction at the moment the computer-controlled aperture will control fiber period exposure. Then by changing the aperture is to rely on the position of the translation stage to trigger. The maximum length of the grating is determined by the total length of the translation stage moves. Experimental results show that the production of the total length of 11mm, a period of $500\mu\text{m}$ of LPFG. Through this testing the experimental and simulated values match thus illustrate the accuracy of this simple method.

2.2.5 Summary of Fabrication Techniques

Techniques	Process	Range
Femtosecond pulse (800nm)	<ul style="list-style-type: none"> Using an infrared femtosecond laser step by step inscription. 	<ul style="list-style-type: none"> Ti:sapphire laser without the use of an amplifier 400 nm frequency-quadrupled pulses from a Nd:glass laser 264 nm
CO ₂ Laser	<ul style="list-style-type: none"> In the process of writing a CO₂ laser, a bare fiber exposed to CO₂ laser beam focusing. 	555 μm to 605μm
Corrugated	<ul style="list-style-type: none"> Used hydrofluoric acid solution to etching to form circumferential axially symmetric periodic structure 	400μm
Flexible	<ul style="list-style-type: none"> This approach extends the point by point write technology 	500 μm

Table 1: Summary of optical fabrication techniques

2.3 Application of Other Optical Fiber Sensor on the Sucrose Sensing

2.3.1 Application of an Optical Fiber Sensor on the Determination on Sucrose and Ethanol Concentration in Process Streams and Effluents of Sugarcane Bio-ethanol Industry

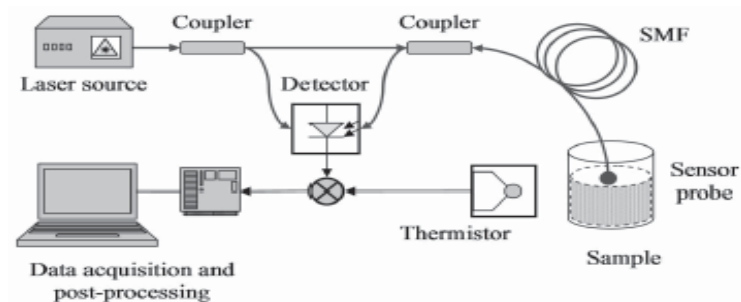


Figure 2.9: Using the optical fiber reflectometer to measurement of liquid solution (Fujiwara and Suzuki, 2012).

Fujiwara and Suzuki (2012) proposed the sensor includes an optical fiber for measuring the reflectance of the liquid mixture. As show in a sample to be analyzed in which the refractive index was identified. The light source is use Fabry-Perot laser diode source to emit its operating wavelength can switch at the 1310nm and 1550nm. In figure 2.9 it can seen the laser source to separated two fiber couple, first fiber couple is measuring the pin photo detector for the monitoring of the laser intensity. Second fiber couple signal is spread by a standard mode fiber optic cable that size is 1m length. The SMF will flat polished end and placed in the liquid after a potion of the light is reflected to detector than to measure by another photo detector. In addition, the thermistor function is to monitor the temperature liquid and the acquired signal is digitized and post- processing.

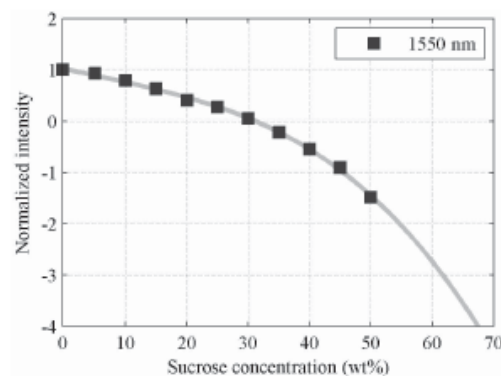


Figure 2.10: is shown the sucrose solution in 1550nm Fujiwara and Suzuki, 2012

As shown in above figure 2.10 is sucrose solution for measuring the sensor that seen when sucrose concentration increase than the reflected intensity will decrease since the refractive index increment of the concentration presented higher sucrose content.

2.3.2 Characteristics Analysis of Chemical Concentration Sensor Based on Three Layer FBG

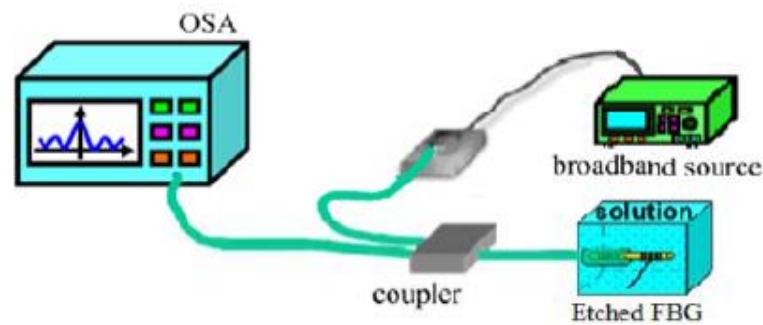


Figure 2.11: shown the experiment setup (Zhaoxia Wu and Xinyan Yu, 2013)

Zhaoxia Wu and Xinyan Yu (2013) proposed this experiment showed the principle and the experiment device for measuring the refractive index modulation fiber Bragg grating sensor using the three layer structure model to testing liquid solution such as sucrose, ethanol and NaCl solution. The measurement apparatus shown in figure 2.11 in this experiment focuses on theoretical analysis of fiber bragg grating chemical sensors and establishment of three layer structure mode to test three different solution at less than 80%.

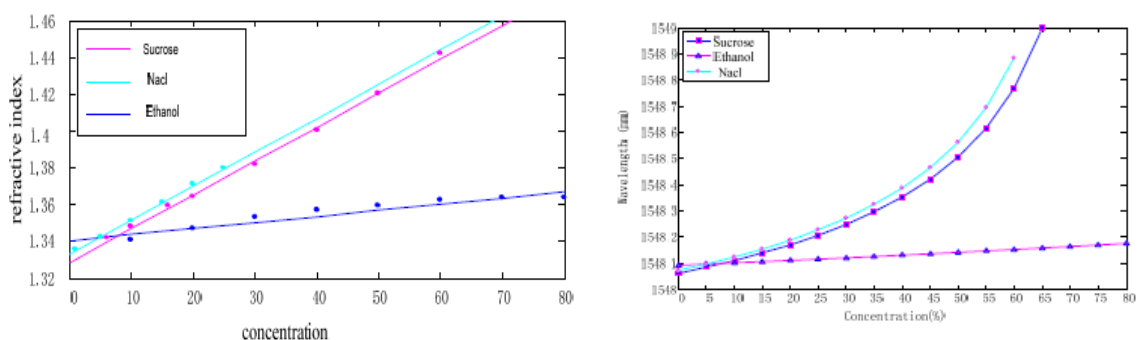


Figure 2-12: (a) differences solution of the concentration and refractive index of the correlation and 2.12(b) the relationship between the wavelength and the concentration of the differences solution (Zhaoxia Wu and Xinyan Yu, 2013).

Therefore, the refractive index of the three concentrations shown in the figure 12 and that can see from the figure 2.12(a) there is no significant difference between the calculated value and the value of the refractive index. So, fixed the cladding radius, FBG with an external solution concentration varying wavelength obtained as shown in figure 2.12 (b). The figure 2.12 (b) shows wavelength in the determination of 0- 80% concentration in external solution is small change.

When measuring NaCl and sucrose the solution concentration changes with wavelength is obvious. Thought characterization and completed the three layer structure of experimental fiber grating sensor that can see the spectrum and sensitivity of different concentration of solution obtained. Meanwhile, the sensor can be used to measure chemical and biological composition or liquid environment.

2.3.3 Fiber Optic Sucrose Sensor Based on Mode-Filtered Light Detection

Mode filtered light fiber optic sensor device consists of a light source system, system of detection, computer and fiber the experimental apparatus shown in figure 2.13. The solution will be pumped to the capillary and then collecting the detection signal by the detector. Sucrose solution refraction measured by Abbe refractometer. The liquid flow rate will affect the signal noise ratio (SNR) of flow rate sensor if the flow rate of the liquid will cause excessive vibration capillary fiber while the flow rate is too slow that can take time to analysis. So, to select the appropriate flow rate is very important.

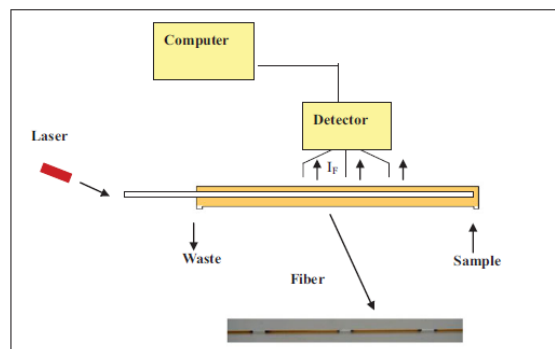


Figure 2.13: mode optical instrument schematic (Jun Zhang and Wenping Cheng, 2013)

Jun Zhang and Wenping Cheng (2013) proposed this experiment a flow rate of 0.76 mL/m was chosen because of low noise sensor and short analysis time. In the experiment with different concentrations 0-30% (w/w) of sucrose solution was continuously measured to give the results as shown by the graph that the sensor range of 0-30% (w/w) are responsive sucrose solution. With increasing concentration of sucrose solution the mode filtered is gradually reduced this result will shown in figure 2.14.

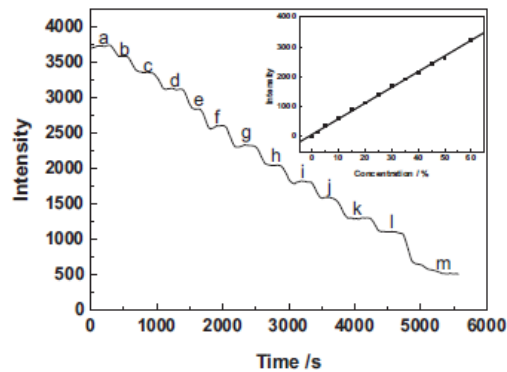


Figure 2-14: filter response mode sensor for different concentrations of sucrose (Jun Zhang and Wenping Cheng, 2013)

2.4 Application of Long Period Fiber Grating on the Sucrose Sensing

2.4.1 Enhanced sucrose sensing sensitivity of long period fiber grating by self-assembled polyelectrolyte multi-layers

Qiushun Li and Xu-lin Zhang (2010) proposed using polyelectrolyte multilayer (PEMS) self-assembly method in the long-period grating surface. The material use is poly (allylamine hydrochloride) (PAH) and poly (sodium-p-styrenesulfonate) (PSS) film and studied their response to sucrose concentration. In the figure 2.15 it can be observed, with the increase in the thickness of overlay the effective refractive index of the cladding mode slightly increases until a critical point is reached.

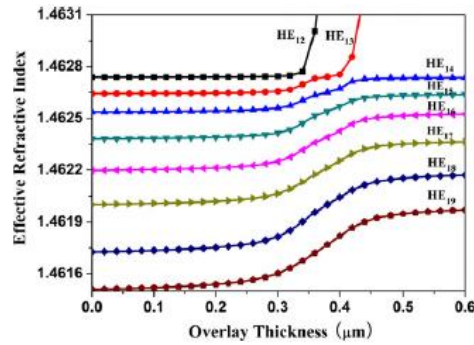


Figure 2.15: the impact of overlay on the effective refractive index of different cladding modes in aqueous solution (Qiushun Li and Xu-lin Zhang, 2010).

Besides, to prove this experiment simulation PEM coated in surface LPFG will developed by multilayer self-assembly techniques. First the LPFG will fix to the Teflon shelves and then with a chemical agent surface treated to produce a negative charge. After that, LPFGs will repeatedly immersed in 1 mg / l of PAH (containing sodium chloride 0.5 M of NaCl) and 1 mg PSS / L (containing sodium chloride 0.5 M of NaCl), to obtain a multilayer film.

As shown figure 2.16 (a) the relationship between the number of bi-layer and film thickness when the film thickness is increasing than the number of bi-layer will increases. Apart from that, the figure 2.16 (b) as shown the attenuation of the amplitude of the central wavelength band increased at the beginning until it reaches a maximum and then decreases with the number of bi-layer increases.

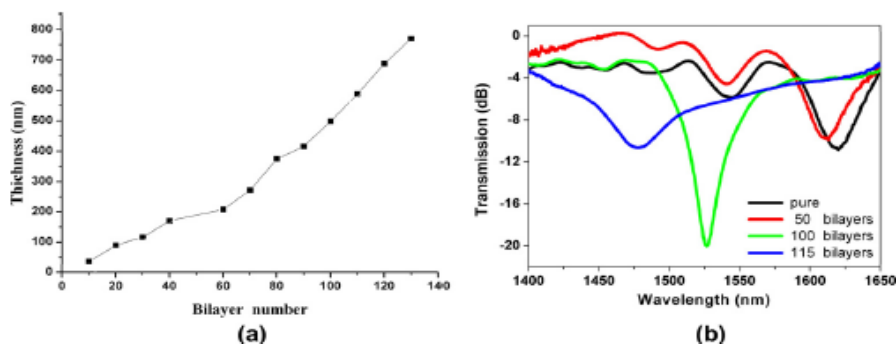


Figure 2-16: (a) relationship between of film thickness and bi-layer number. 2.16 (b) the relations between of attenuation band and number of PEM central wavelength (Qiushun Li and Xu-lin Zhang, 2010).

Next is continuous the experiment using PEM coated LPFGs to test concentrations of sucrose solution by controlling their thickness as shown in figure 2.17(a), 2.17 (c) and 2.17 (e). In figure that seen for pure and PEM coated LPFGs the attenuation band centre wavelength are gradually shifted to the short wavelength with an increase in the concentration of sucrose solution. Use PEM technique overlay will greatly improve the sensing of sucrose sensitivity to compare with pure LPFGs.

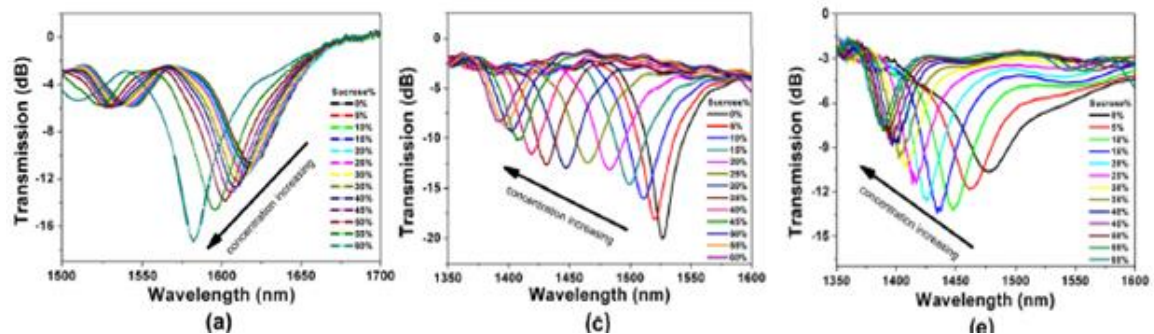


Figure 2.17: experiment results of LPFGs transmission spectra at different sucrose solution 2.17 (a) pure LPFGs 0-60%, 2.17 (c) 100 bi-layers 20-25% and 2.17 (e) 115 bi-layers 0-5% (Qiushun Li and Xu-lin Zhang, 2010).

2.4.2 Optical Glucose Sensor Based on a Fiber Bragg Grating Concatenated with a long period Grating

In order to achieve simultaneous measurement both sucrose solution concentration and temperature Ming-Yue Fu and Hung-Ying Chang (2014) proposed use a FBG cascaded a LPFG to prove monitoring changes in the reflection wavelength and reflected power. LPFG is forward transmission mode with the same core base to the cladding mode coupling and FBG is the backward cladding mode wave vector. So it cans satisfaction the phase matching condition between the two modes as FBG-LPFG and induced-channel λ_{BL} on the shorter wavelength side of the Bragg wavelength λ_{BL} as shown in figure 2.18.

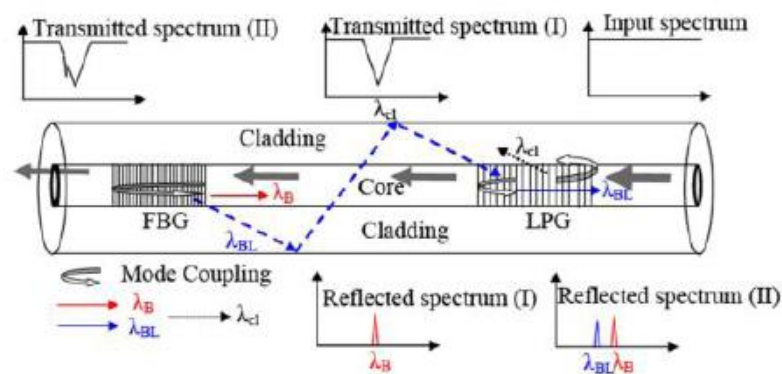


Figure 2.18: Modular fiber grating structure diagrams (Ming-Yue Fu and Hung-Ying Chang, 2014).

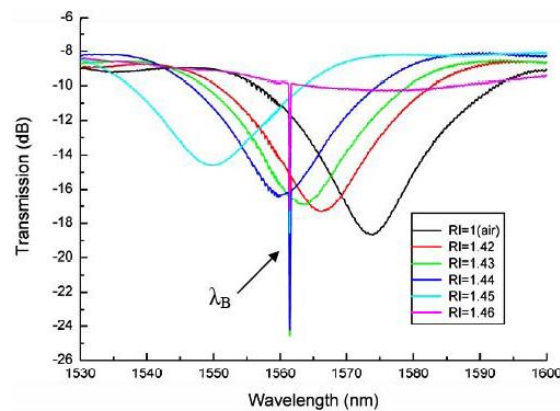


Figure 2.19: transmission spectra of a FBG-LPFG (Ming-Yue Fu and Hung-Ying Chang, 2014)

Figure 2.19 displays the transmission spectrum of a FBG-LPFG for refractive indices ranging from 1.42 to 1.46. The graph shows that as the refractive index of the cladding increases, the resonance wavelength of the LPFG Bragg wavelength λ_{BL} shifts toward shorter wavelengths. For measuring the concentration of glucose and temperature, the sensing head is connected in series with an amplified spontaneous emission (ASE) light source and an optical spectrum analyzer (OSA) to monitor changes in the grating spectrum. The sensor is placed within the wafer surface and the container. The containers will be filled with different salinities and immersed into a tank with a controllable heater. At a constant temperature of 25°C, the glucose solution concentration is increased from 1% to 26% in increments of 5%. Figure 2.20 (a) shows the Bragg wavelength, constant wavelength, and the difference in reflected power between

Bragg wavelength and induced wavelength is changed as a function of the applied glucose solution. Figure 2.20 (b) shows the relationship between the Bragg wavelength shift ($\Delta\lambda$) and temperature as well as the relationship between the difference of reflective power change (ΔP) and temperature.

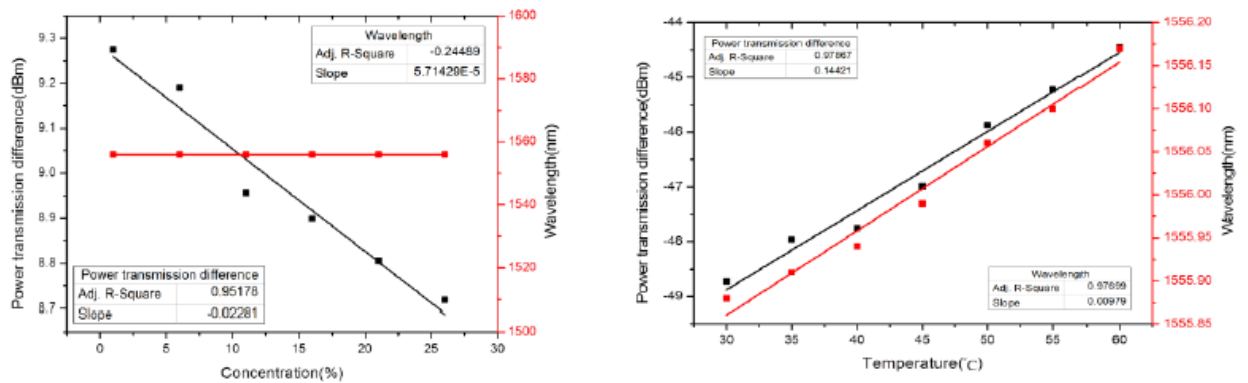


Figure 2.20: (a) and (b) is relationship of different of power transmission between concentration of glucose solution and temperature (Ming-Yue Fu and Hung-Ying Chang, 2014).

Based on FBG-LPFG dual composite structure parameters of the optical transmission sensor for sucrose solution concentration and temperature for measurements at the same time, that can proved the characteristics of the FBG sensors combined as photochemical sensor with high sensitivity.

2.4.3 Summary Application of an Optical Fiber Sensor on the Determination on Sucrose

Type of optic fiber	Technique	Sensitivity Value
Standard single-mode fiber cable	<ul style="list-style-type: none"> Optical fiber reflectometer 	(0-50%) 27.78w/m ²
Fiber bragg grating	<ul style="list-style-type: none"> Three layer FBG 	(0-50%)9nm
Fiber	<ul style="list-style-type: none"> Mode filtered light fiber optic sensor 	(0-30%) 32kw/ m ²
LPFG	<ul style="list-style-type: none"> Polyelectrolyte multilayer (PEMS) 	(0-60%) 840.58nm
FBG-LPFG	<ul style="list-style-type: none"> FBG connected in series with a LPFG for the mode coupling 	(6-26%) 154.8nm

Table 2: summary of optic fiber for sucrose sensing

CHAPTER 3

METHODOLOGY

3.1 Introduction

This chapter will illustrate on how to construct the long period fiber grating by self-assemble multilayer. It consists of two parts, fabrication of long period fiber grating included using single pass and double pass techniques, and coating of long period fiber grating.

For the fabrication the fiber part, it would like to melt the bottom part of the fiber. From the fabrication fiber method, it involves certain process to prepare the fiber which is removed the polymer surface of fiber and aliment of the fiber. After then both end of were connected to LED light transmitter to check connection and the initial mass of the load used is 14g as well as each section of the fiber would setup exposing for 10 times.

In the coated fiber part consists of two substances which are positive charged polyelectrolyte PDDA (poly-diallyldimethylammonium chloride) and negative charged PSS (poly-sodium styrenesulfonate); used this two solution to coat the multilayer. Next, using long period fiber grating with the layer by layer to test in technique as single pass and double pass.

The figure 3.1 shows the project flow chart. First of all, we need to understand the background of the project that can identify the problem. For this project is enhanced sensing of long period fiber grating by self-assembled polyelectrolyte multi-layers exhibited for the optimal sensitivity to 60-70% sucrose solution. Therefore, in this chapter 2 literature review has shows several techniques to enhanced sensing of long period fiber grating so we must learn and understand the long period fiber grating.

3.2 Project Flow Chart

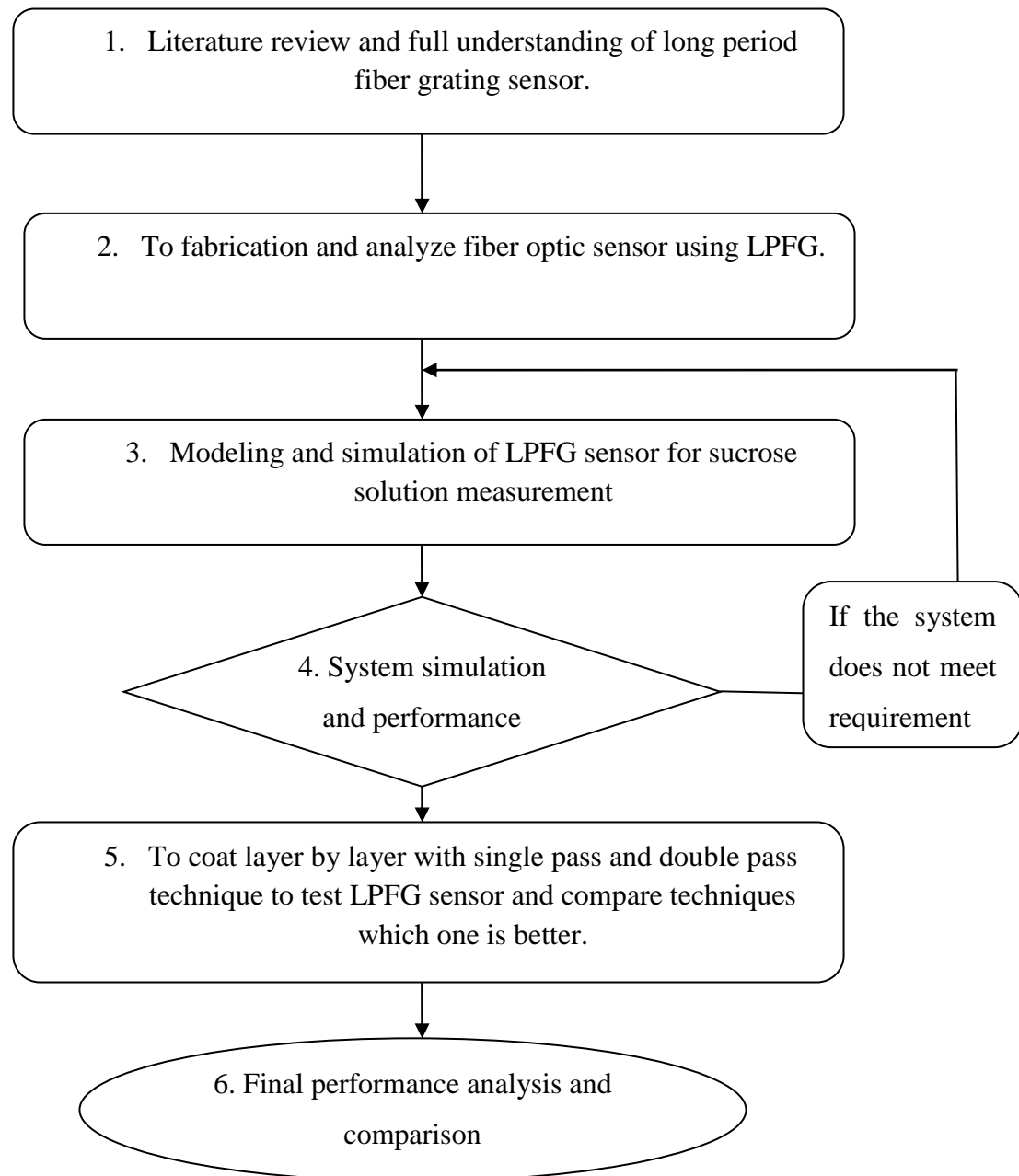


Figure 3.1: Project flow chart.

3.2.1 Fabrication of Long Period Fiber Grating

In this project the fabrication of an arc-induced LPFG is shown in figure 3.2. The setup process of the long period fiber grating is use a specific method of periodically changing the effective refractive index of the fiber which are changes in periodically will occur to encourage the mode coupling of light propagating in the core and cladding.

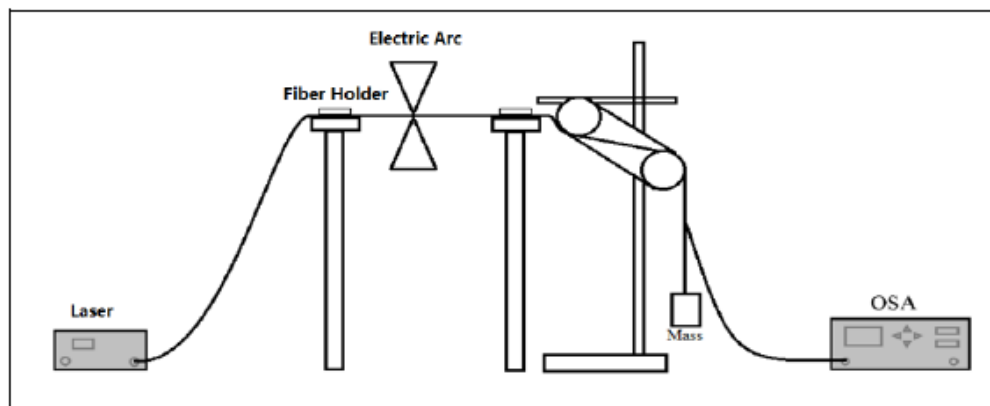


Figure 3.2: an electric arcing fabrication system for LPFG

The figure 3.3 shows a computer will set the time for controlling the voltage applied to the electric on the electrodes for electric arcing. At the same time, the motorized stage (X and Y axis) is to control the electrodes position, move along the bare fiber which fixed by fiber clamp at both ends. The motorized stage will move the electrodes to left side for fixed period before arc discharge and the maximum distance is based on the grating periods set. After completion of each period, it will discharge and move to next position until the maximum distance reach. The fiber deformation of the cladding caused by arcing which is showed in figure 3.3.

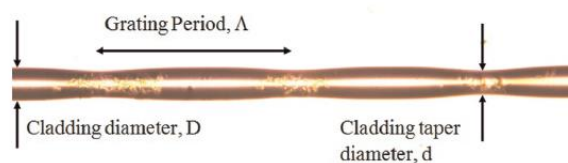


Figure 3.3: periodic perturbation crated by electric arcing along the optical fiber

(Yun-Thung Yong, 2014).

Besides that, in the end of the fiber put certain weight when electric to electrodes for electric arc the fiber is melted by the high temperature. So under heavy tension the melted portions of the fiber will attenuated therefore the fiber structure is formed long period fiber grating. Transmission spectra shown in figure 3.4 is the period the fabrication for making grating period $650\mu\text{m}$ and the 26 grating period it is at each point discharge time is 1 seconds and weight is 18g. The transmission power is around -43dB and the notch form between 1546.4nm to 1548.8nm.

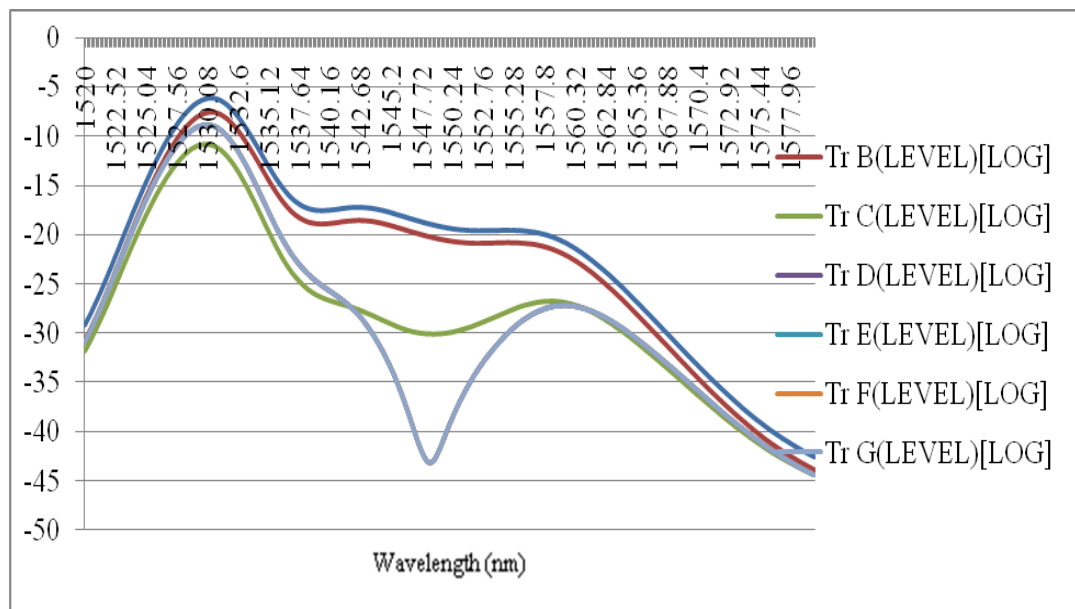


Figure 3.4: transmission spectra of an arc- induced LPFG 260315-650-1-18-26-D-04

3.2.2 Material Preparation

a) Sucrose Solution Preparation

The procedure to make concentration sucrose solution is used the formula to calculate as sucrose% (w/w) = $100 \times \text{Weight Sucrose} / (\text{Weight Sucrose} + \text{Weight Water})$. In order to determine the amount of sucrose used, the weight of water is fixed to 25g then mix with different weight sucrose for each solution. The prepared 11 sample of sucrose solutions as 0%, 10%, 20%, 30%, 40%, 45%, 50%, 55%, 60%, 65% and 70%. After completion of sucrose solution, digital refractometer was used to check the refractive index of solution and listed in table 3.

Concentration %w/w	Sucrose (g)	Water (ml)	Refractive Index (RI)
0	0.00	25	1.3330
10	2.78	25	1.3478
20	6.25	25	1.3639
30	10.72	25	1.3812
40	16.80	25	1.3999
45	20.50	25	1.4100
50	25.00	25	1.2010
55	30.60	25	1.4300
60	37.50	25	1.4419
65	46.50	25	1.4500
70	58.30	25	1.4654

Table 3: Refractive indices of sucrose solutions

b) Multilayer Preparations

In this project is referred by Qiushun Li and Xu-lin Zhang (2010) used polyelectrolyte PDDA (poly-diallyldimethylammonium chloride) and PSS (poly-sodium styrenesulfonate) for long period fiber grating (LPFG) surface modification to prepare sensitive film of sucrose solution. To study the coating PDDA and PSS film in surface LPFG sensitivity for sucrose solution function.

First, the LPFG is fixed surface to the watch glass and then rinsed with deionised water before start to immerse LPFG with PDDA and PSS. After the LPFG put other watch glass and put into solution (33.33% (w/w)) immerse for 10 minutes and then rinsed with deionised water then dry LPFG first before next process. Following by PSS (5% (w/w)) immerse for 10 minutes then rinsed with deionised water then dry LPFG first before next process, thus completing a first bi-layer by self-assembled polyelectrolyte see in figure 3.5 (a) and (b). To repeat alternated the above steps to get 50 bi-layer PDDA/PSS multilayer was reached. Figure 3.5 (a) is a schematics diagram of the self-assembly process and figure 3.5 (b) is a schematic view of a polyelectrolyte self-assembly principles.

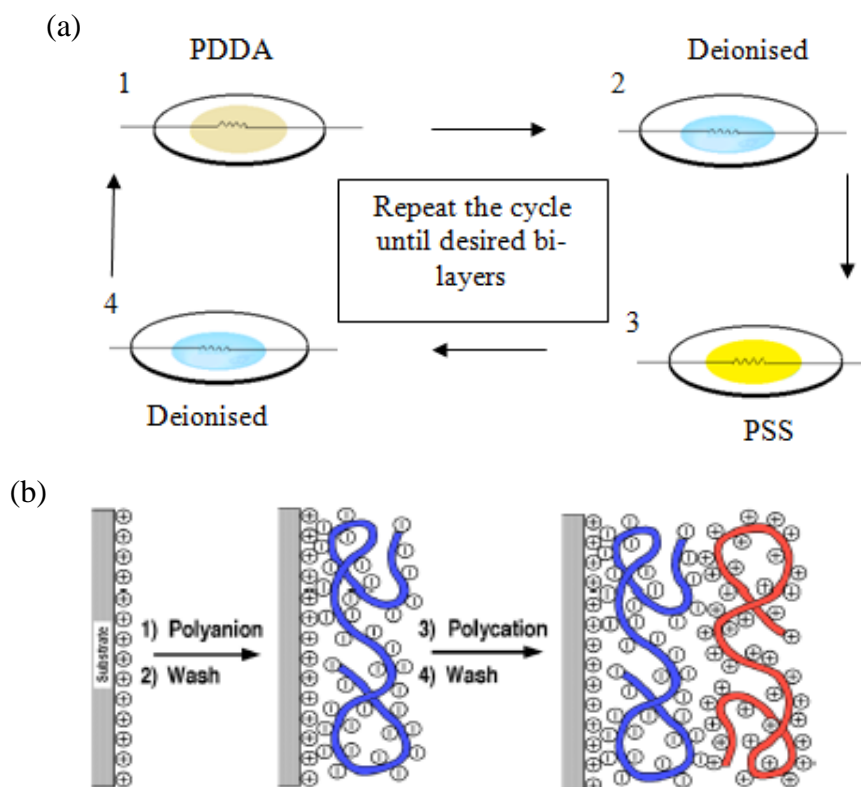


Figure 3.5: (a) and (b) Scheme of multilayer fabrication process and basic principle.

3.2.3 Instrument Preparation

After that make a complete material of the long period fiber grating in the second step is to design and analyze long period fiber grating sensor. In this project most main important components and additional component are definitely know it consists:









	
(a) optical spectrum analyzer	(b) low noise optical amplifier
	
(c) ProsKit 8PK-326 3-Hole Fiber Optic Stripper	(d) fiber optic cutter Fc-7
	
(e) digital refractometer	(f) fusion splicer or splicing machine
	
(g) fiber SMF-28	(h) fiber circulator

Table 4: list instrument

3.2.4 Setup Techniques of Single Pass and Double Pass

First of all, I prepared 3 LPFG that had different number of the grating as 35, 38 and 39 for single pass with uncoated normal test and single pass with layer by layer; and also prepared 3 LPFG that had different number of the grating as 33, 35 and 38 for double pass with uncoated normal test and double pass with layer by layer for the testing.

The actual experiment model setup of single pass system is referred by Yun-Thung Yong (2014) will be design and used to measurement sucrose sensing sensitivity of long period fiber grating with uncoated normal test and LBL test. The setup of the single pass configuration, the light source will enter first circulator than pass through the LPFG under test and transmitting into the second circulator goes to OSA. The diagram below is the single pass configuration.

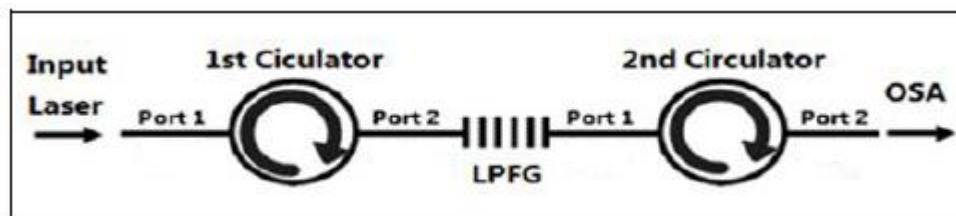


Figure 3.6: LPFG single pass configuration

Next, the actual experiment model setup double pass system will be design and used to measurements refractive index (RI) of long period fiber grating with uncoated normal test and LBL test. The setup of the double pass configuration, first of all, the light source will enter first circulator than pass through the LPFG under test and transmitting into the second circulator. Next, the light source will re-enter into second circulation pass through the LPFG and transmitting towards into the optical spectrum analyzer. Figure 3.7 illustrates show the setup double pass configuration long period fiber grating system.

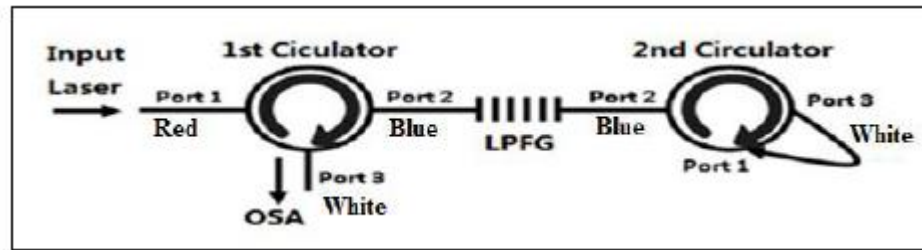


Figure 3.7: LPFG double pass configuration

After finished designed output port of the optical circulator of the system the simulation mode that can start to measurement sucrose solution of the system that is using an OSA (optical spectrum analyzer) from machine YOKAGAWA AQ63370C to performance results. If the double pass setup model system does not meet the necessary condition shall I do again in the previous of the step to simulation model and to solve the model of the LPFG sensor array system and then to test model until I get the expected results.

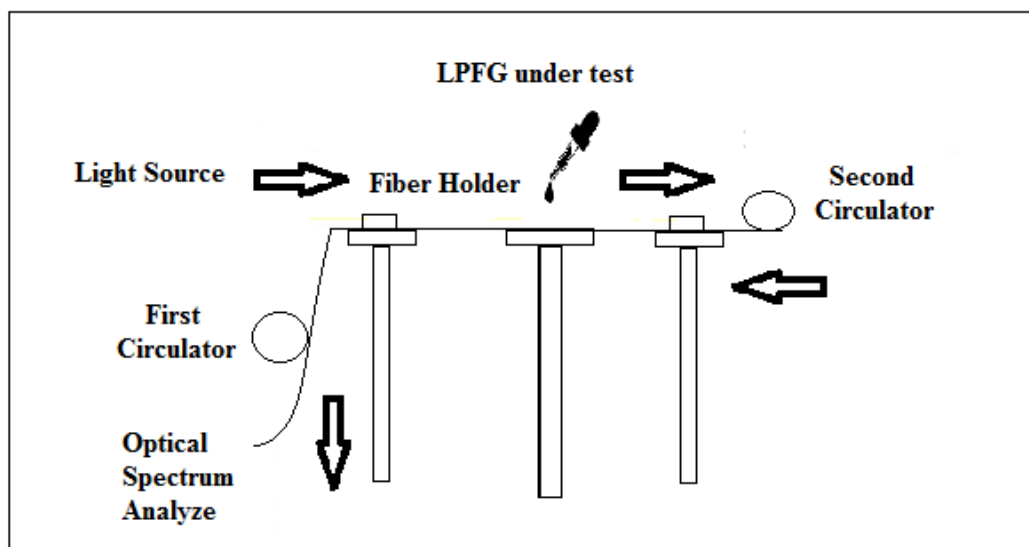


Figure 3.8: Refractive index testing setup

Last, I was test sucrose solution from 0 to 70% using two techniques of single pass and double pass. The LPFG that has grating was place in the middle of the test plate. Then the grating of the LPFG was fully covered by the different concentration of sucrose solution and every time do tested I using deionised water cleaned the grating on the LPFG in order to get a precise value. Then I was using the LPFG to test which method was better to enhanced sensing sensitivity such as normal test of

single pass and double pass and LBL test of single pass and double pass. In the end, the model of the system will performance and display the result on the OSA and I am satisfied the LPFG sensor model system performance.

CHAPTER 4

RESULTS AND DISCUSSIONS

4.1 Result of Sucrose Solution Test

Different of sucrose concentration will used to test sensing sensitive of long period fiber grating. In figure 4.1 that can see the dependence of the concentration on refractive index of sucrose solution when the sucrose solution increasing the refractive index also increases.

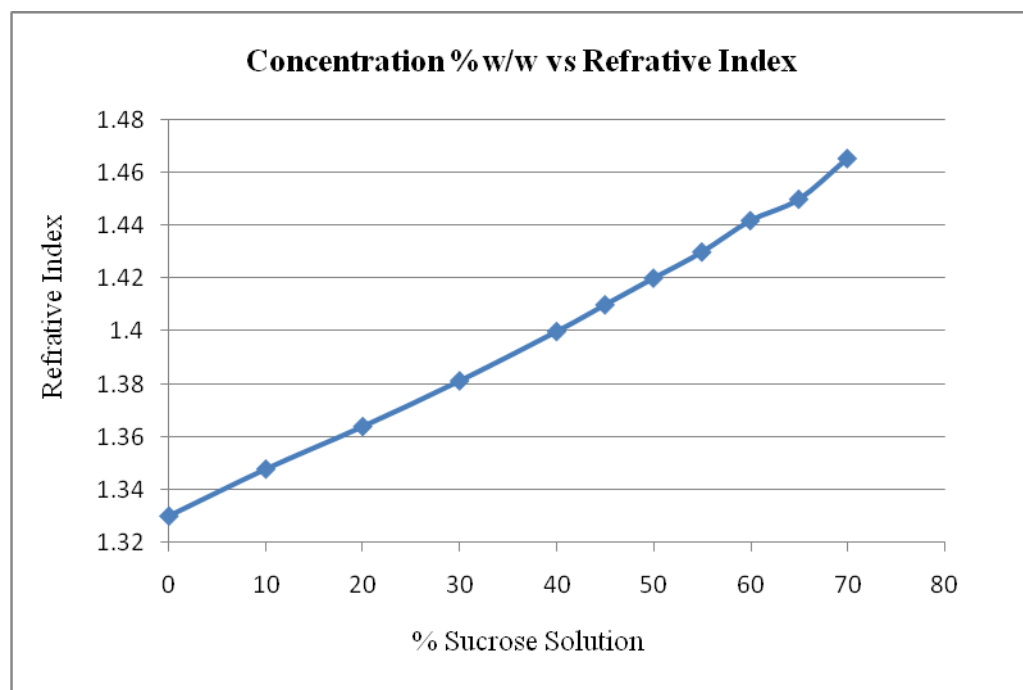


Figure 4.1: The relationship between sucrose solution and refractive index

According to the Snell's law when the light source passing through from air into a medium the constant, n ($= \sin i / \sin r$) known as the refractive index of the medium. It is a measure that how much a ray of light is refracted when passing through from air/vacuum through a medium. The refractive index of a material is greater show that it is denser and can refract light through a large angle. This means that the sucrose solution is increasing the refractive index also increases.

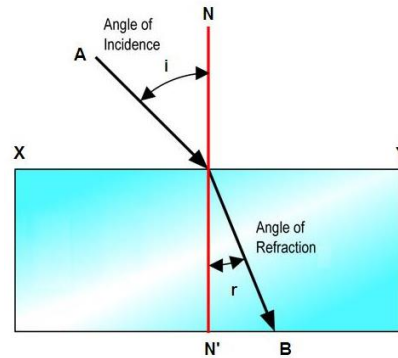


Figure 4.2: principle of Snell's Law

The basic principle of the optical waveguide is an optical fiber transmission of reflected light. As shown in figure 4.3 fiber structures we can see the head face surface are smooth and flat.

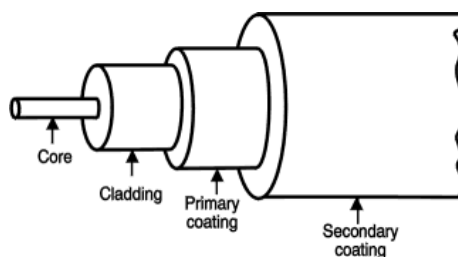


Figure 4.3: fiber structure

When light rays is passing through into optical fiber that is angle of incident θ_0 , the refracted light rays will be approaching the normal line that is angle of refraction β , where β is satisfy of the Snell's law $n_0 \sin \theta_0 = n_1 \sin \beta$. The refractive index of n_0 is external environment refractive index and n_1 is refractive index of the core. At the light ray incident θ_1 on the interface of fiber core and cladding boundary surface when light ray incident θ_1 is greater than or equal to critical angle θ_c so now

the refracted ray had fully reflected. Wherein θ_c is satisfies $\sin \theta_c = n_2 \sin 90 / n_1$, the n_2 is refractive index of the fiber cladding and θ_1 is optical fiber total reflection critical incident angle. After that, the light ray inside the fiber will occurred equal or greater than θ_1 angle incidence to recurrent total internal reflection. This reflection is called “Total Internal Reflection” in below figure 4.3(a) shown principle of total internal reflection.

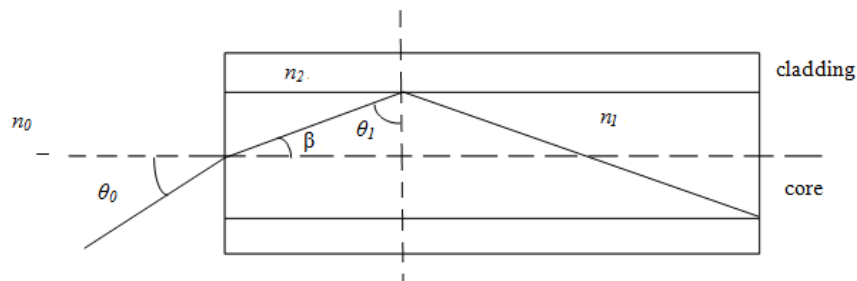


Figure 4.4: (a) Total internal reflection

This principle is come from Snell’s law when the internal refractive index has to higher than the external in order to have a total reflection. Since the refractive index of sucrose solution (0-70%) is 1.333 to 1.46 is between the optical fiber refractive index of the cladding is 1.45 and the core is 1.46 therefore the light incident in the optical fiber within a certain angular range through the entire fiber the loss does not induced.

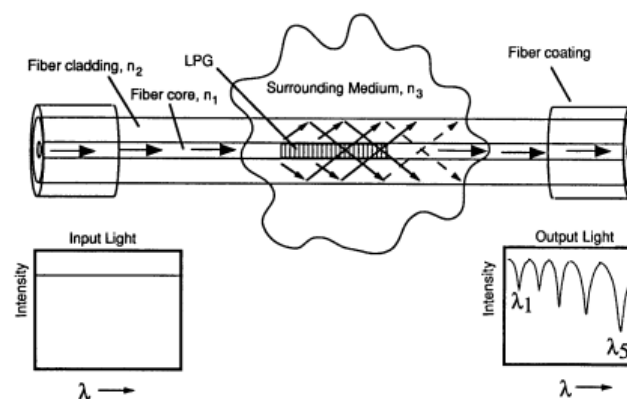


Figure 4.4: (b) schematic of the based LPG external sensor measuring the refractive index (Patrick, 1998)

In addition, this theory is come from Patrick (1998), the central wavelength of the resonance peak refractive index changes with sucrose solution (surrounding medium). When the refractive index of sucrose solution changes from 1.00 to 1.44

the central wavelength of the resonance peak shifted to the short wavelength direction and the more obvious the higher the refractive index change. Beside, when sucrose solution in a slight change in the between refractive index 1.45 to 1.46, the transmission spectrum can be observed different. This is because the refractive index of the cladding is about 1.45 when the refractive index of sucrose solution is approximately equal to 1.45 the cladding mode occurs off that cannot be propagated in the fiber cladding since the notch depth of power transmission will decrease and shown in below as single pass and double pass result.

4.2 Single Pass Test Result

4.2.1 Single Pass with Uncoated Normal Test

i. Grating -35

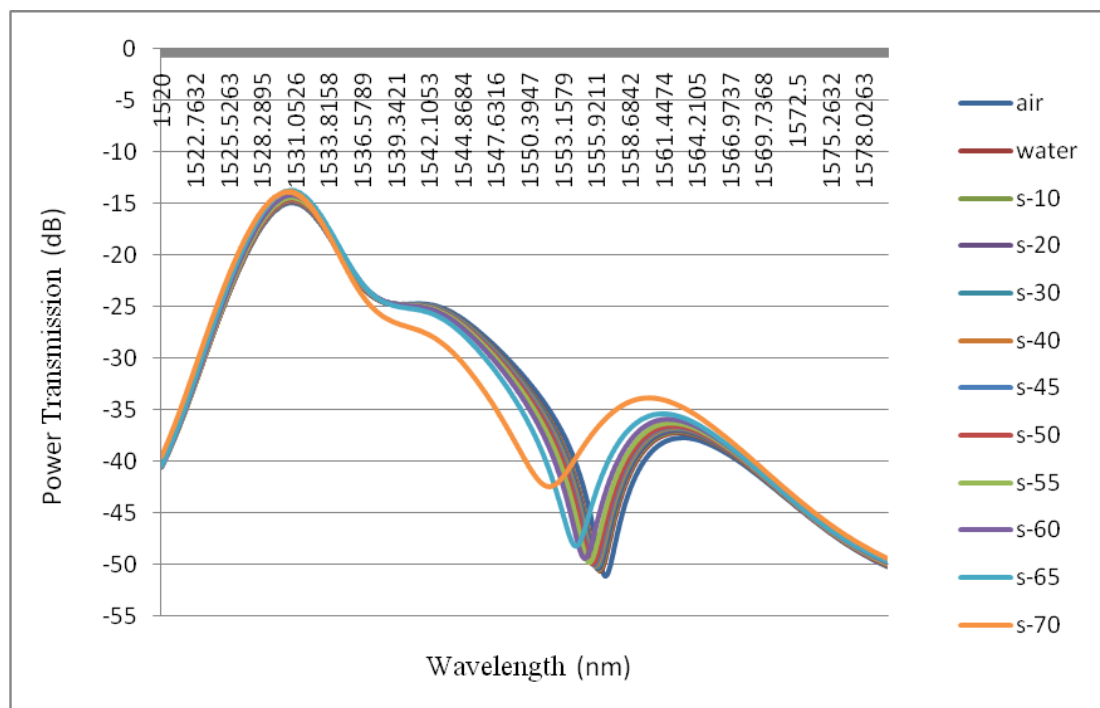


Figure 4.5: Grating 35-Transmission spectra at different sucrose solution (0-70%) using single pass with uncoated technique

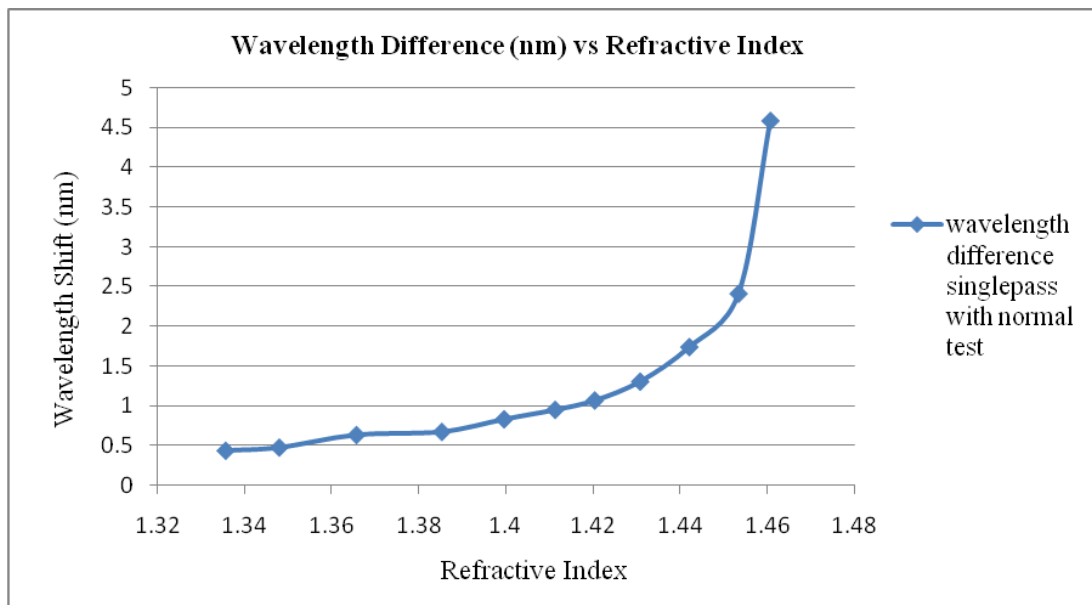


Figure 4.6: Grating 35-Resonance wavelength shift of LPFG with different refractive index

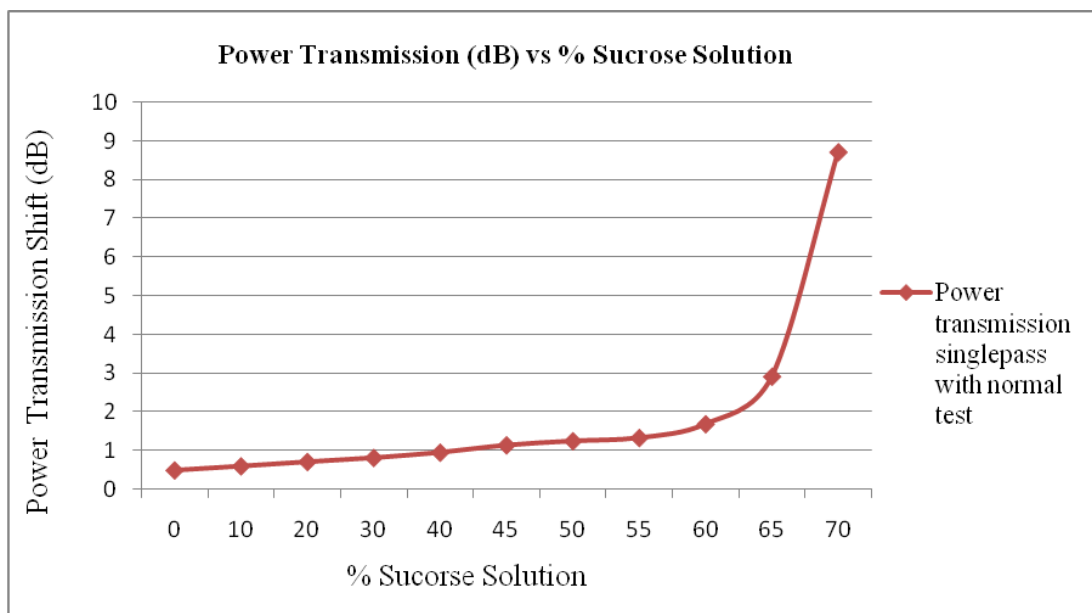


Figure 4.7: Grating 35-Power transmission shift of LPFG with different sucrose using single pass with uncoated technique

ii. Grating-38

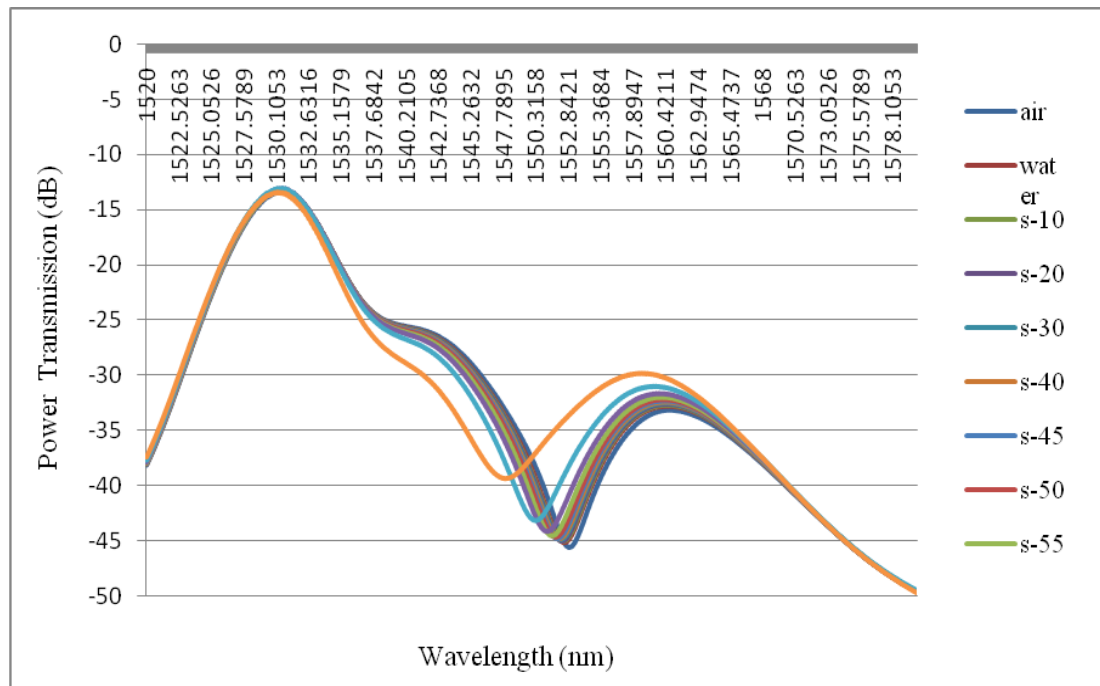


Figure 4.8: Grating 38-Transmission spectra at different sucrose solution (0-70%) using single pass with uncoated technique

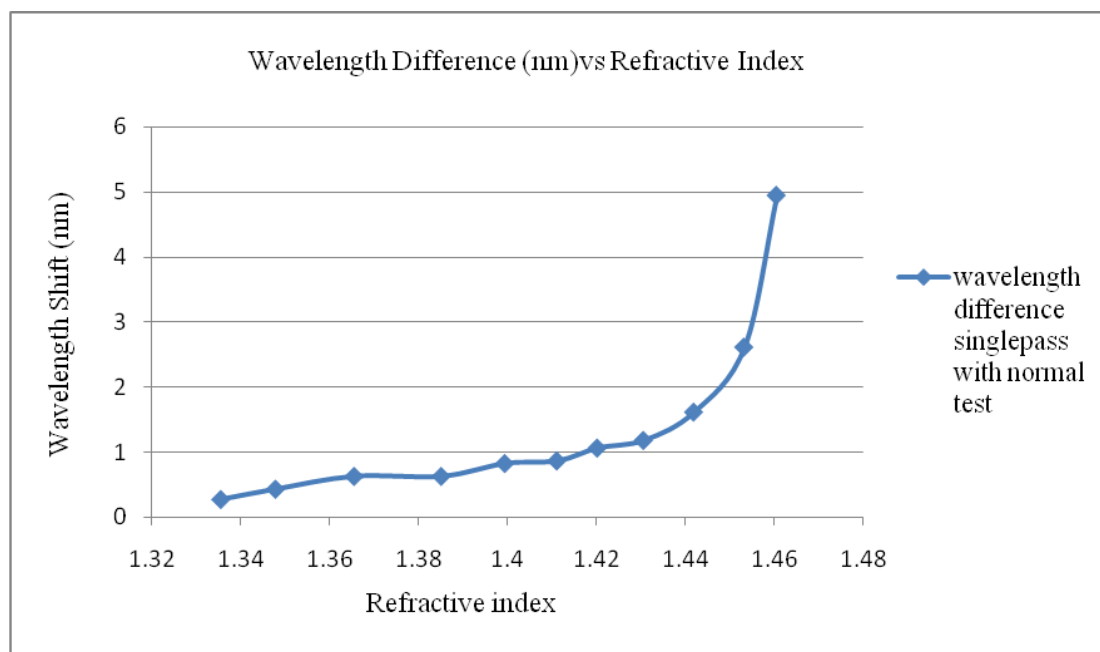
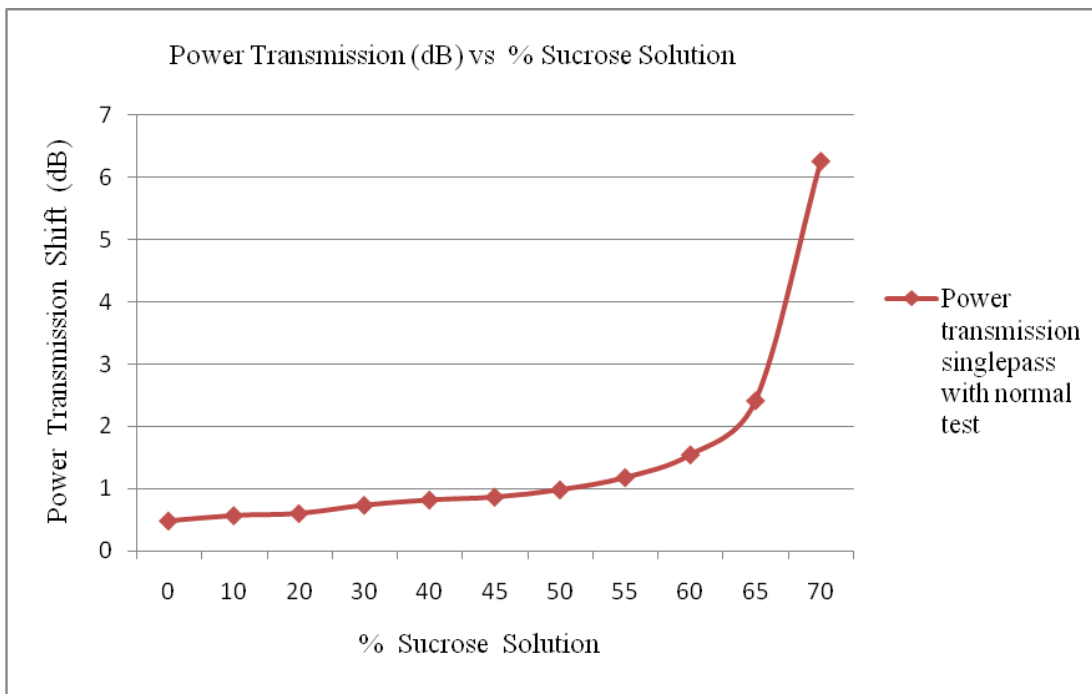


Figure 4.9: Grating 38-Resonance wavelength shift of LPFG with different refractive index using single pass with uncoated



(c)

Figure 4.10: Grating 38-Power transmission shift of LPFG with different sucrose solution using single pass with uncoated technique

iii. Grating-39

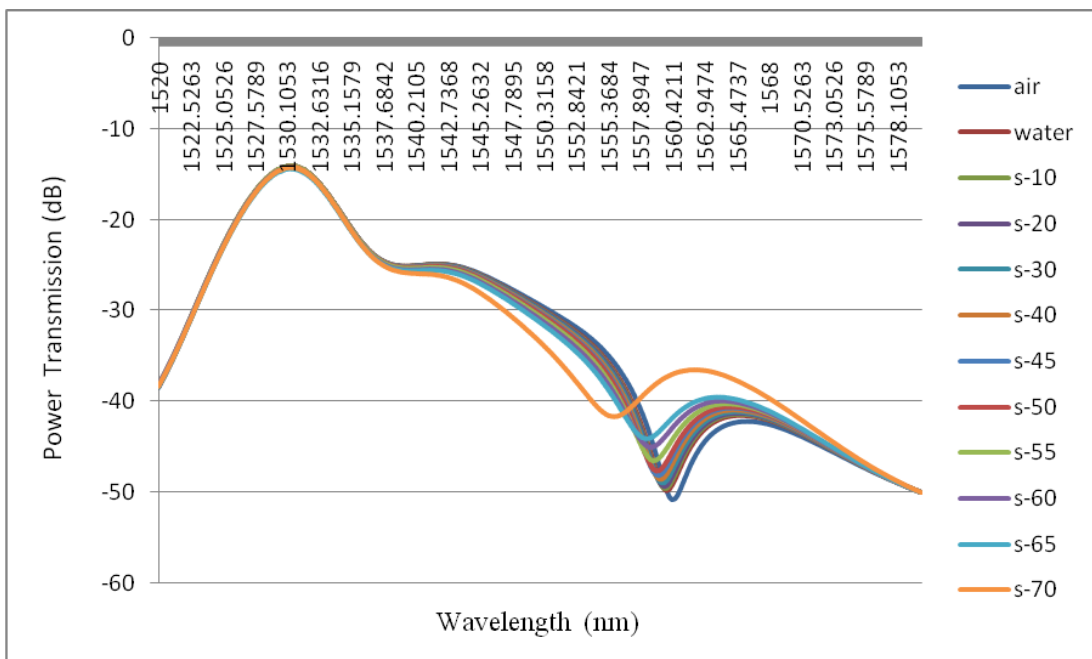


Figure 4.11: Grating 39-Transmission spectra at different sucrose solution (0-70%) using single pass with uncoated technique

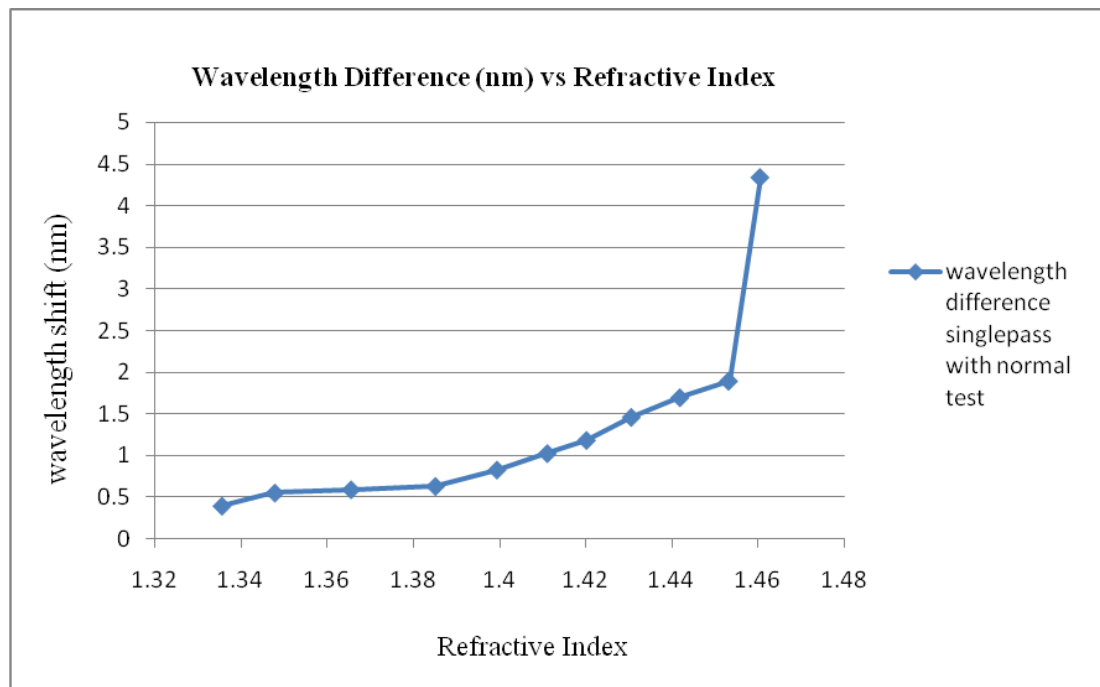
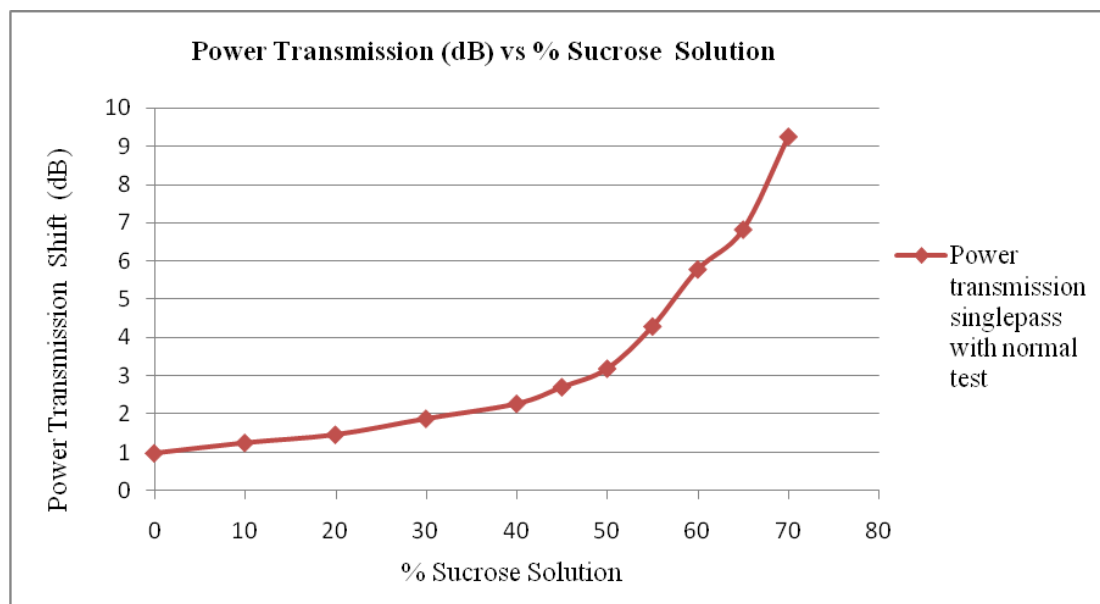


Figure 4.12: Grating 39-Wavelength shift of LPFG with different refractive index using single pass with uncoated technique



(c)

Figure 4.13: Grating 39-Power transmission shift of LPFG with different sucrose solution using single pass with uncoated

Referring by above graph for the single pass with uncoated test we can see that the three different LPFG of the grating as 35, 38 and 39 is show from figure 4.3 to 4.13 for the transmission spectra at different sucrose solution, wavelength shift and power transmission shift. From the transmission spectra we can see the from 0% to 70 % is gradually increasing the resonance wavelength is left shift and power transmission is shift up. In this test, the optimal concentration of sucrose solution is 70% increasing the refractive index of the solution from 1.333 to 1.4654. The LPFG grating of 35, 38 and 39 exhibited a total left shift is 4.579nm, 4.947nm and 4.3421nm when concentration of sucrose solution increasing. The measurement LPFG power transmission of grating 35, 38 and 39 a total shift up is 8.72dB, 6.25dB and 9.236dB.

4.2.2 Single Pass with Layer by Layer Test

i. Grating-35

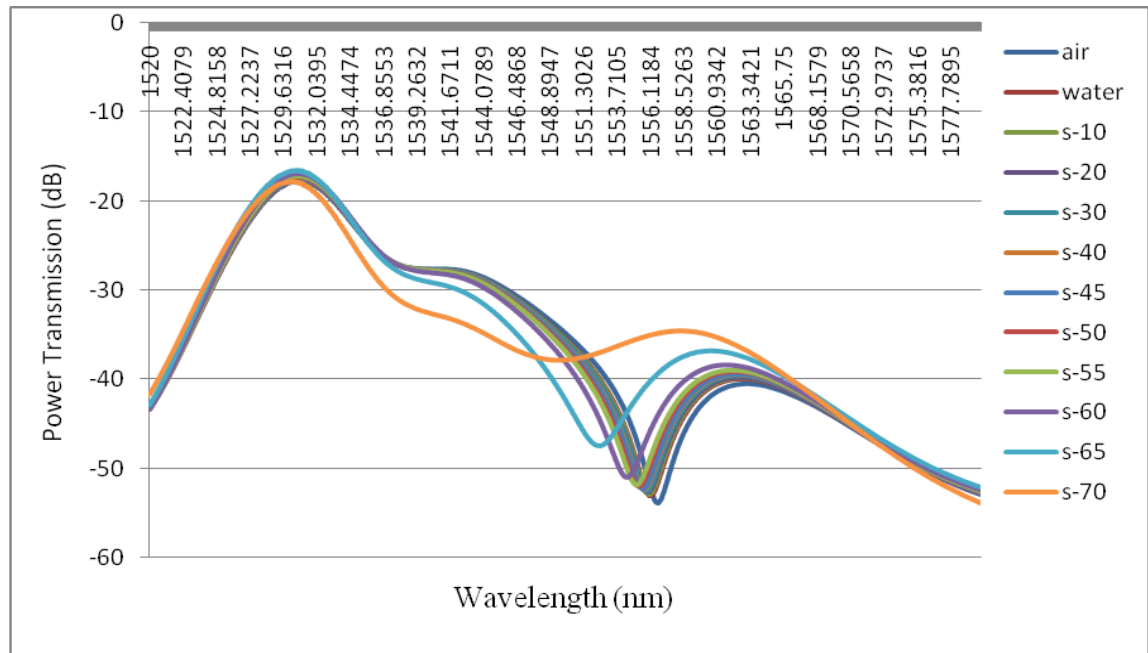


Figure 4.14: Grating 35-Transmission spectra at different sucrose solution (0-70%) using single pass with layer by layer technique

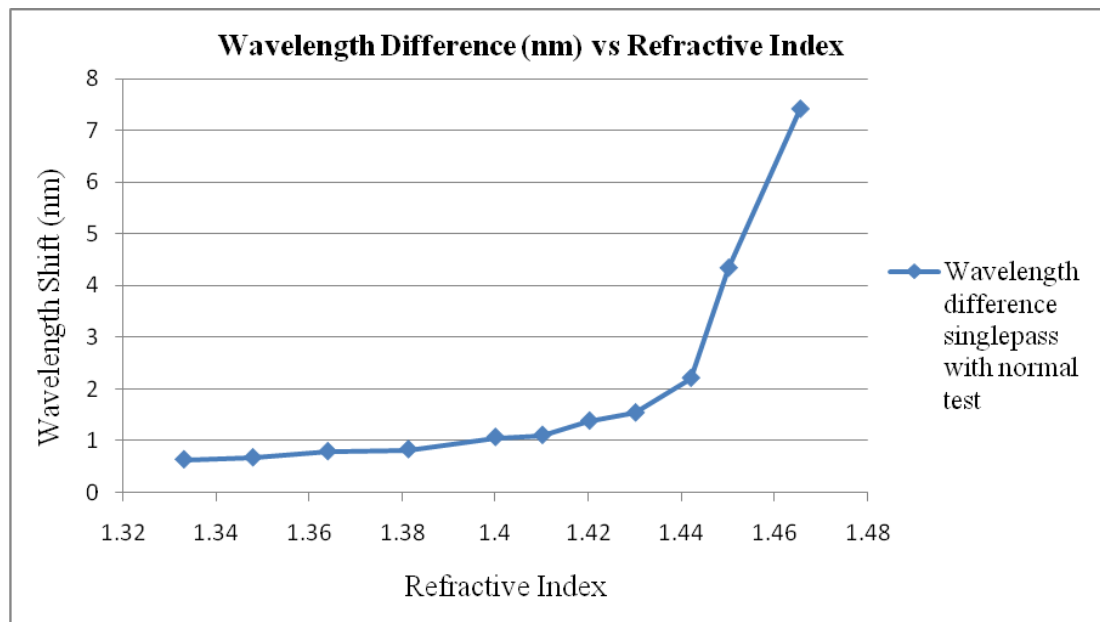


Figure 4.15: Grating 35-Wavelength shift of LPFG with different refractive index using single pass with layer by layer technique

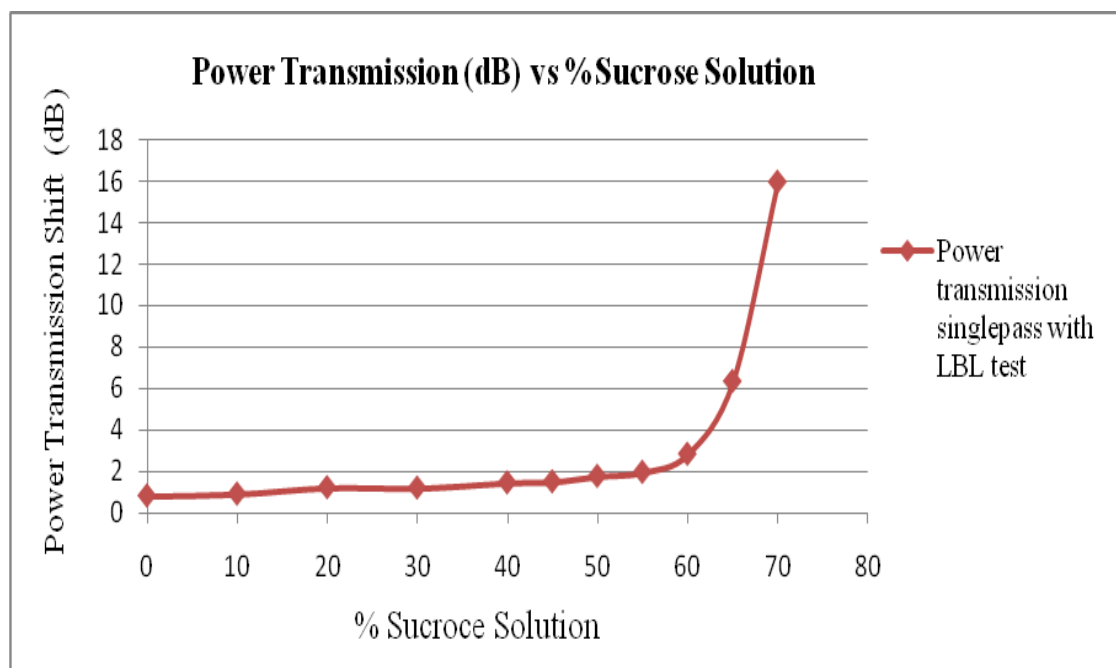


Figure 4.16: Grating 35-Power transmission shift of LPFG with different sucrose solution using single pass with layer by layer technique

ii. Grating-38

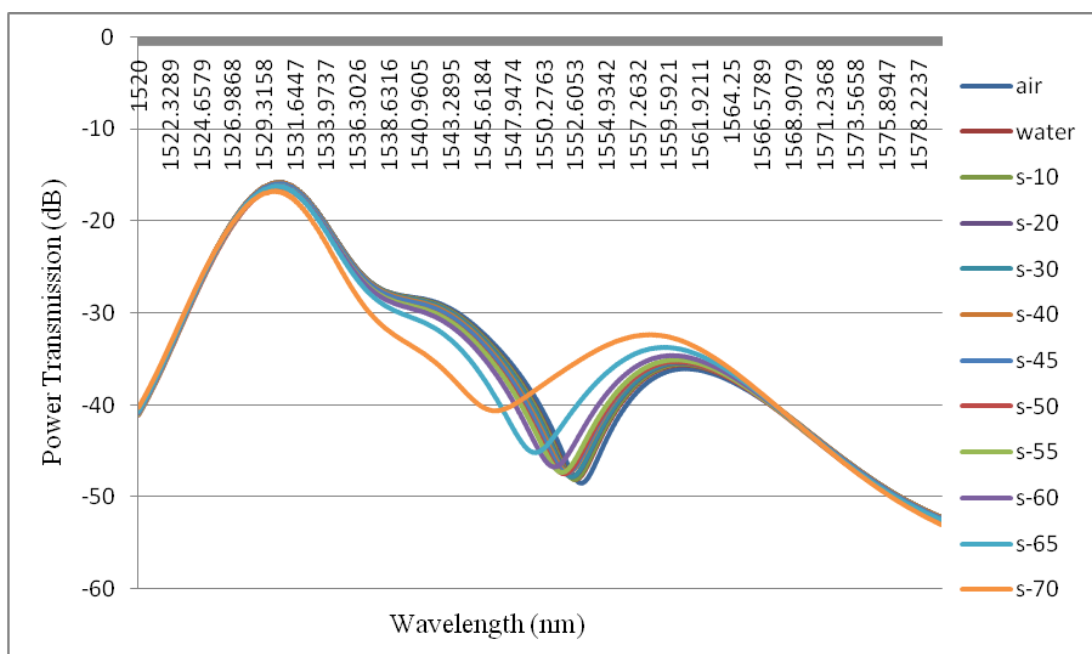


Figure 4.17: Grating 38-Transmission spectra at different sucrose solution (0-70%) using single pass with layer by layer technique

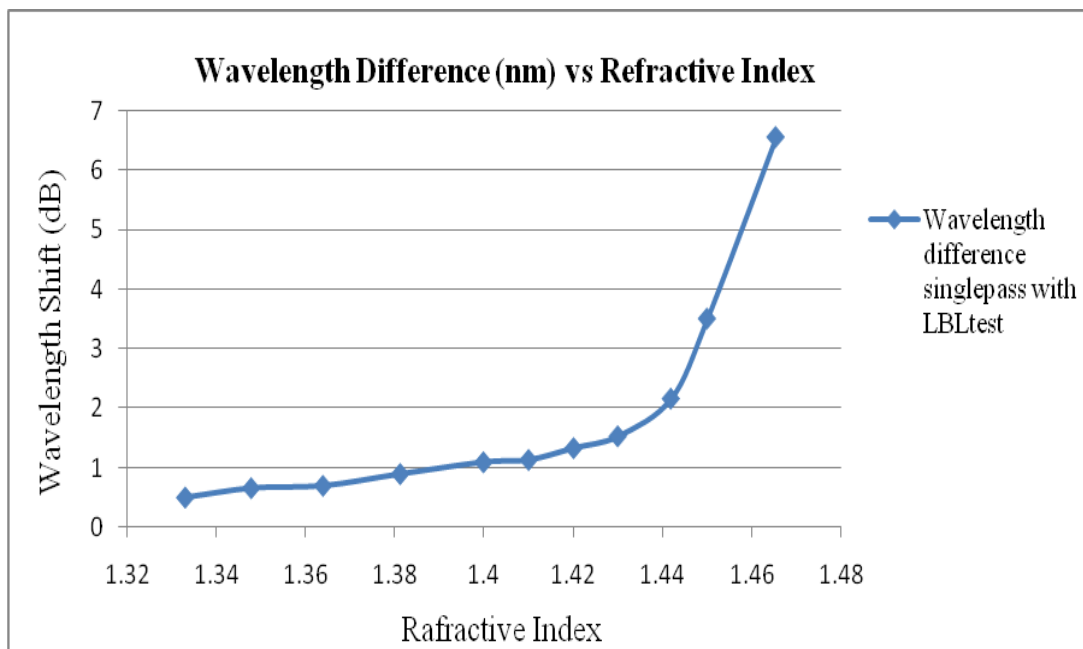


Figure 4.18: Grating 38-Wavelength shift of LPFG with different refractive index using single pass with layer by layer technique

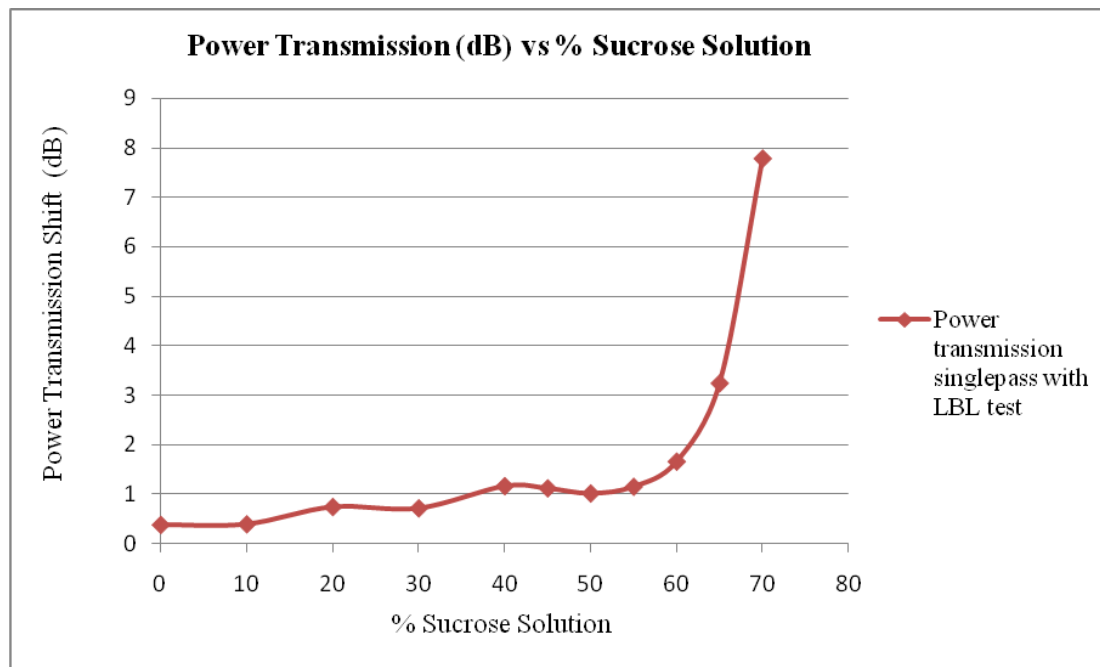


Figure 4.19: Grating 38-Power transmission shift of LPFG with different sucrose solution using single pass with layer by layer technique

iii. Grating-39

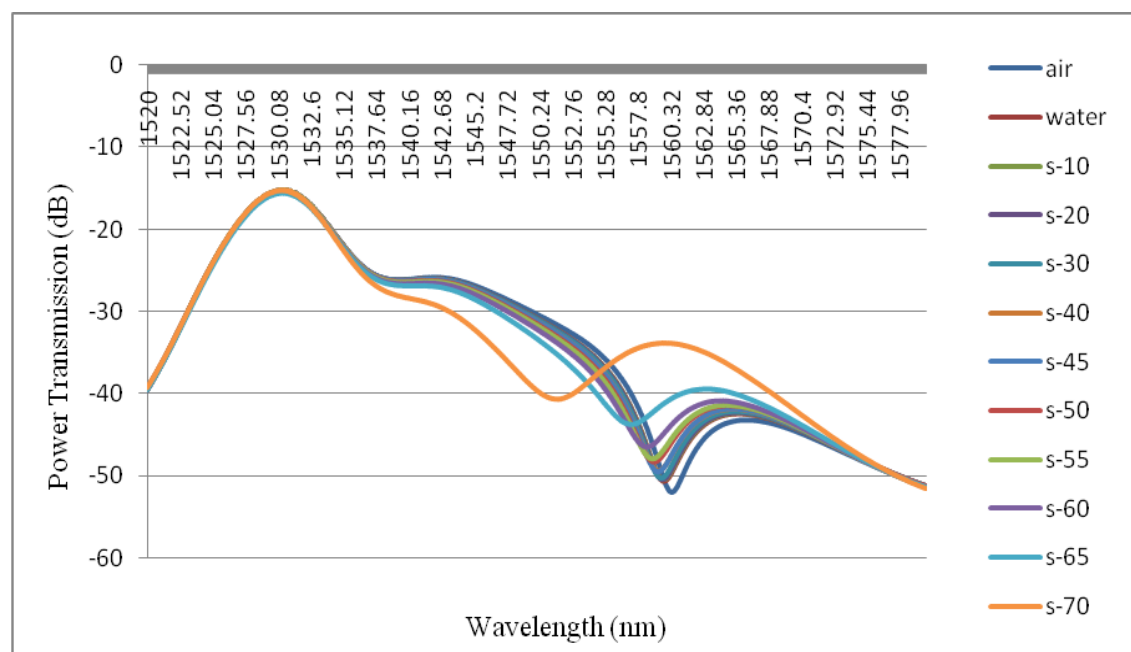


Figure 4.20: Grating 39-Transmission spectra at different sucrose solution (0-70%) using single pass with layer by layer technique

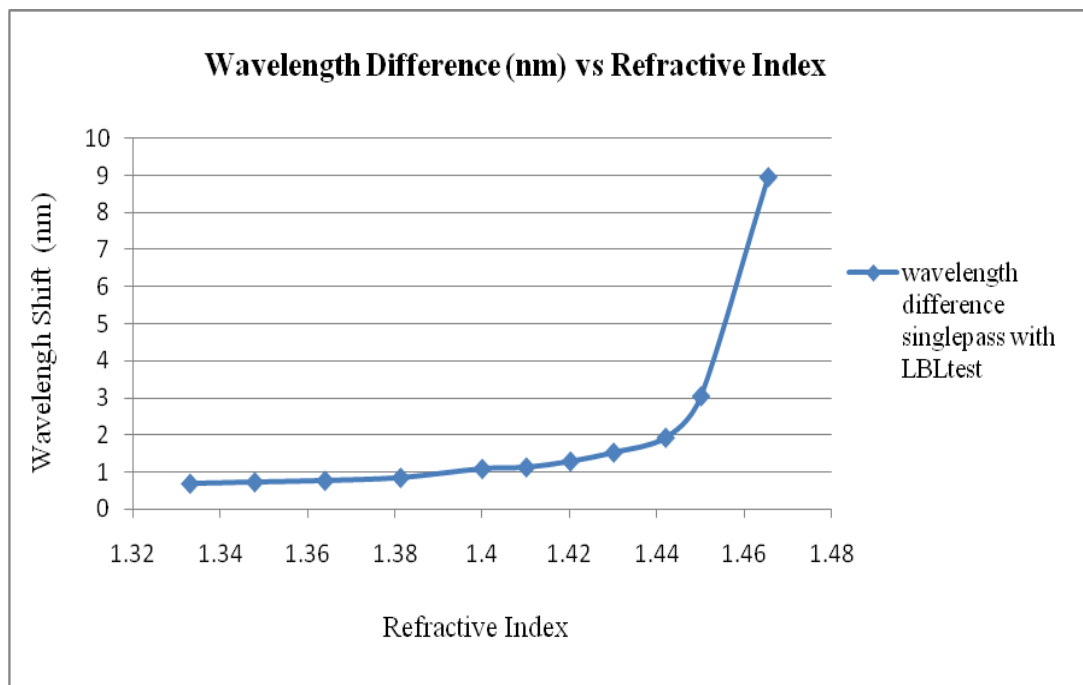


Figure 4.21: Grating 39-Wavelength shift of LPFG with different refractive index using single pass with layer by layer technique

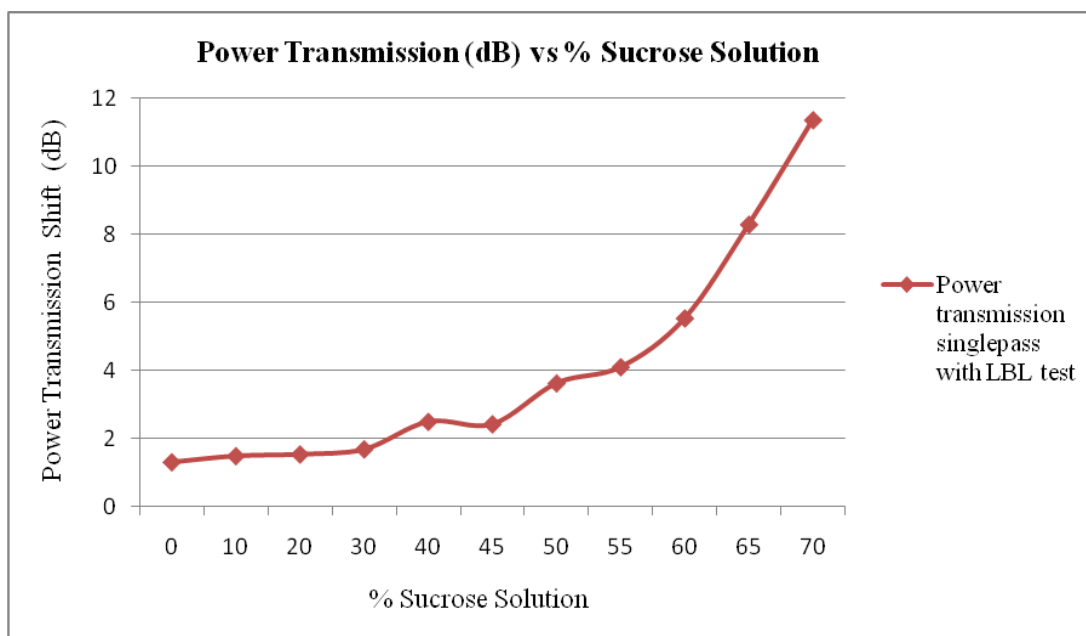


Figure 4.22: Grating 39-Power transmission shift of LPFG with different sucrose solution using single pass with layer by layer technique

In order to enhanced sucrose sensing sensitivity of LPFG, I using single pass with layer by layer techniques to surface coated LPFG with a multilayer PDDA (poly-diallyldimethylammonium chloride) and PSS (poly-sodium styrene suffocate. As we can see above transmission spectra LPFG of grating 35, 38 and 39 from the air central wavelength left shift to concentration of sucrose solution 70% was gradually shift as 7.421nm, 6.5527nm and 8.96nm. The measurement LPFG power transmission of grating 35, 38 and 39 a total shift up is 15.961dB, 7.776dB and 11.38dB.

4.2.3 Compared Between Single Pass with Uncoated Test and Single Pass with LBL Test

i. Grating-35

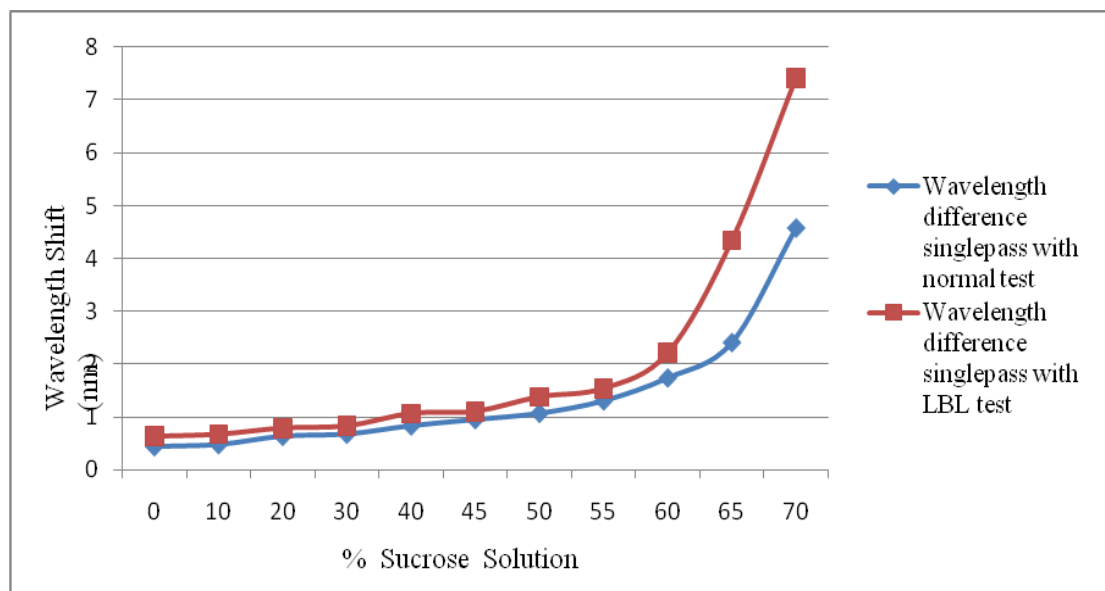


Figure 4.23: Grating 35-Different wavelength shift between singlepass uncoater and layer by layer techniques.

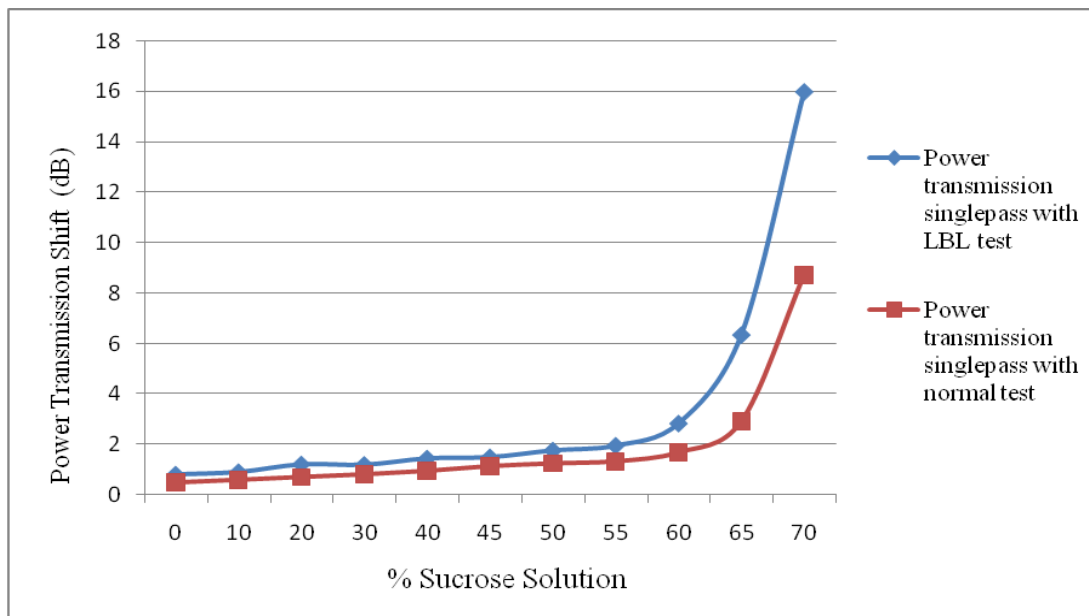


Figure 4.24: Grating 35-Different power transmission shift between singlepass uncoater and layer by layer techniques.

ii. Grating-38

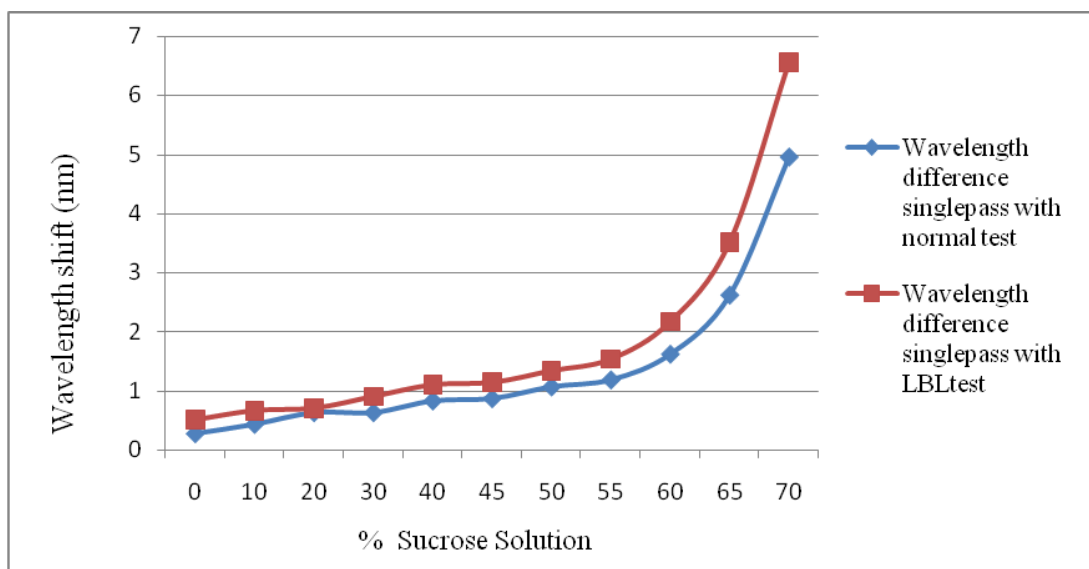


Figure 4.25: Grating 38- Different wavelength shift between singlepass uncoater and layer by layer techniques.

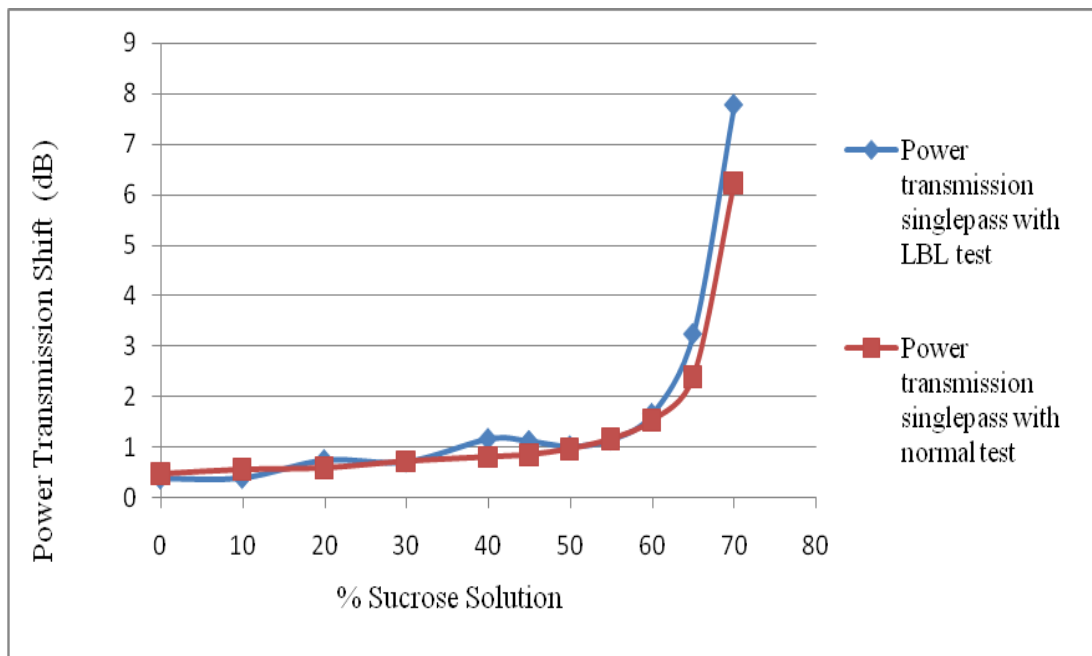


Figure 4.26: Grating 38-Different power transmission shift between singlepass uncoater and layer by layer techniques.

iii. Grating-39

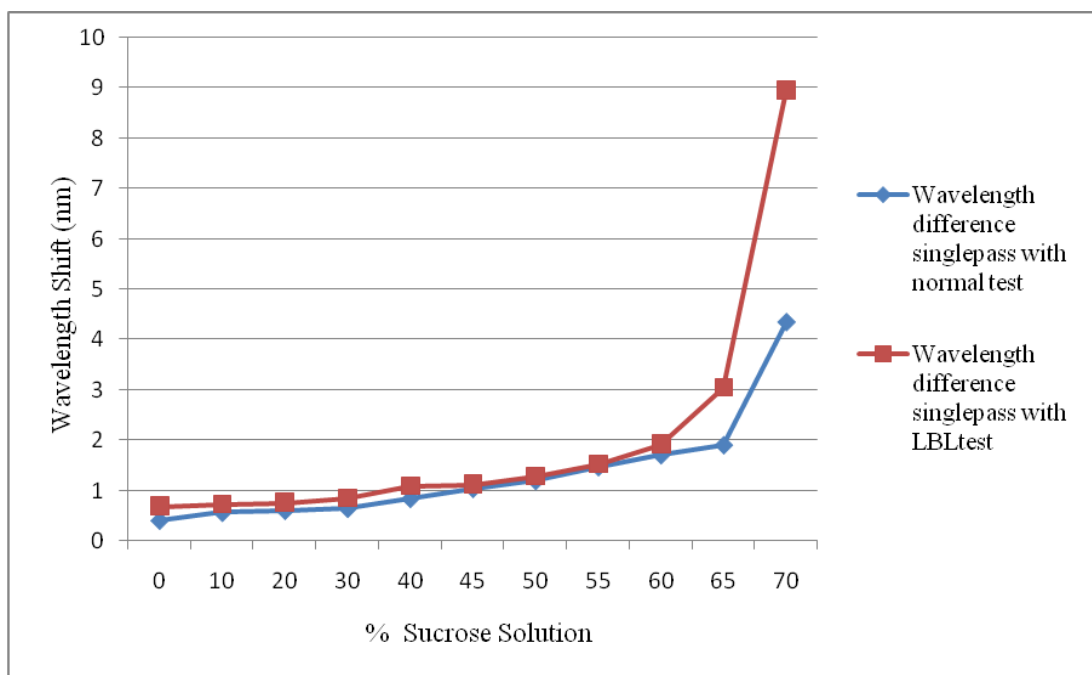


Figure 4.27: Grating 39- Different wavelength shift between singlepass uncoater and layer by layer techniques.

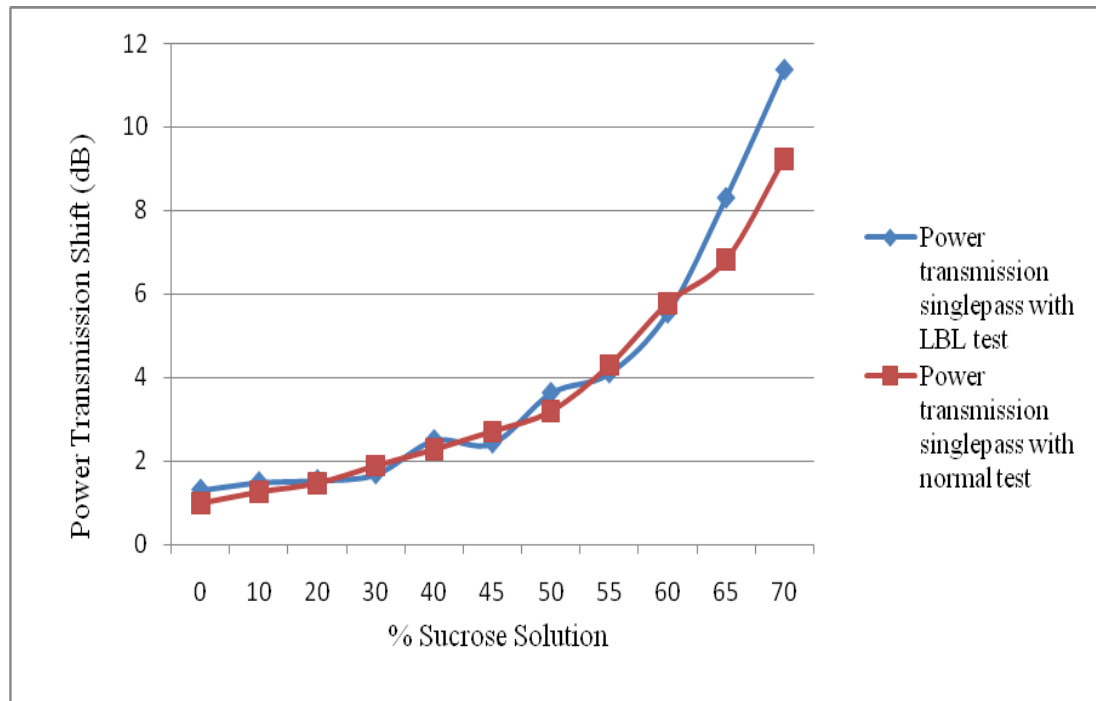


Figure 4.28: Grating 39-Different power transmission shift between singlepass uncoater and layer by layer techniques.

The above figure shows the three different fiber grating as 35, 38, and 39 the graph is clearly to show different wavelength shift between singlepass uncoater and layer by layer techniques. It is significant sensitive of concentration (60-70%) as show in figure 4.23, 4.25 and 4.27. In figure 4.27 is maximum shift of 8.96 nm occurs when the concentration of sucrose from 0% to 70% using single pass with layer by layer compared to the single pass with uncoter the maximum wavelength shift of 4.3421nm that means this is double wavelength shift in single pass with layer by layer techniques. The different power transmission shift between single pass with uncoated and layer by layer is significant sensitive of concentration (60-70%) as shows in figure 4.24,4.26 and 4.28. The single pass with layer by layer to show the figure 4.24 is maximum power transmission shift from 0% to 70% of 15.961dB to compare with the single pass with uncoated the power transmission shift of 8.72.

4.3 Double Pass Test Result

4.3.1 Double Pass with Uncoated Normal Test

i. Grating-33

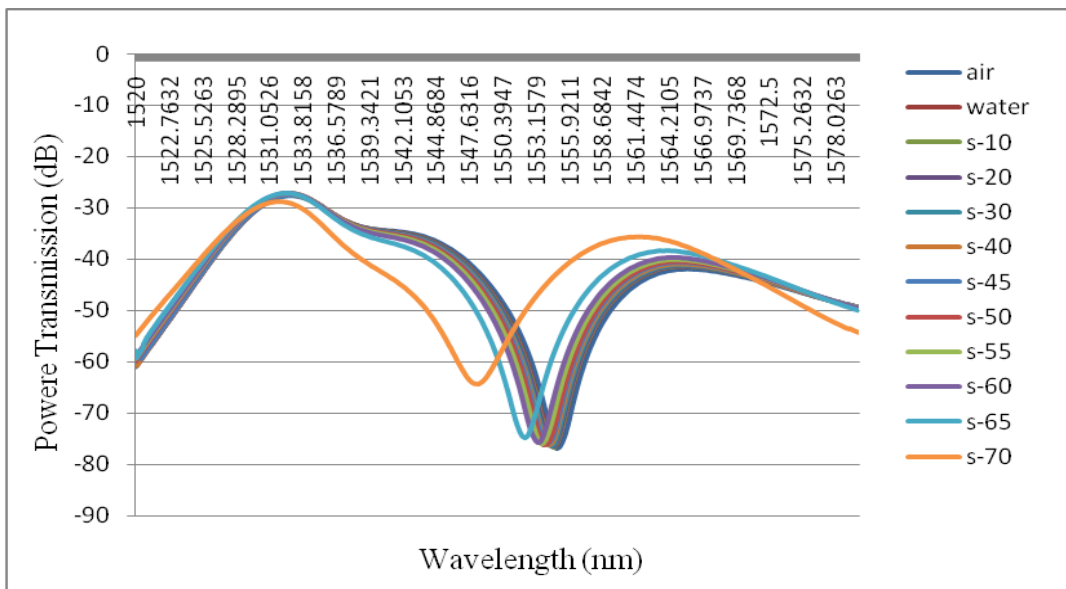


Figure 4.29: Grating 33-Transmission spectra at different sucrose solution (0-70%) using double pass with uncoated technique

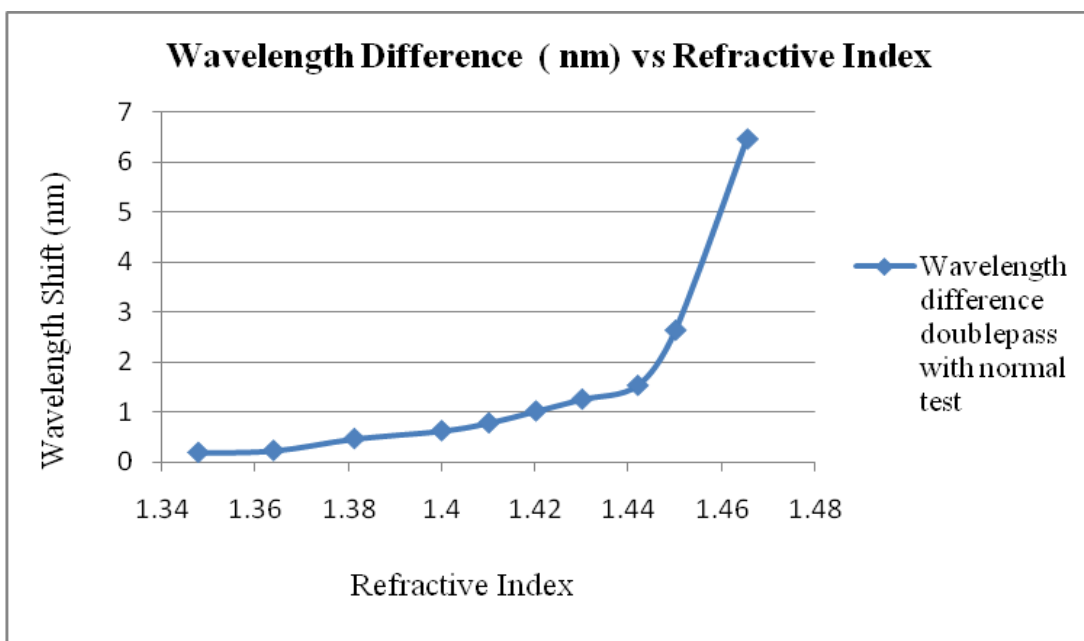


Figure 4.30: Grating 33-Wavelength shift of LPFG with different refractive index using double pass with uncoated technique

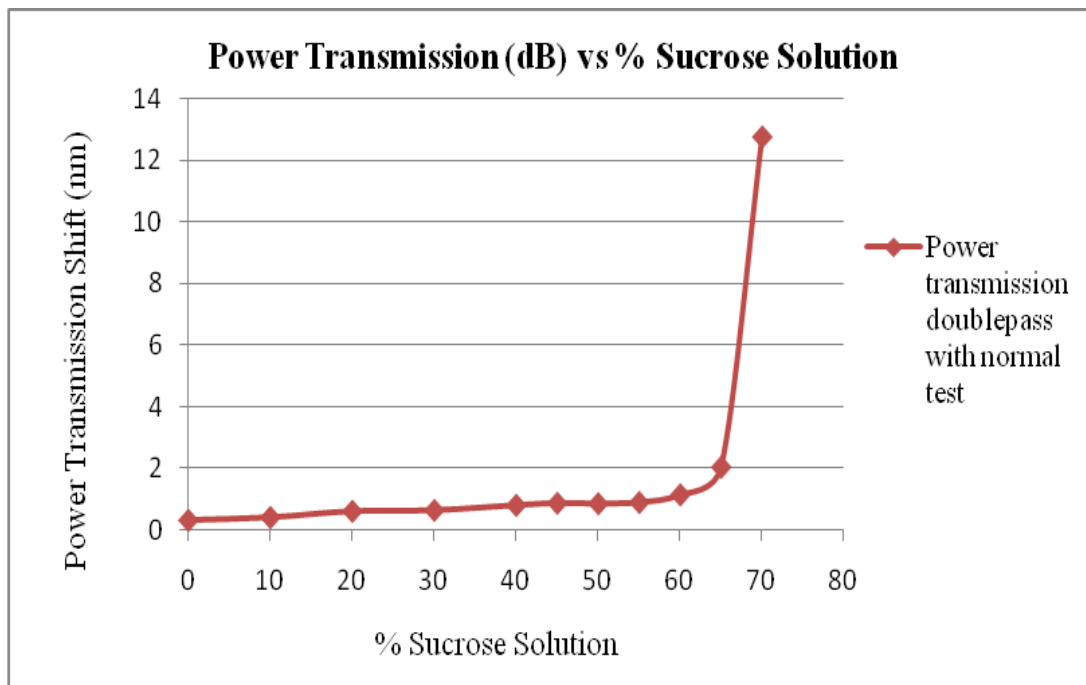


Figure 4.31: Grating 33-Power transmission shift of LPFG with different sucrose using double pass with uncoated technique

ii. Grating-35

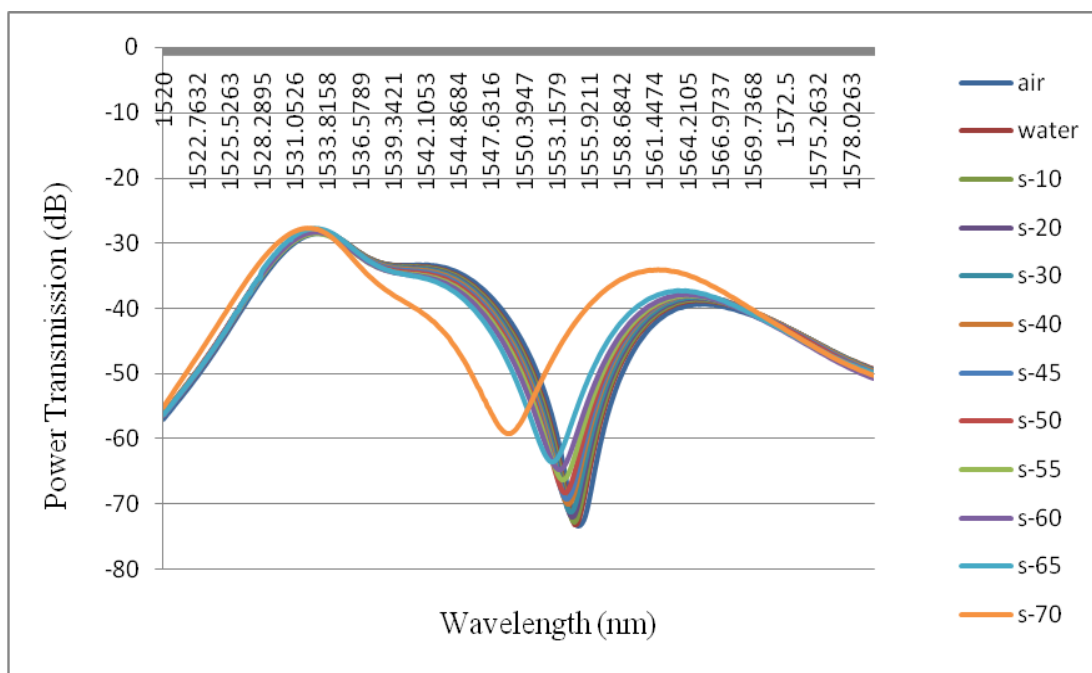


Figure 4.32: Grating 35-Transmission spectra at different sucrose solution (0-70%) using double pass with uncoated technique

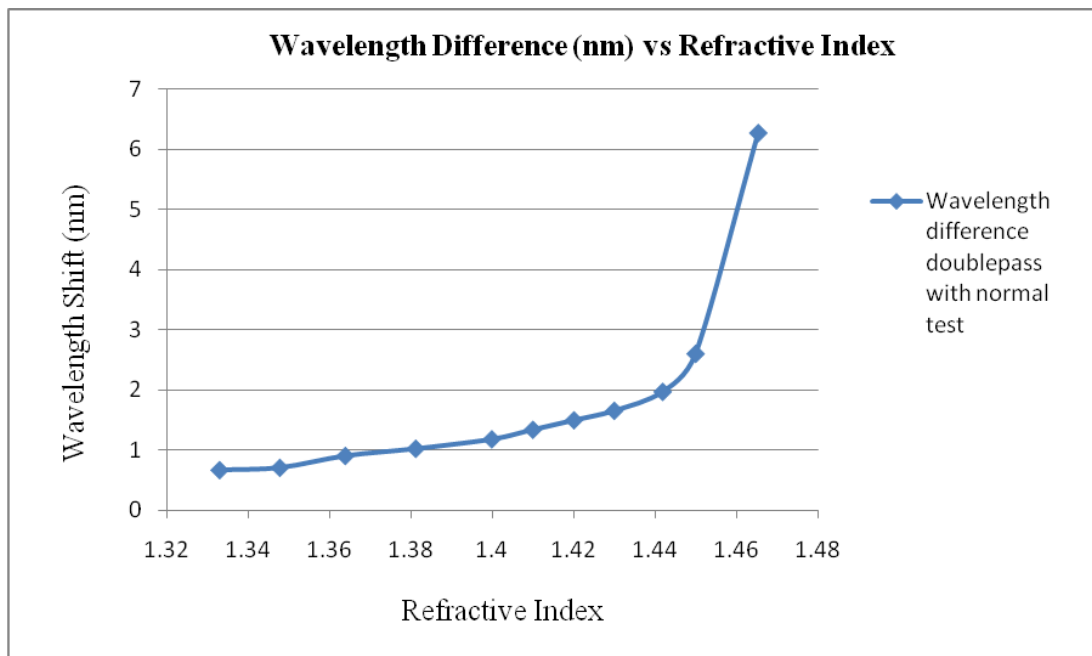


Figure 4.33: Grating 35-Wavelength shift of LPFG with different refractive index using double pass with uncoated technique

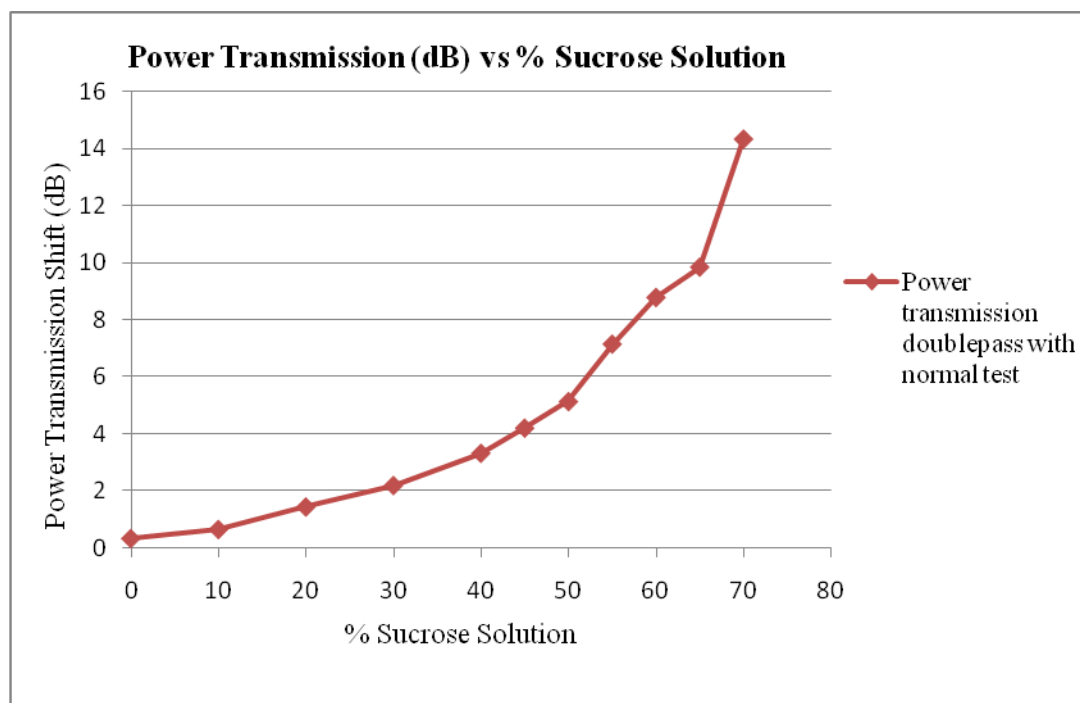


Figure 4.34: Grating 35-Power transmission shift of LPFG with different sucrose using double pass with uncoated technique

iii. Grating-38

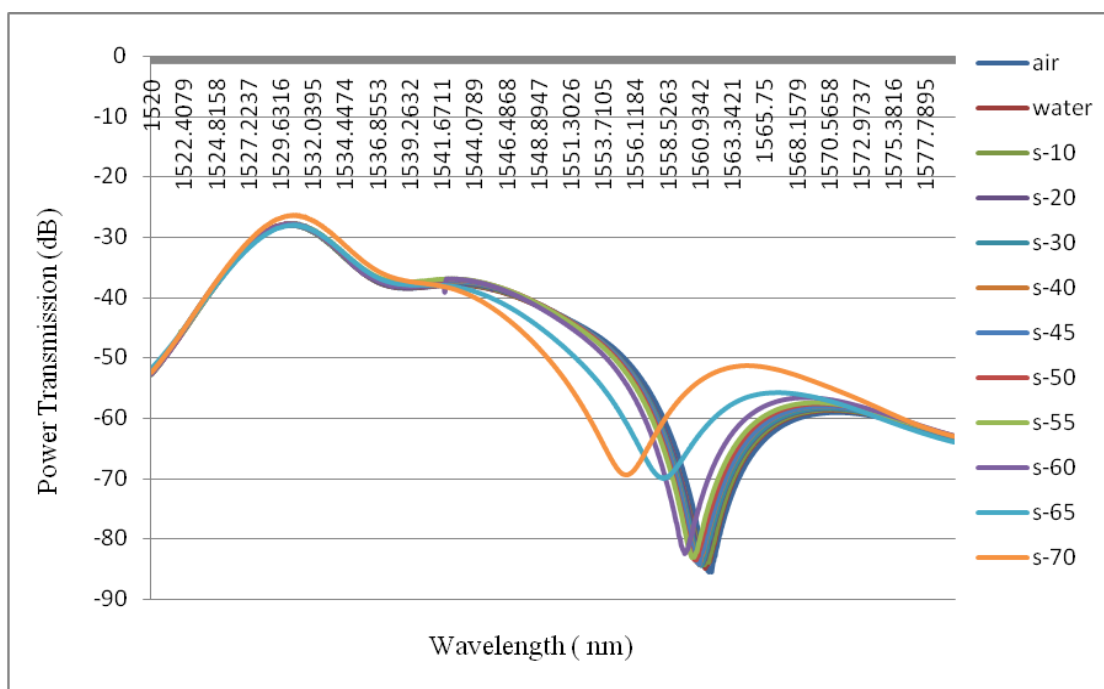


Figure 4.35: Grating 38-Transmission spectra at different sucrose solution (0-70%) using double pass with uncoated technique

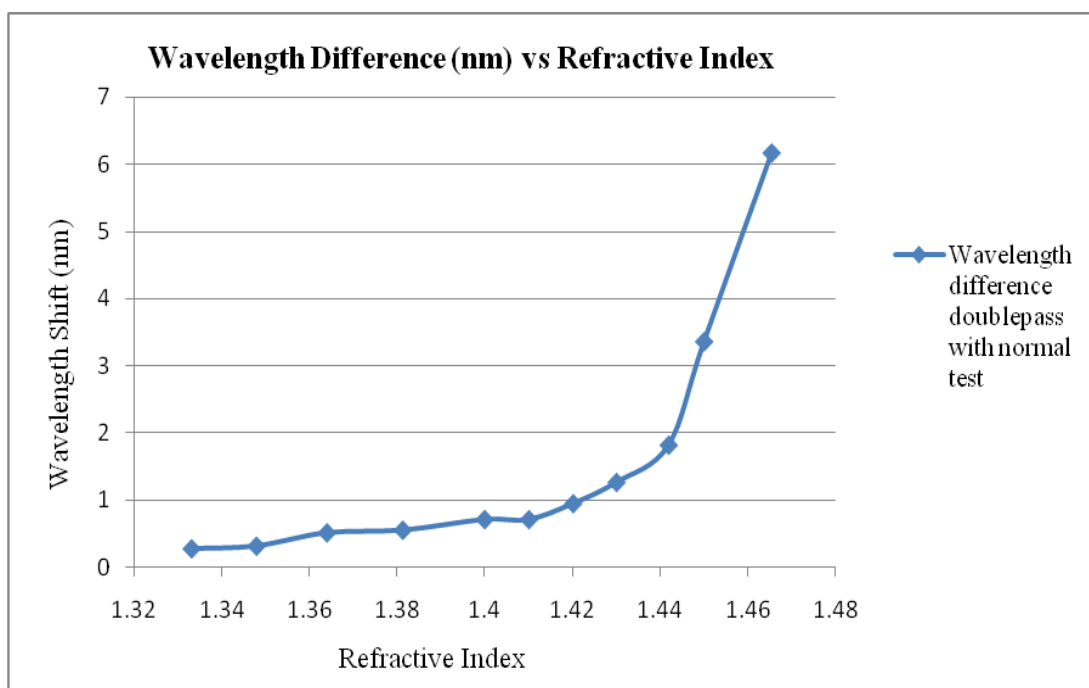


Figure 4.36: Grating 38-Wavelength shift of LPFG with different refractive index using double pass with uncoated technique

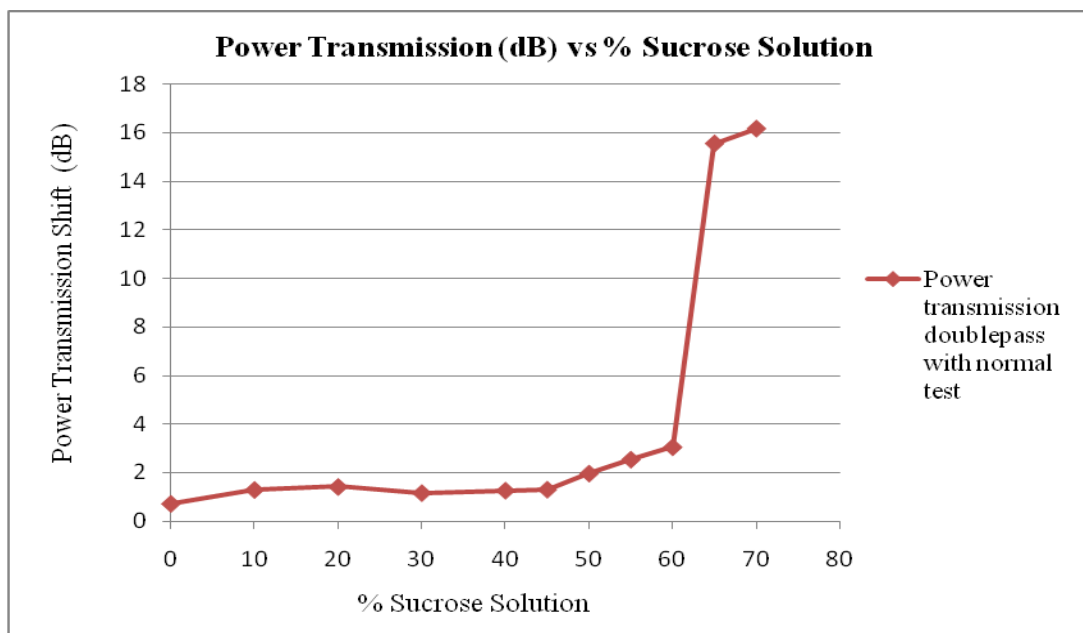


Figure 4.37: Grating 38-Power transmission shift of LPFG with different sucrose using double pass with uncoated technique

In above figure shows from 4.29 to 4.37 is using double pass with uncoated techniques. From the transmission spectra we can see the from 0% to 70 % is gradually increasing the resonance wavelength is left shift and power transmission is shift up. In this test, the optimal concentration of sucrose solution is 70% increasing the refractive index of the solution from 1.333 to 1.4654. The LPFG grating of 33, 35 and 38 exhibited a total left shift is 6.4737nm, 6.2763nm and 6,1579nm when concentration of sucrose solution increasing. The measurement LPFG power transmission of grating 33, 35 and 38 a total shift up is 12.751dB, 14.31dB and 16.179dB.

4.3.2 Double Pass with Layer-by-Layer Test

i. Grating-33

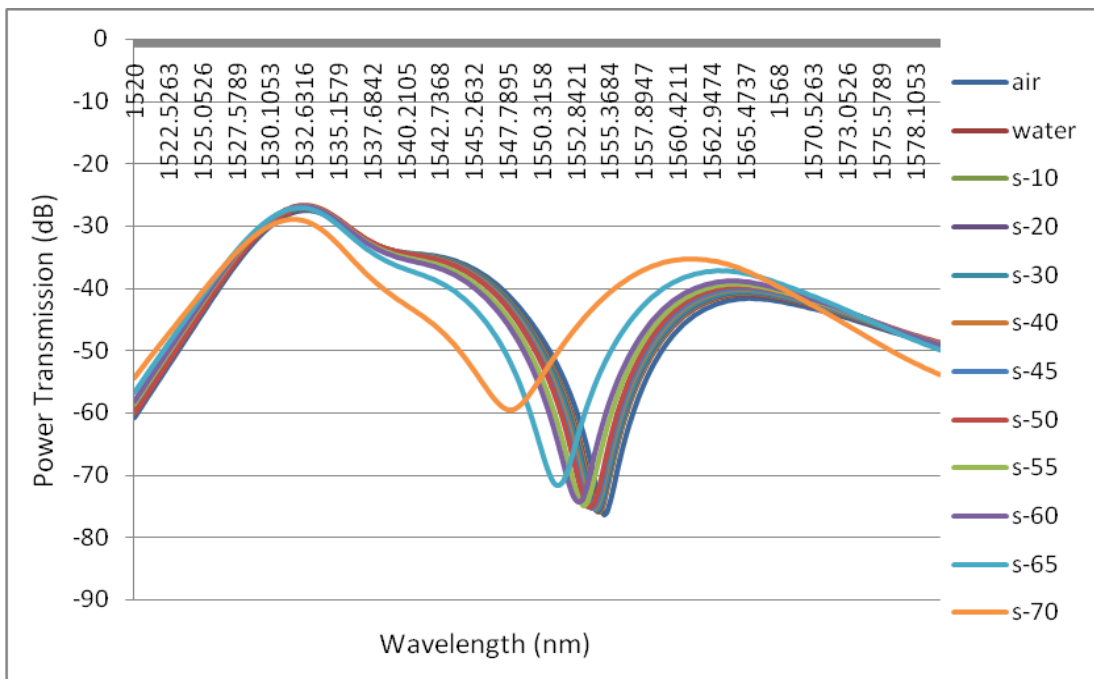


Figure 4.38: Grating 33-Transmission spectra at different sucrose solution (0-70%) using double pass with coated technique

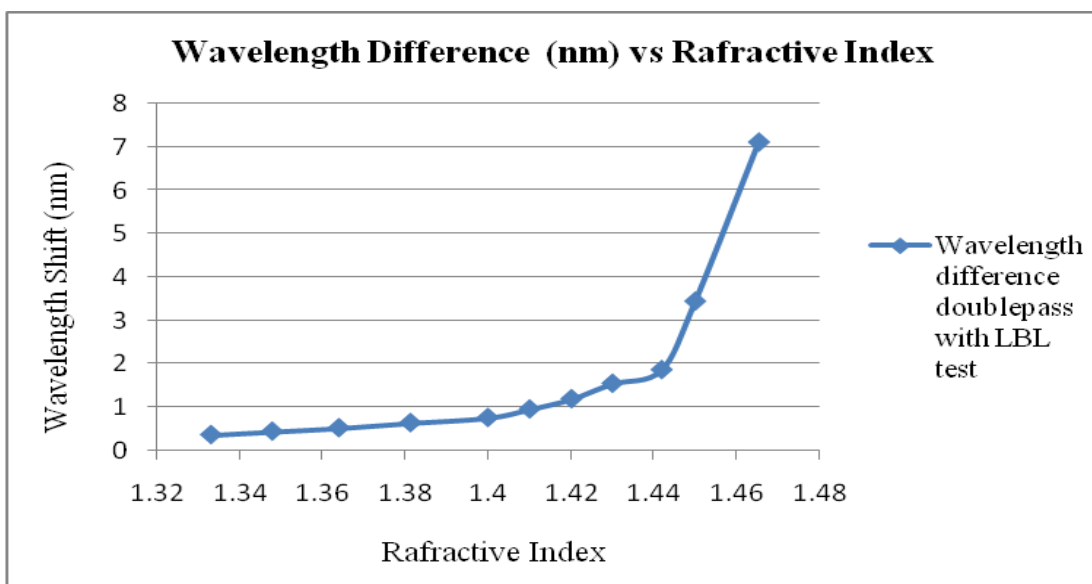


Figure 4.39: Grating 33-Wavelength shift of LPFG with different refractive index using double pass with coated technique

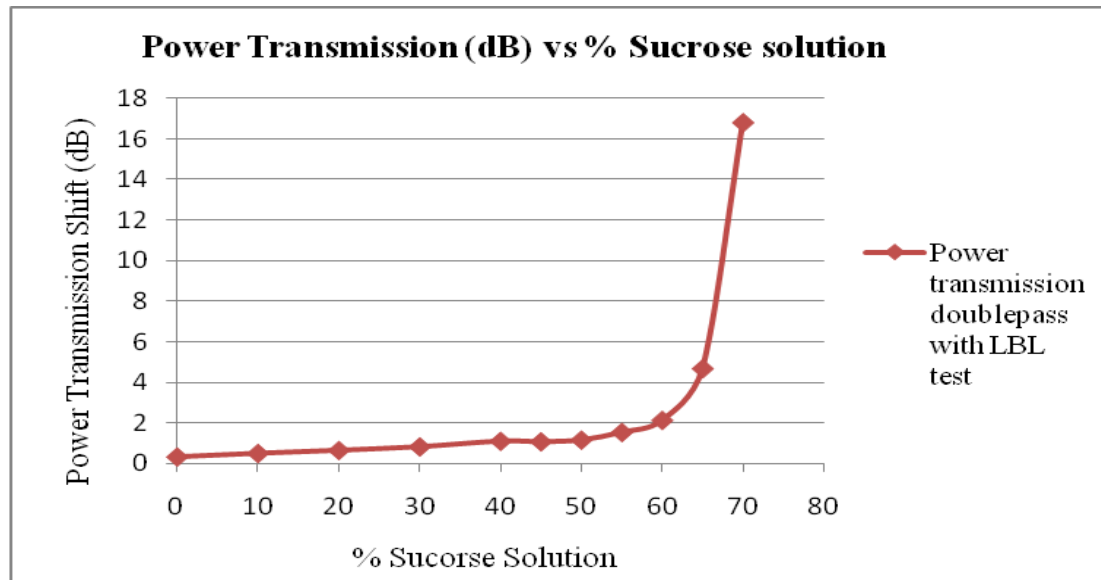


Figure 4.40: Grating 33-Power transmission shift of LPFG with different sucrose using double pass with coated technique

ii. Grating-35

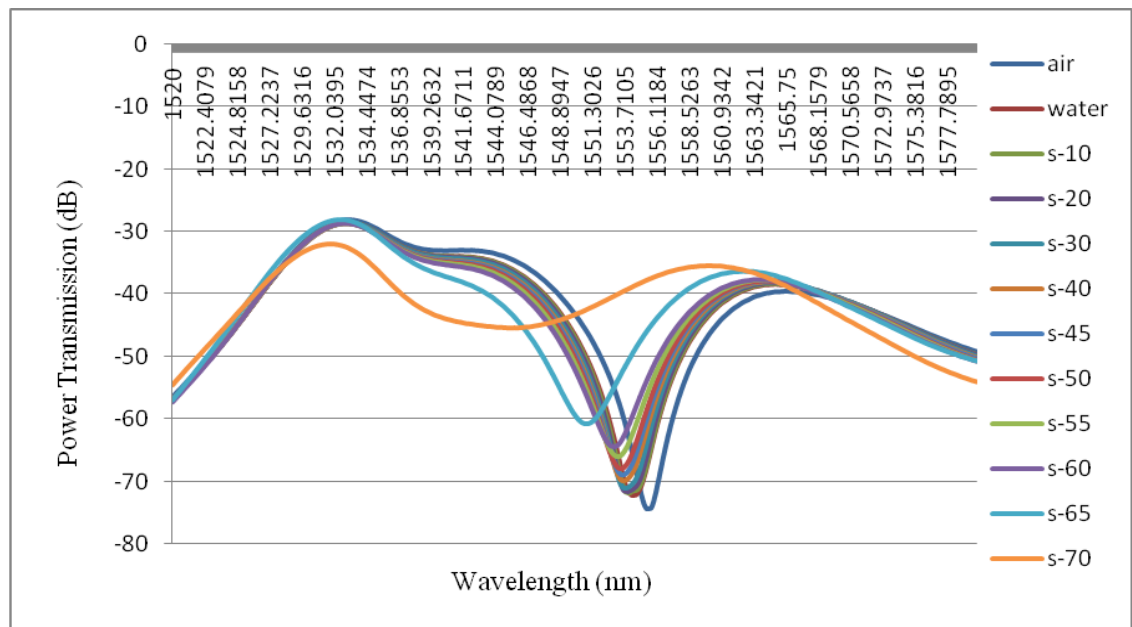


Figure 4.41: Grating 35-Transmission spectra at different sucrose solution (0-70%) using double pass with coated technique

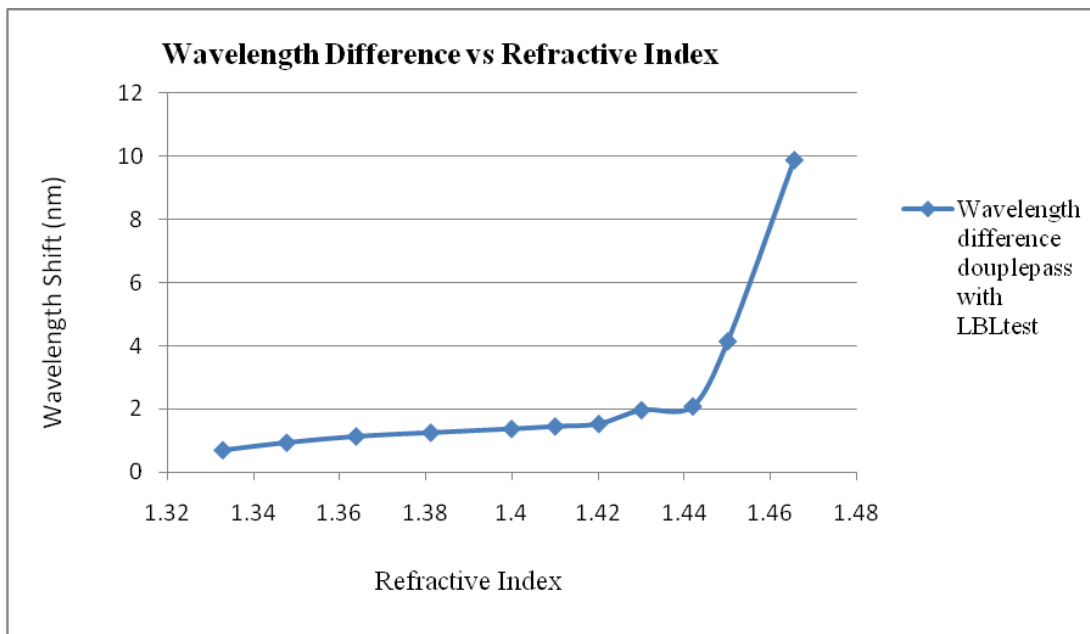


Figure 4.42: Grating 35-Wavelength shift of LPFG with different refractive index using double pass with coated technique

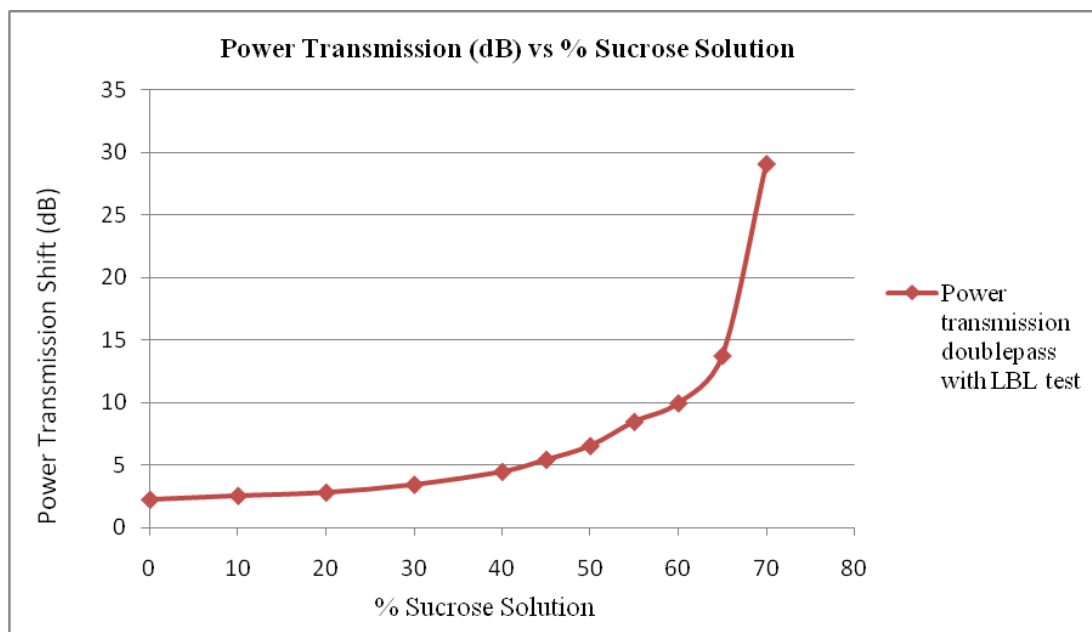


Figure 4.43: Grating 35-Power transmission shift of LPFG with different sucrose using double pass with coated technique

iii. Grating -38

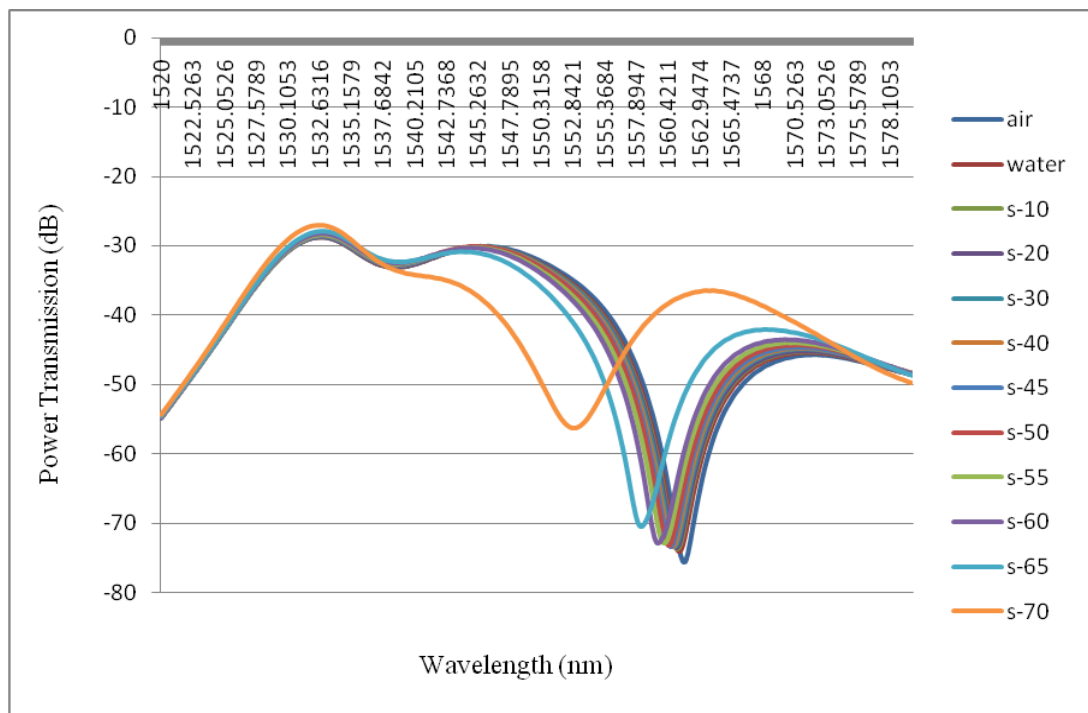


Figure 4.44: Grating 38-Transmission spectra at different sucrose solution (0-70%) using double pass with coated technique

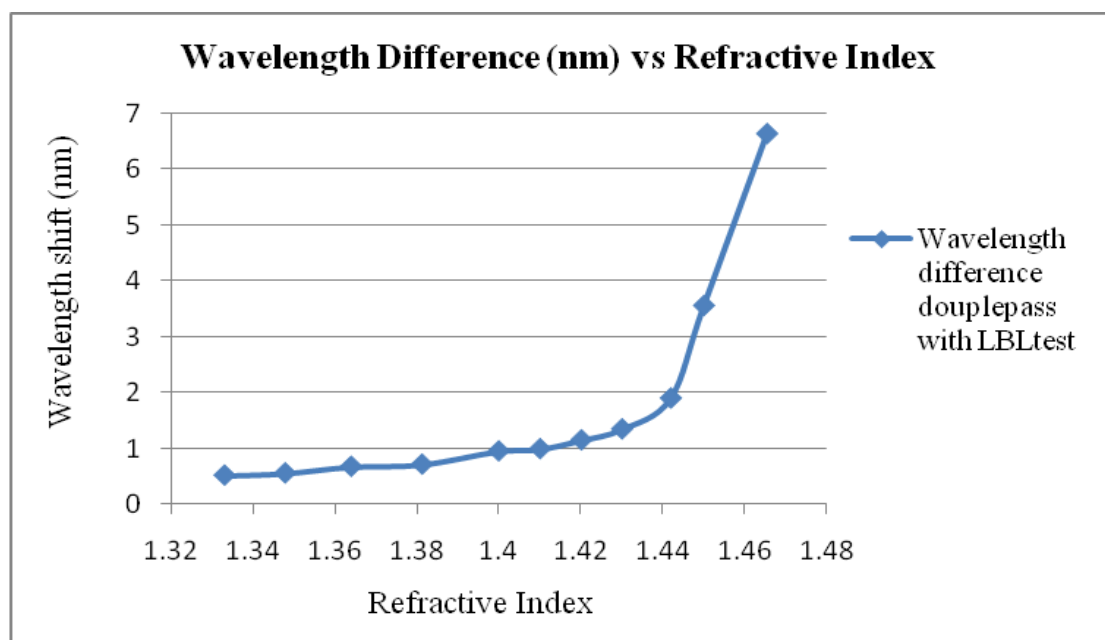


Figure 4.45: Grating 38-Wavelength shift of LPFG with different refractive index using double pass with coated technique

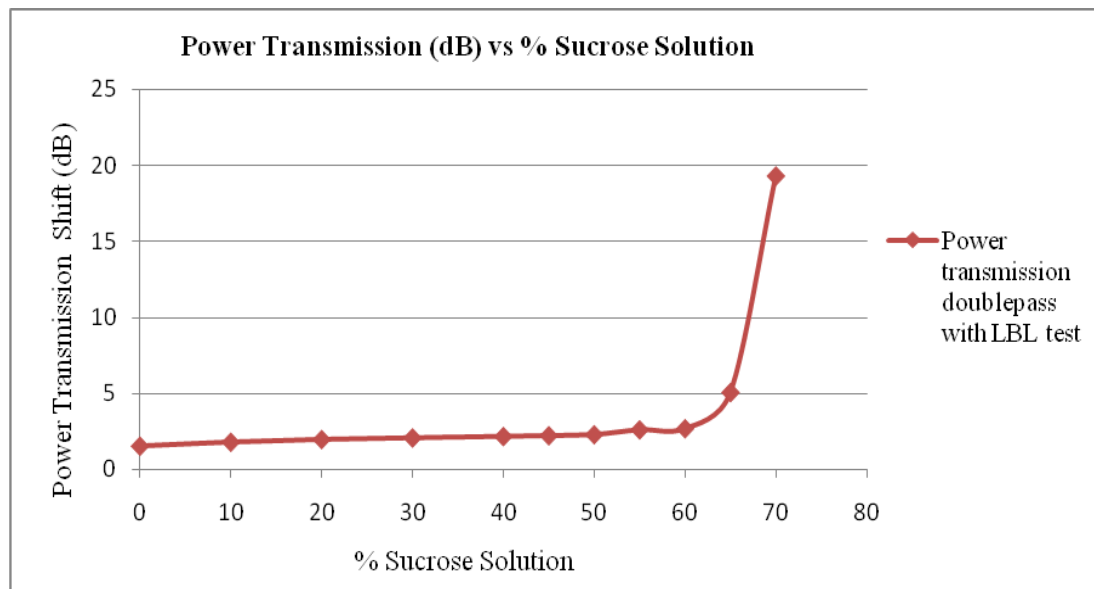


Figure 4.46: Grating 38-Power transmission shift of LPFG with different sucrose using double pass with coated technique

From above figure 4.38 to 4.46 I using double pass with layer by layer techniques to surface coated LPFG with a multilayer PDDA (poly-diallyldimethylammonium chloride) and PSS (poly-sodium styrene sulfonate). As we can see above transmission spectra LPFG of grating 33, 35 and 38 from the refractive index air is 1.333 central wavelength left shift to concentration of sucrose solution 70% the refractive index is 1.4606 was gradually shift as 7.106nm, 9.8684nm and 6.316nm. The measurement LPFG power transmission of grating 35, 38 and 39 a total shift up is 16.828dB, 29.086dB and 19.29dB.

4.3.3 Compare Between Double Pass with Uncoated Normal Test and Double Pass with LBL Test

i. Grating-33

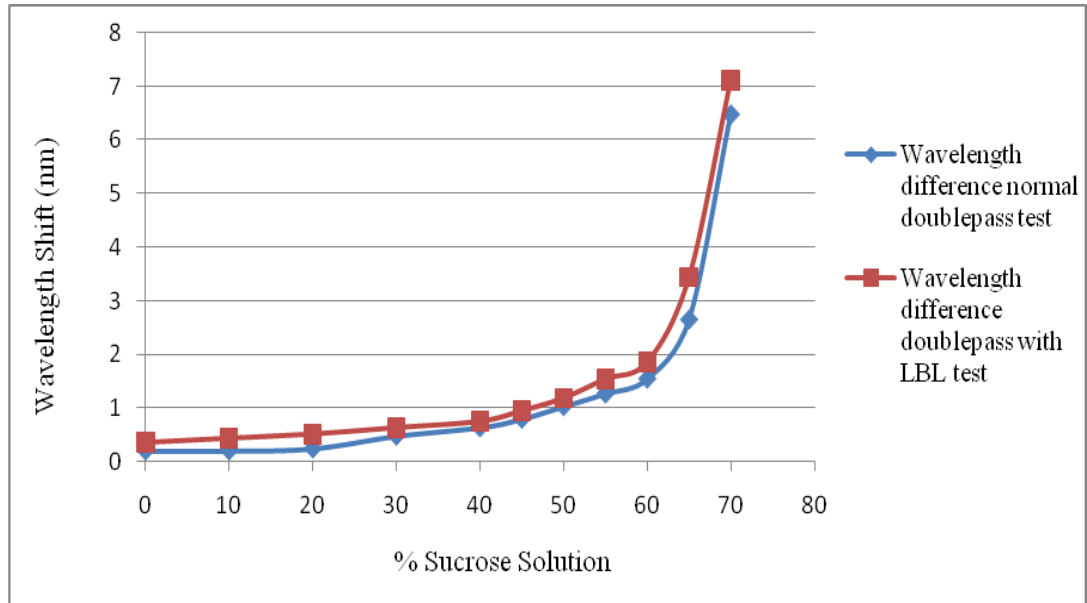


Figure 4.47: Grating 33- Different wavelength shift between double pass uncoater and layer by layer techniques.

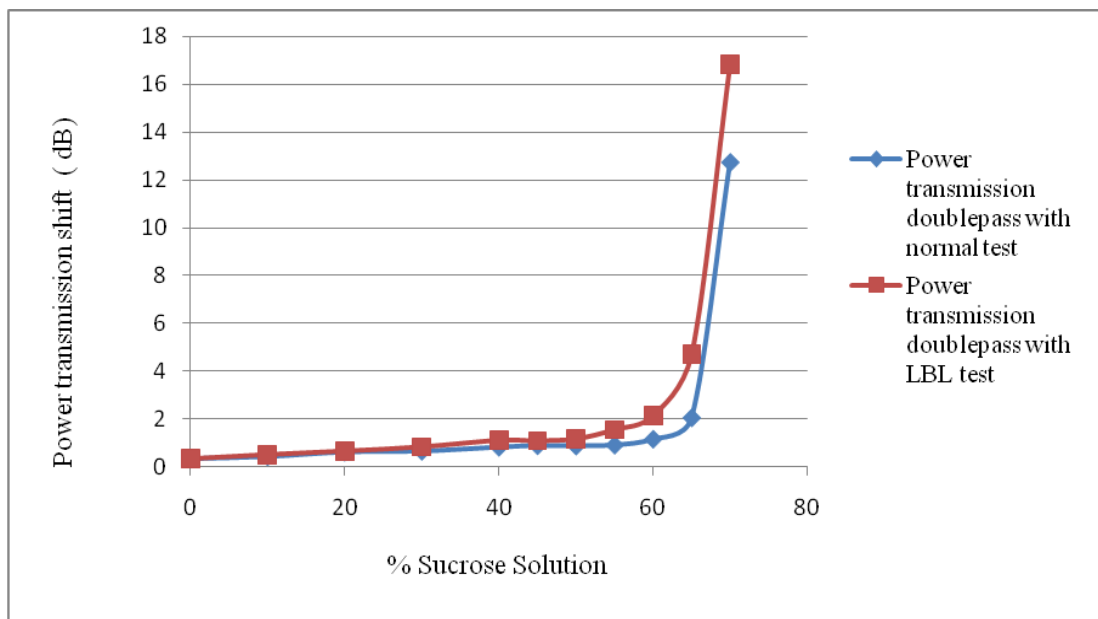


Figure 4.48: Grating 33- Different power transmission shift between double pass uncoater and layer by layer techniques.

ii. Grating-35

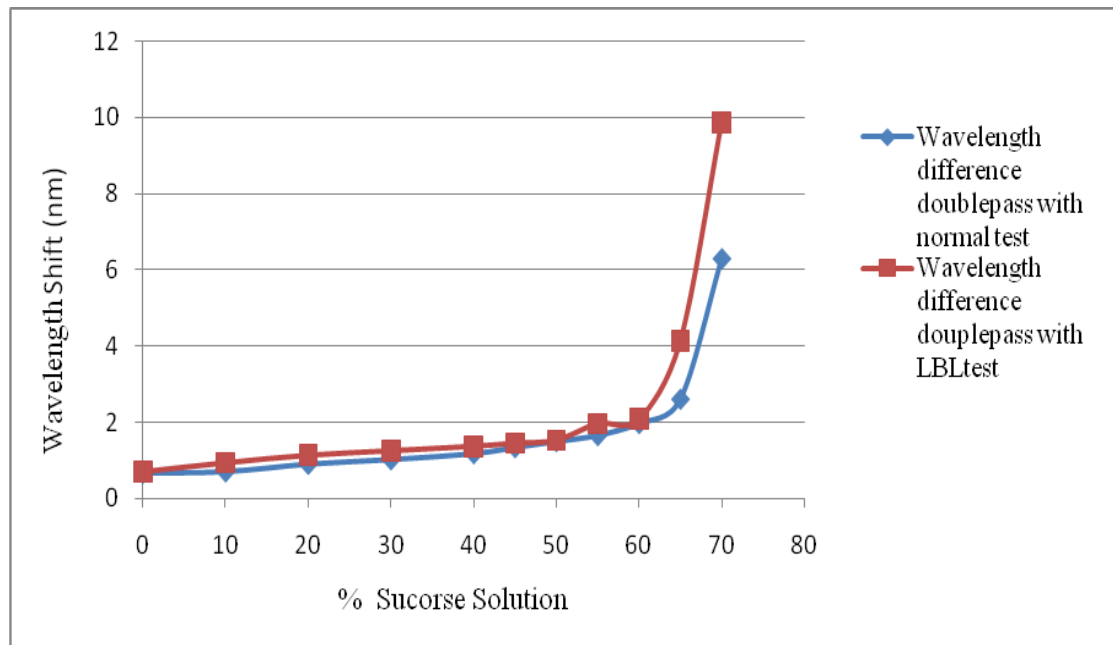


Figure 4.49: Grating 35- Different wavelength shift between double pass uncoater and layer by layer techniques.

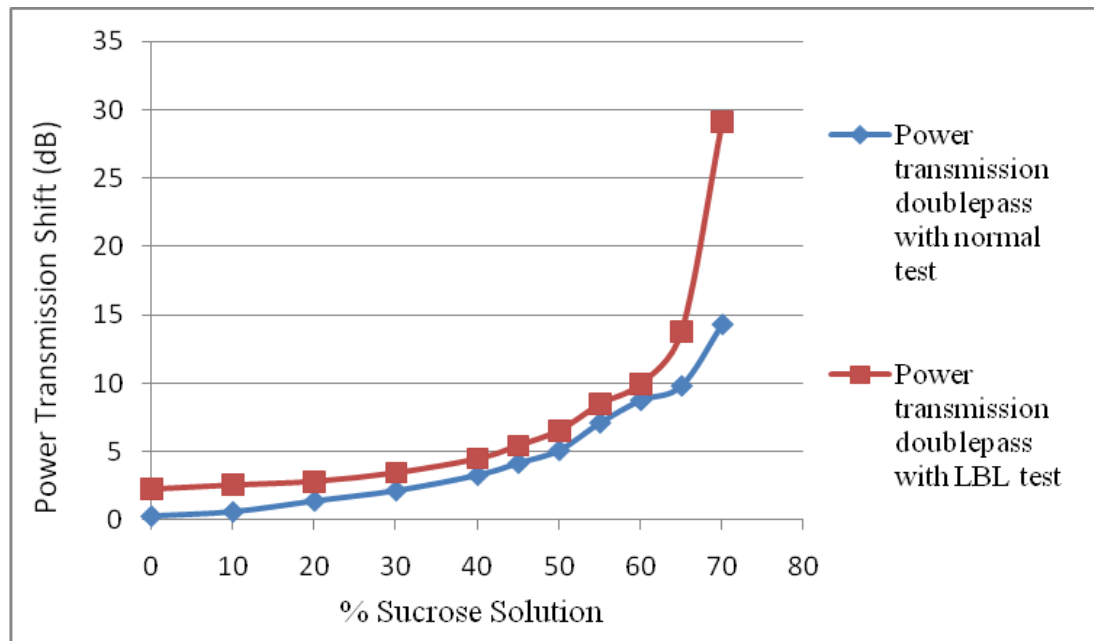


Figure 4.50: Grating 35- Different power transmission shift between double pass uncoater and layer by layer techniques.

iii. Grating-38

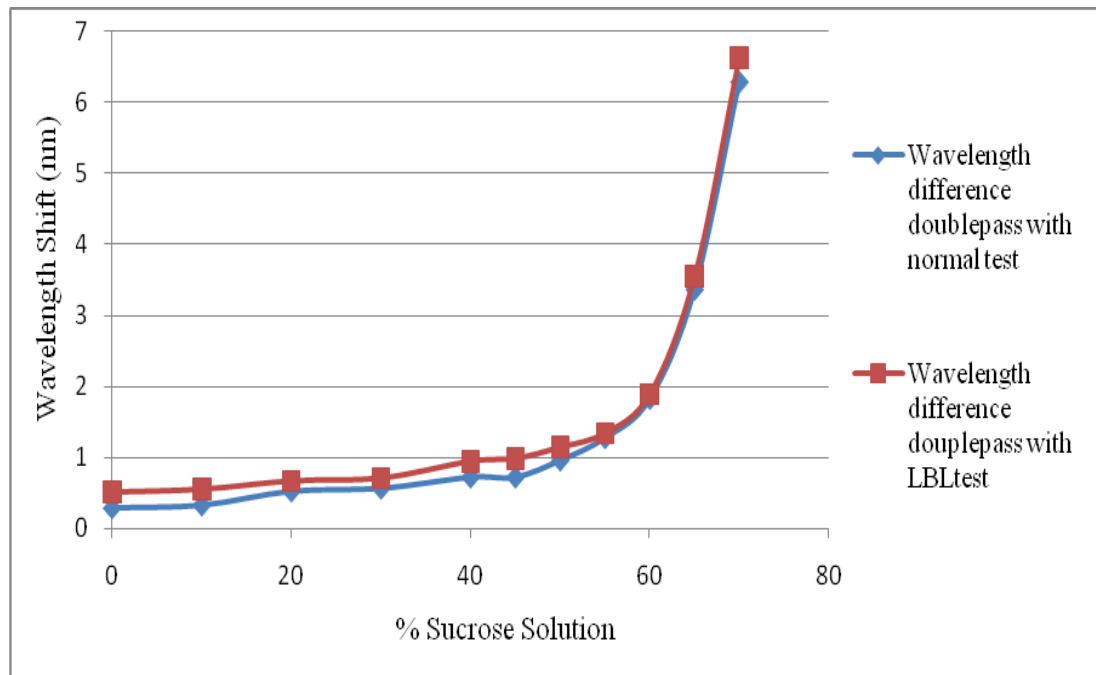


Figure 4.51: Grating 38- Different wavelength shift between double pass uncoater and layer by layer techniques.

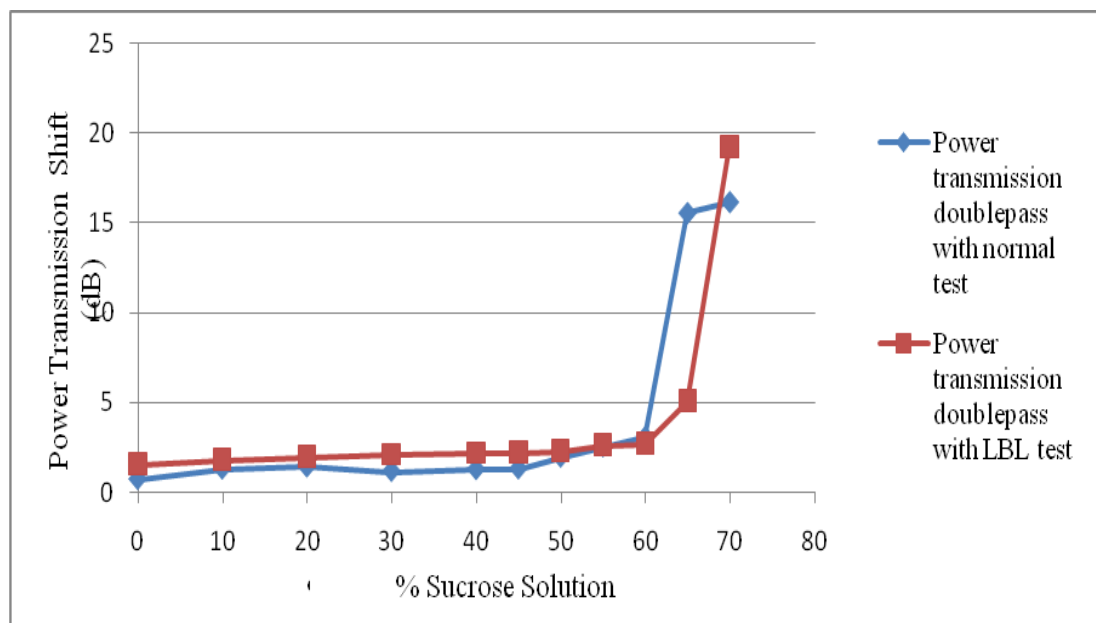


Figure 4.52: Grating 38- Different power transmission shift between double pass uncoater and layer by layer techniques.

By comparison double pass between uncoated and layer by layer test, the graph shows above from figure 4.47 to 4.52 for the sucrose solution of 0% until 70%. As the percentage of sucrose solution increase, the wavelength shift also increase.

According to above graph, the grating of 33 and 38, the wavelength shift in double pass uncoated and layer by layer is not much different between. For example, the figure 4.51 show the double pass with normal test on concentration (70%) is 6.1579nm and double pass with layer by layer is 6.636nm.

Referring to the figure 4.48, 4.50 and 4.52 as seen the power transmission of double pass with layer by layer is more increased compared with double pass with uncoated normal test. For example as shown in figure 4.50, using technique of layer by layer the maximum power shift from sucrose solution 0% to 70% is 29.086dB compared with using uncoated the maximum power shift from sucrose solution 0% to 70% is 14.31dB.

4.4 Comparison of Air between Single Pass and Double Pass

4.4.1 Single Pass

i. Grating -35

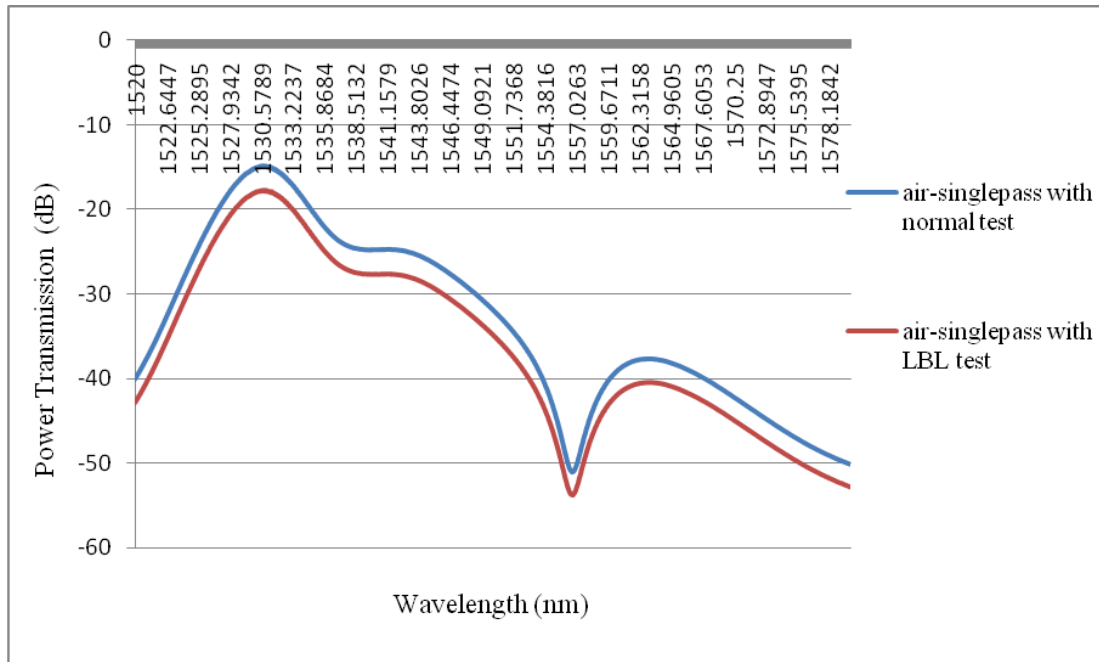


Figure 4.53: Grating 35- Different air wavelength shift between single pass uncoated and layer by layer test

ii. Grating- 38

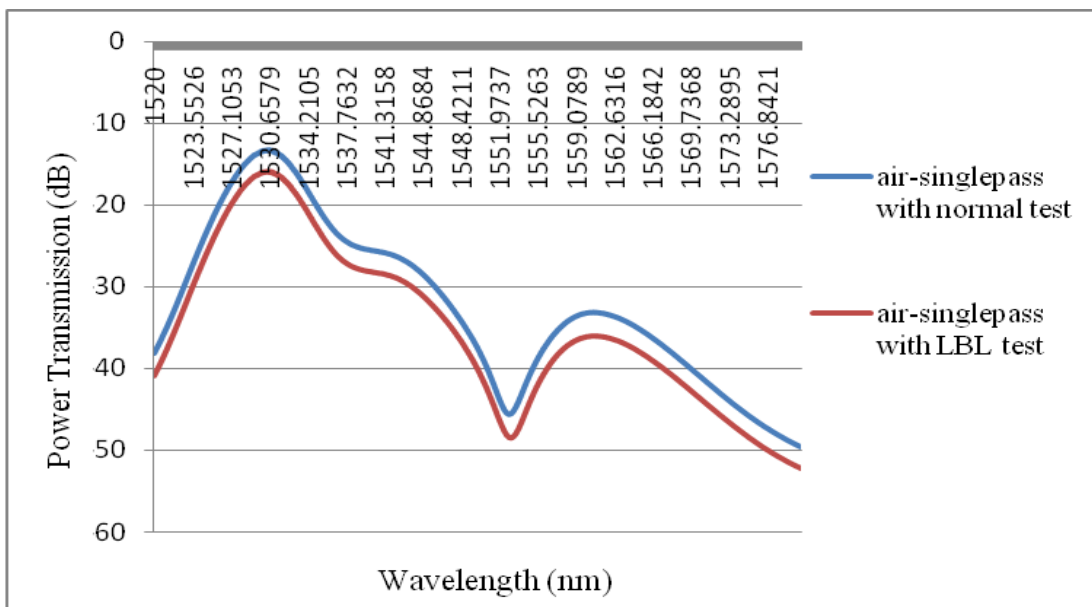
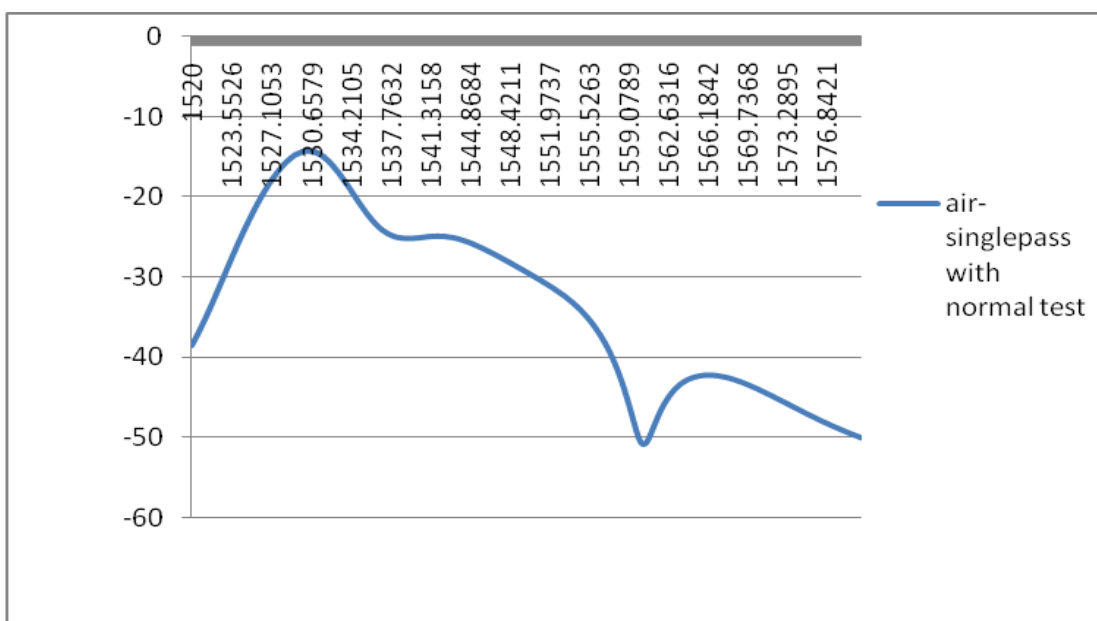


Figure 4.54: Grating 38- Different air wavelength shift between single pass uncoated and layer by layer test

iii. Grating -39



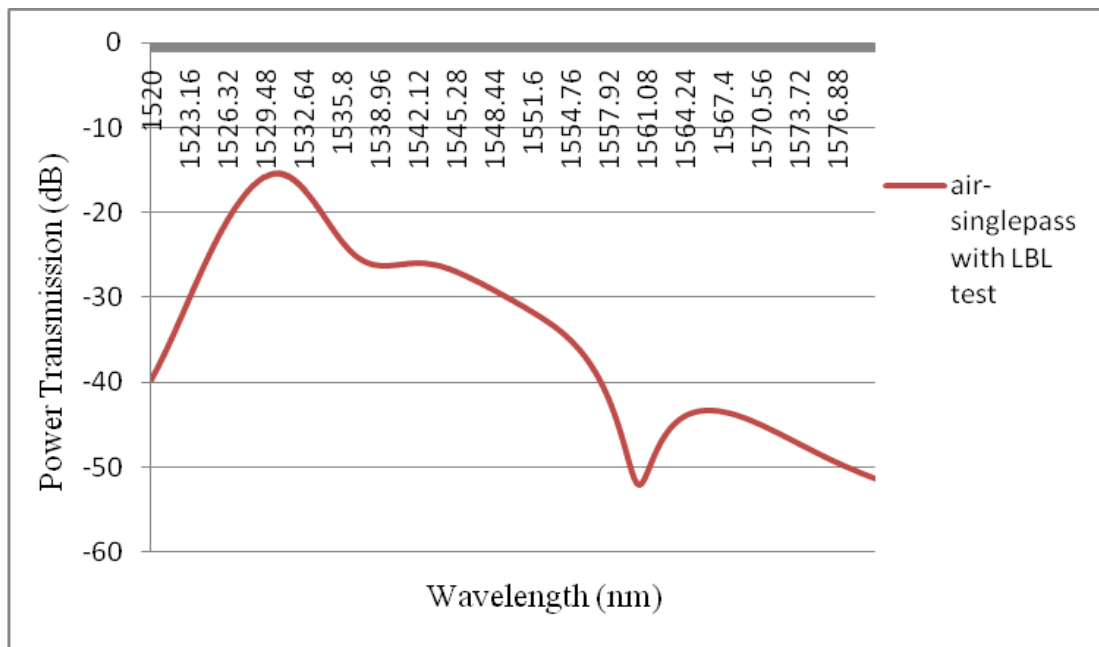


Figure 4.55: Grating 39- Different air wavelength shift between single pass uncoated and layer by layer test

4.4.2 Double Pass

i. Grating -33

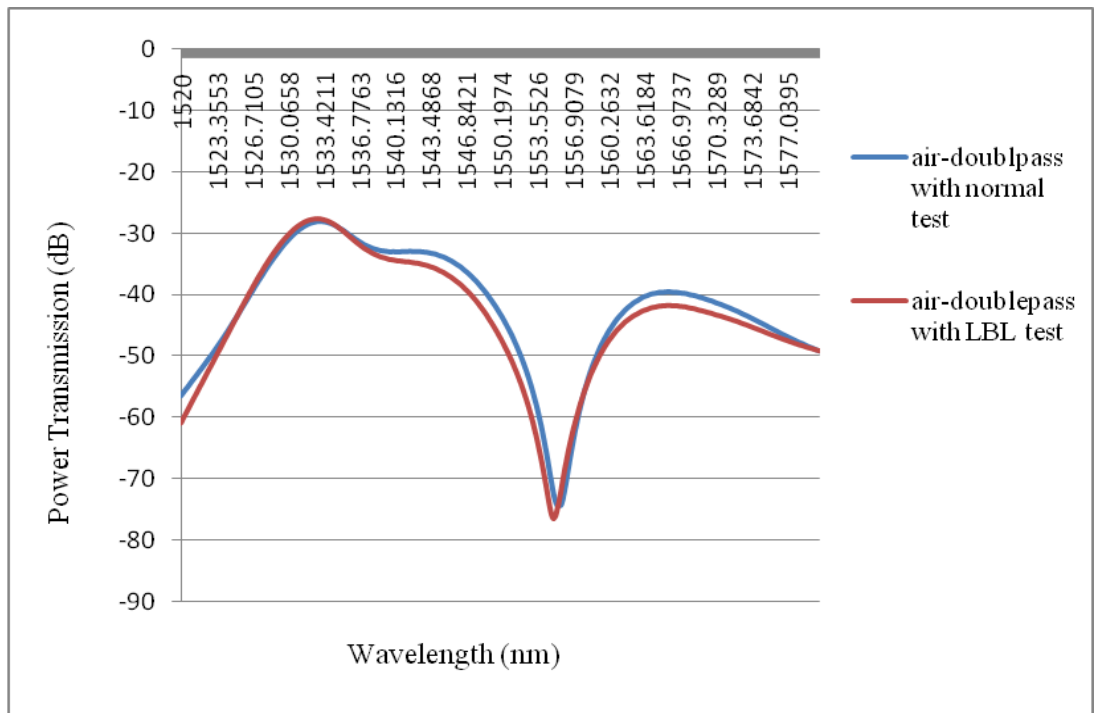


Figure 4.56: Grating 33-Different air wavelength shift between double pass uncoated and layer by layer test

ii. Grating -35

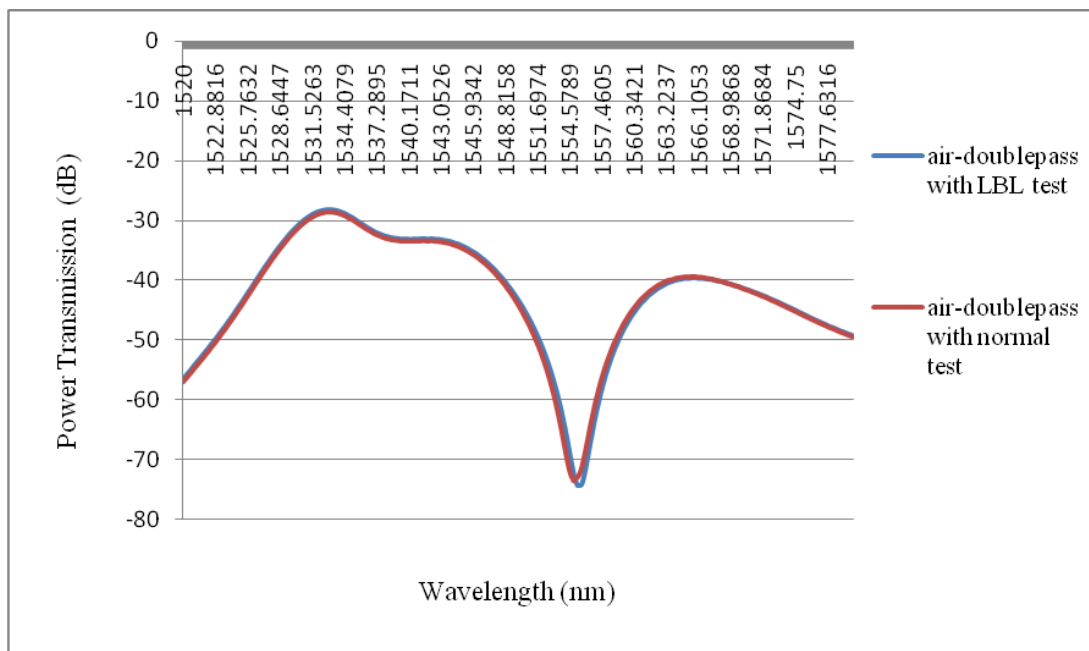


Figure 4.57: Grating 35-Different air wavelength shift between double pass uncoated and layer by layer test

iii. Grating -38

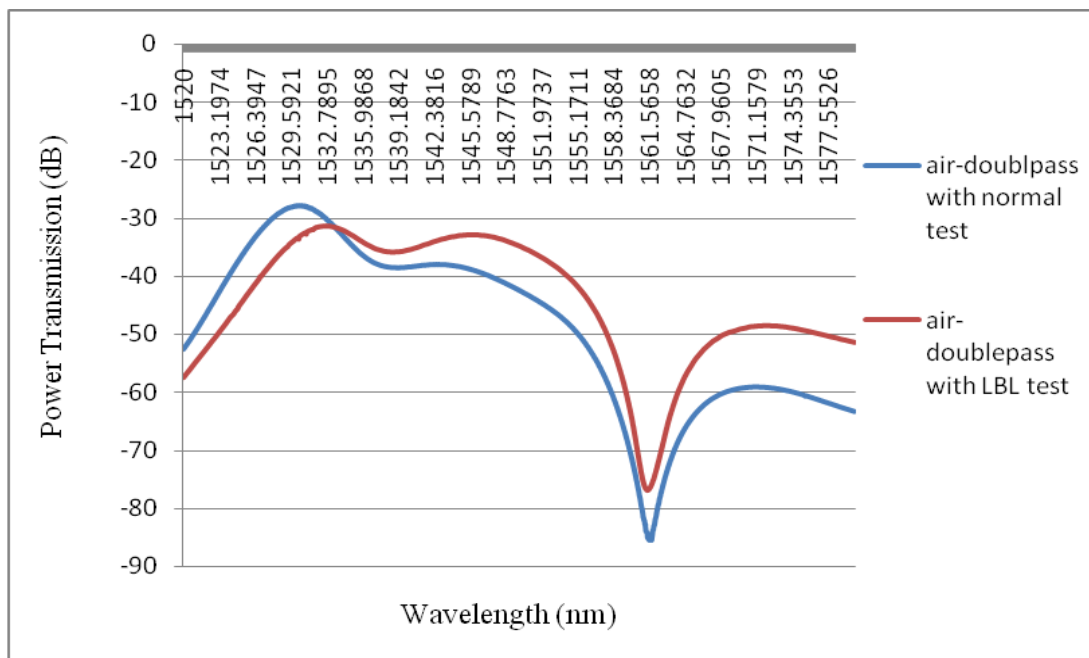


Figure 4.58: Grating 38-Different air wavelength shift between double pass uncoated and layer by layer test

Be referring to the from figure 4.53 to figure 4.55 they show the different air resonance wavelength test as single pass with uncoated and single pass with layer by layer for air resonance wavelength. As we see the using technique of polyelectrolyte layers in single pass test the notch depth of the power transmission more drop than normal test. For example the figure 4.53 to 4.55 the distance between single pass with normal and layer by layer is 2.2619dB, 2.8dB and 1.13dB.

Meanwhile, the figure from 4.56 to 4.58 shows the double pass with uncoated and layer by layer test. Using the double pass between uncoated and layer by layer in figure 4.57 not much different the distance between is 0.765dB but in figure 4.56 the distance between is 1.989 dB. In figure 4.58 the double pass with normal test is more drop than double pass with layer by layer the distance between is 8.636dB.

4.5 Compare Same Grating between Single Pass and Double Pass

i. Grating-35

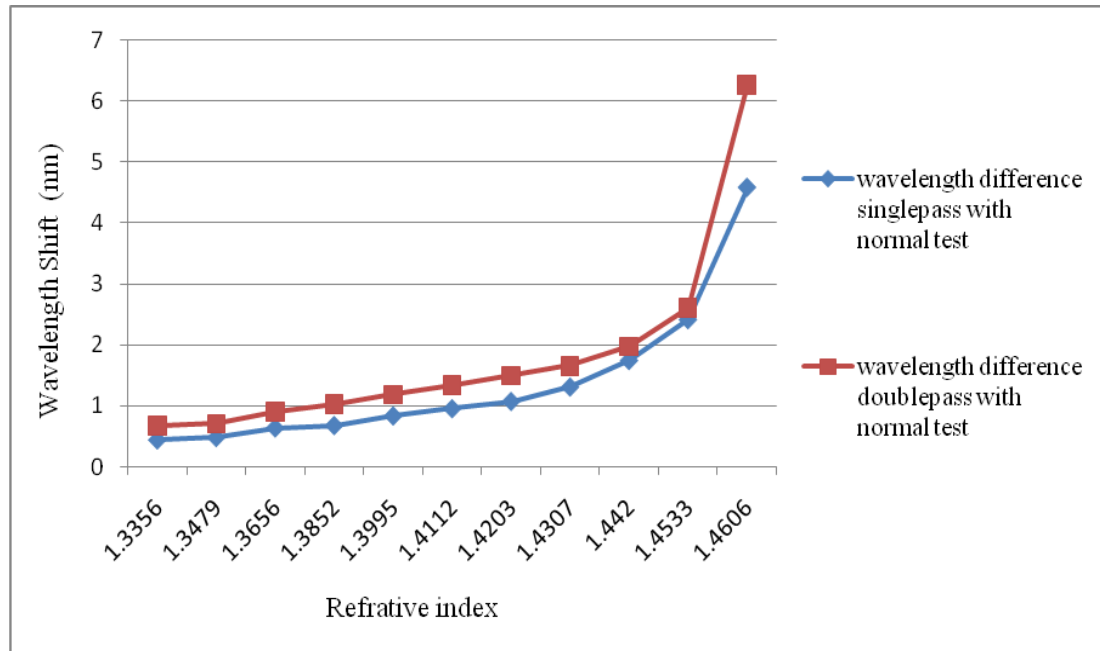


Figure 4.59: Grating 35-Different wavelength shift between single pass with uncoater and double pass with uncoated techniques

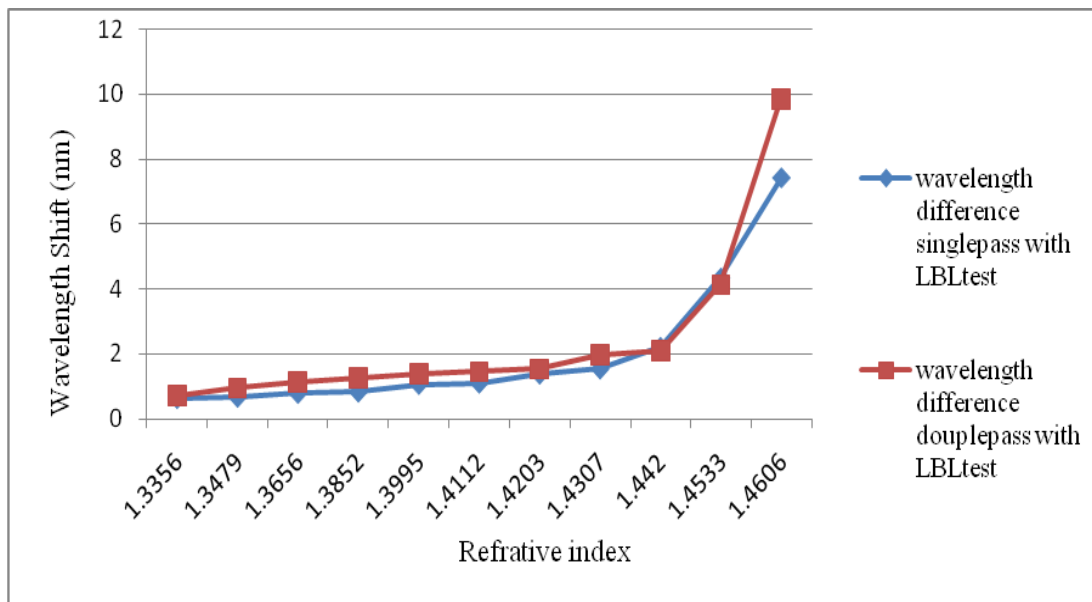


Figure 4.60: Grating 35- Different wavelength shift between single pass with layer by layer and double pass with layer by layer techniques

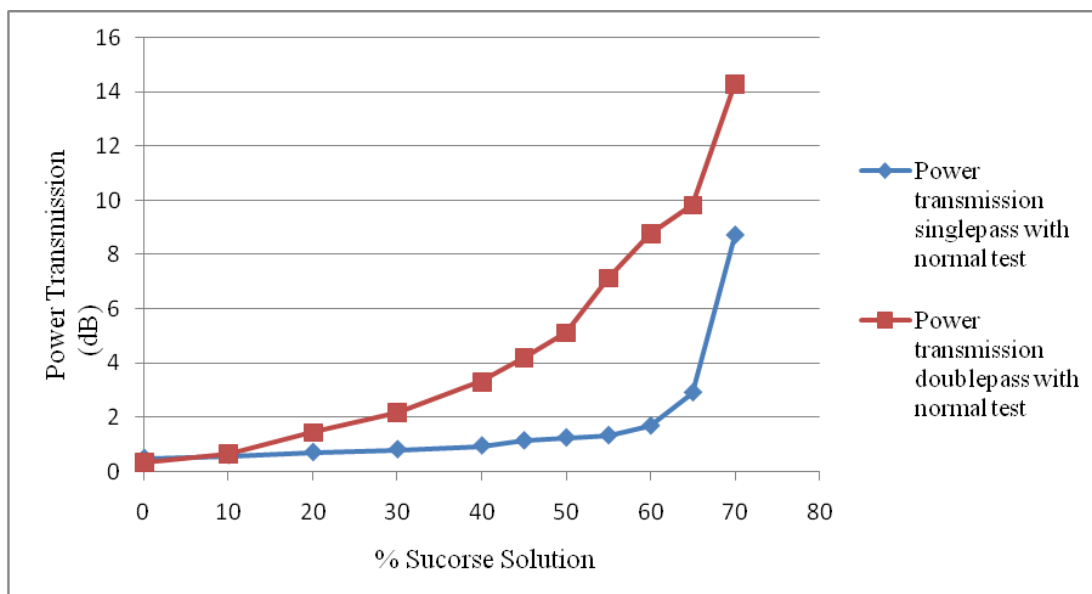


Figure 4.61: Grating 35- Different power transmission shift between single pass with uncoater and double pass with uncoated techniques

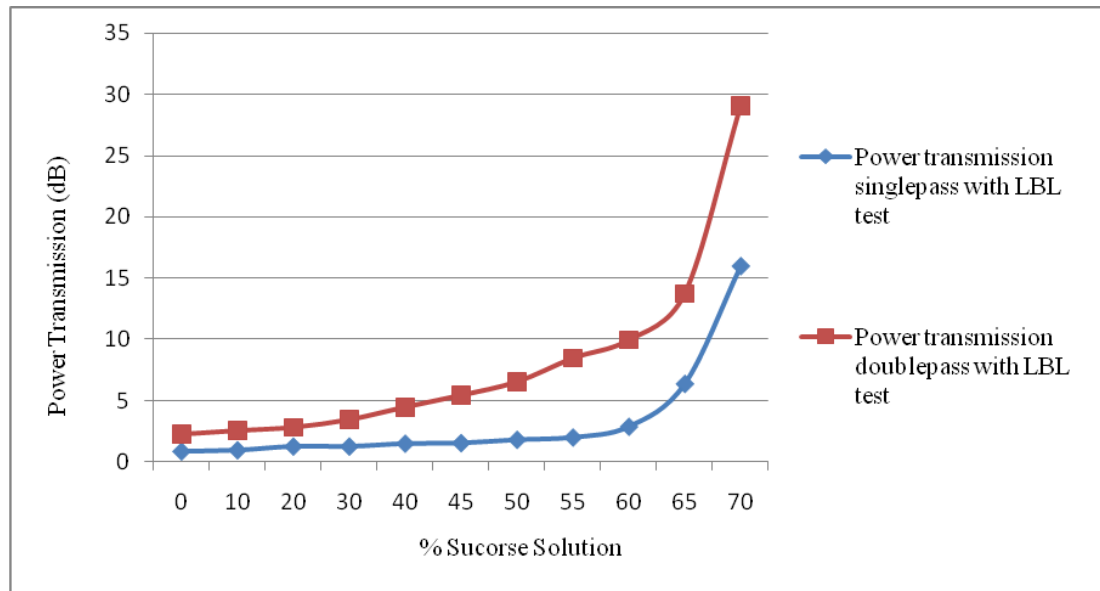


Figure 4.62: Grating 35- Different power transmission between single pass with layer by layer and double pass with layer by layer techniques

From the figure 4.59 to 4.62 shown to compare two different LPFG using same grating is 35. As we can see the above figure 4.59 and 4.60 shows using the normal test and layer by layer test. When refractive index is gradually increasing the wavelength shift also increasing and the refractive index from 1.333 to 1.4606 the double pass with normal test maximum wavelength shift is 6.2763nm to compare the single pass with normal test the refractive index is 4.579; double pass with LBL the maximum wavelength shift is 9.8684nm to compare single pass with LBL the maximum wavelength shift is 7.421nm.

By referring the figure 4.61 is show measurement the power transmission shift of the two tests as single pass with normal test and double pass with normal test while figure 4.62 show two tests as single pass with LBL test and double pass with LBL test. Figure 4.61 using the double pass with normal highest increasing at 14.31dB from concentration 0% to 70% compared to single pass with normal test is 8.72dB. Beside, figure 4.62 shows using LBL technique in two tests as single pass and double pass as we see the figure highest increasing at 29.086dB from concentration 0% to 70% in double pass with LBL test compared to single pass with LBL test is highest increasing is 15.961 dB.

ii. Grating -38

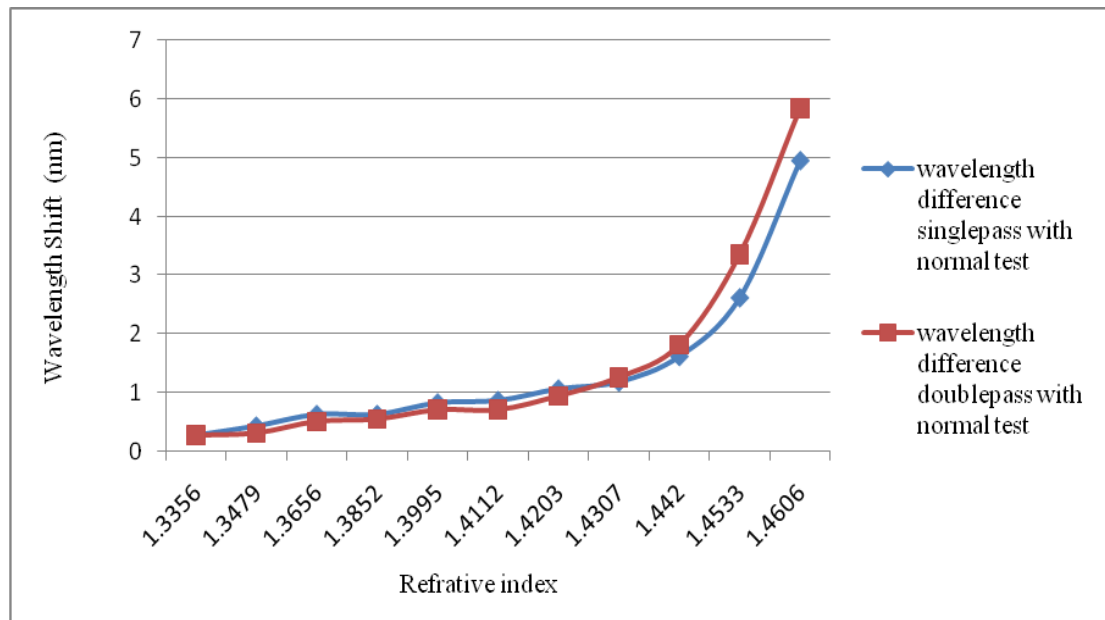


Figure 4.63: Grating 38- Different wavelength shift between single pass with uncoater and double pass with uncoated techniques

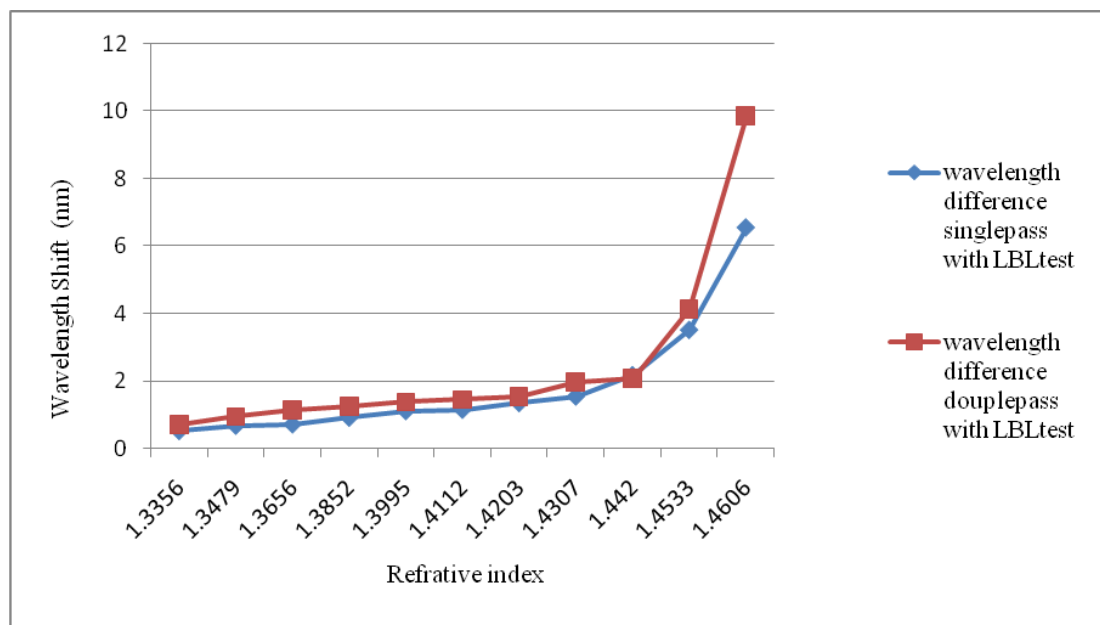


Figure 4.64: Grating 38- Different wavelength shift between single pass with layer by layer and double pass with layer by layer techniques

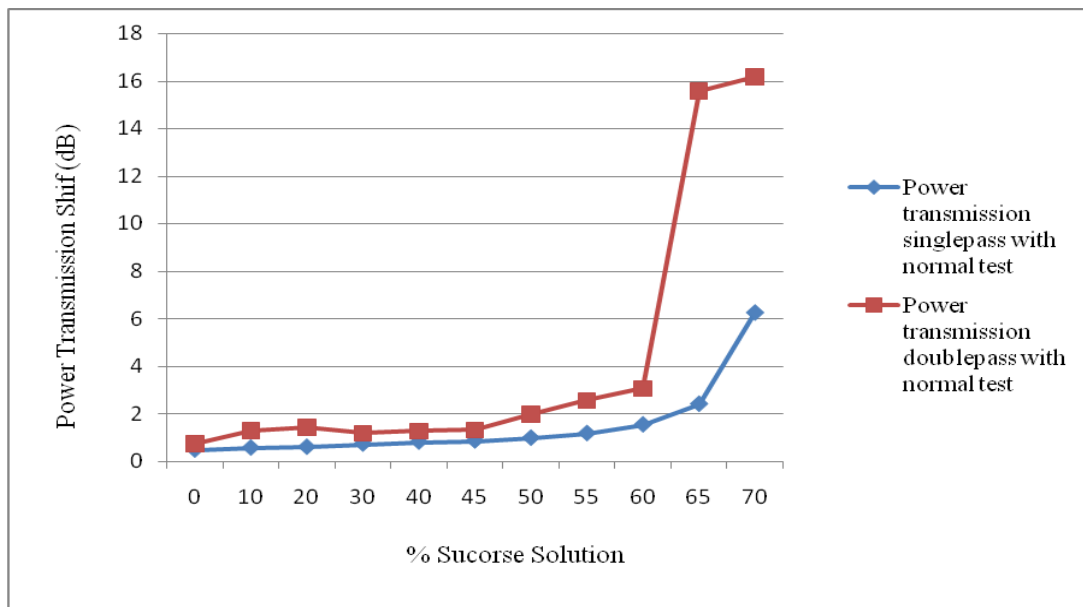


Figure 4.65: Grating 38- Different power transmission shift between single pass with uncoater and double pass with uncoated techniques

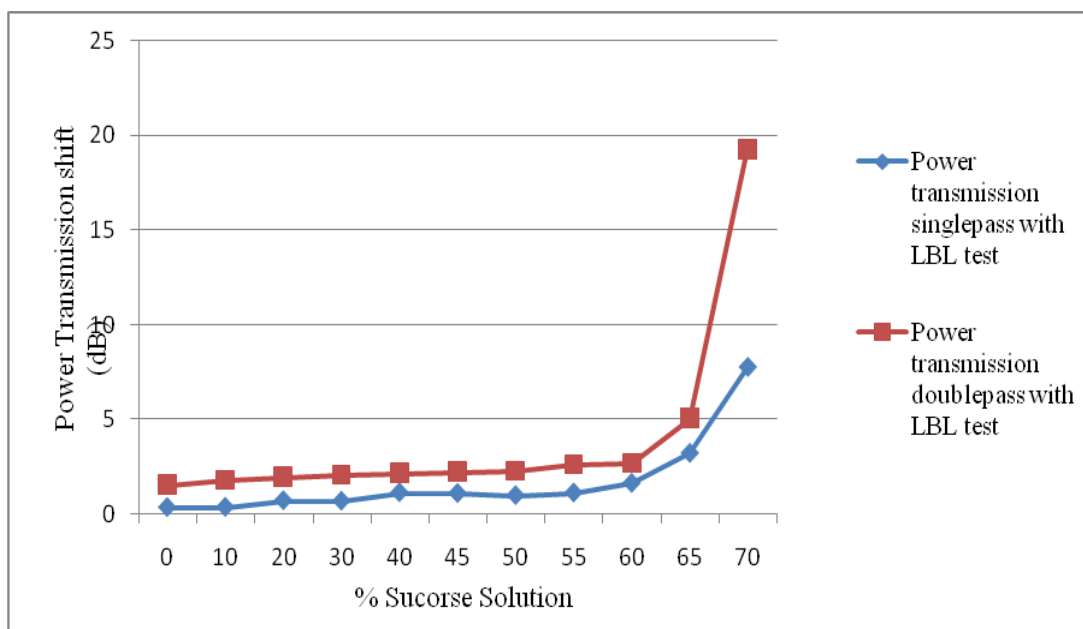


Figure 4.66: Grating 38- Different power transmission between single pass with layer by layer and double pass with layer by layer techniques

In figure 4.63 and 4.64 shows the compared different wavelength shift of the two techniques as single pass with normal test and double pass with normal test meanwhile figure 4.65 and 4.66 is measurement the power transmission shift in single pass with LBL and double pass with LBL. From the data collected, it is

evident that the increasing of the double pass with normal test and double pass with LBL are influenced by the sucrose solution.

From figure 4.63 the wavelenth shift between single pass with normal test is 4.947nm and double pass with normal test is 5.8421nm that the a little different. Figure is 4.64 show most increasing wavelenght shift in double pass with LBL is 9.8684nm compared to single pass with LBL is 6.5527nm. Next, the figure from 4.65 and 4.66 is power transmission shift versus percentage sucrose solution it is clear using double pass with normal is highest than single pass with normal. Beside, using double pass with LBL the power shift is 12.298dB highest than single pass with LBL the power shift is 7.776dB.

4.6 Discussion

Long period fiber grating had a refractive index of the different material sensitive performance and for different environments with different refractive index sensitive ability. The sensitive capability of long period fiber grating can be improved through coating method to form a thin film on fiber surface.

Figure 4.41, 4.17, 4.20, 4.38, 4.41 and 4.44 shows the transmission spectra response of long period grating coated PDDA/PSS film at different concentration of sucrose. In order to achieve a sufficient response, when coated the LPFG the temperature is 24⁰C and every time tested will switch off air condition. As can be seen from above figure when the percentage of sucrose solution increasing, the LPFG transmission spectra gradually shift. Relationship of coated PDDA/PSS film in LPFG with percentage sucrose solution can be further analyzed clear from the graph as wavelength shift versus refractive index and power transmission shift versus percentage sucrose solution. As can seen from using single pass techniques figure 4.15, 4.16,4.18, 4.19, 4.21, 4.22 and double pass technique figure 4.39,4.40, 4.42, 4.43, 4.45, 4.46 with the concentration from 0% to 70% the wavelength and power transmission will shift.

After coating with 50 bi-layers using in techniques of single pass and double pass, the LPFG show significant sensitive in high concentration (65-70%) the result

as show in above wavelength shift versus refractive index and power transmission shift versus percentage sucrose solution. When the concentration of sucrose solution within the range of 0% to 55% sucrose solution with the central wavelength of the slope smaller linear trend; and when the concentration of sucrose solution within the range of 60% to 70% sucrose solution with the central wavelength of the slope large linear trend. Therefore, considering normal test in the single pass with double pass and multilayer of single pass and double pass to show figures 4.59,4.62 and 4.60, 4.64 corresponding to the concentration of sucrose solution and the refractive index of the relationship between media the linear response of the refractive index of the respectively medium 1.333- 1.43 and 1.4419-1.4654.

In this project, two techniques single pass and double will be used to test sucrose solutions by observing the resonance wavelength shift during changed in refractive index. Using double pass technique is better than single pass technique because in LPFG resonance wavelength depth notch almost twice compared to single pass technique. For example grating are 35 in different air wavelength LPFG shown in 4.53 and 4.57 and it also shows a significant effect power transmission in double pass techniques. In order to determine the concentration of sucrose solution is significant effect power transmission, I will comparison two different tests as normal test of single pass with double pass and coated LPFG of single pass with double pass the result shows in figure 4.61, 4.62, 4.65 and 4.66. As we see the result, the double pass with normal test and double pass with LBL test is twice power transmission shift.

In the double pass with normal test the grating of 38 LPFG got the wrong data shown in figure 4.35. From the data collector, when test concentration (70%) the wavelength will shift left and power transmission will shift up than concentration (60%) but in different concentration the power transmission in distance difference is 0.61nm. That is because when testing finished concentration (60%) to clean the LPFG, the relax of tension caused by touching the LPFG led to fiber holder cannot tighten the LPFG. Besides that, each test is set to be same but there is a period of time in order to meet other FYP student settings the previous setting will changed. So when I tested double pass with normal test and double pass with LBL the setup is different therefore the LPFG will occurred loss induced are shown in figure 4.58.

CHAPTER 5

CONCLUSION AND RECOMMENDATIONS

5.1 Conclusion

Using techniques of double pass with PDDA/PSS film, it will enhance the sensing capability of LPFG during testing of various concentration of sucrose solution. During the preparation of PDDA/PSS film, the self-assembled technique was used to modify the fiber surface. Although this technique can improve the sensing through the thickness of thin film from the molecular level, one of the main drawback is very time consuming to build the optimal bi-layers. Since the thickness of each layer consists a tiny nanometers while LPFG surface films are typically assembled tens or hundreds of layers which can take several days to complete. Therefore, this project used the techniques of double pass with coated PDDA/PSS film to compensate the reduction of number of layers and yet maintain the comparable refractive index sensitivity on sucrose solutions in power referenced sensing.

5.2 Recommendations

Using the same LPFG fiber to verify the refractive index sensitivity performance for single pass and double pass technique, this can isolate the refractive index sensitivity caused by various LPFG performance. In addition, the same LPFG coated 50 bi-layers and followed by 100 bi-layer in double pass technique, it will able to to verify the thickness of thin film layers effect. Besides that, when assemble polyelectrolyte need to pay attention to immerse LPFG in full the PDDA/PASS solution because it

can influence the coating layer results prior to verify the refractive index sensitivity.

REFERENCES

- Lim, C.Y. and Wang, L.A., 2000. Corrugated long period fiber grating as band rejection filters. *Journal of Applied IEEE*, [E-journal] 1, pp. 20 – 22. Available through: Univerisiti Tunku Abdul Rahman Library Website <http://library.utar.edu.my> [Accessed 06 April 2015].
- Chan, H.M., Alhassen, F., Tomov, Ivan V., and Lee, Henry P., 2008. Fabrication and Mode Identification of Compact Long-Period Grating Written by CO₂ Laser. *Journal of Applied IEEE*, [E-journal] 20(8), pp. 611-613. Available through: Univerisiti Tunku Abdul Rahman Library Website <http://library.utar.edu.my> [Accessed 06 April 2015].
- Everall, L.A., Fallon, R.W., Williams, J.A.R., Zhang, L. and Bennion, I., 1998. Flexible fabrication of long-period in fiber gratings. *Journal of Applied IEEE*, [E-journal], pp. 513-514. Available through: Univerisiti Tunku Abdul Rahman Library Website <http://library.utar.edu.my> [Accessed 06 April 2015].
- Kryukov, P.G., Larionov, Yu.V., Rybaltovskii, A.A., Zagorul ko, K.A., Dragomir, A., Nikogosyan, D.N. and Ruth, A.A., 2003. Long-period fibre grating fabrication with femtosecond pulse radiation at different wavelengths. *Journal of Microelectronic Engineering* 69(2003), pp. 248-255.
- Fujiwara, E., Ono, E. and Suzuki, C.K., 2012. Application of an Optical Fiber Sensor on the Determination of Sucrose and Ethanol Concentration in Process Streams and Effluents of Sugarcane Bioethanol Industry. *Journal of Applied IEEE*, [E-journal] 12(9), pp. 2839-2843. Available through: Univerisiti Tunku Abdul Rahman Library Website <http://library.utar.edu.my> [Accessed 06 April 2015].
- Zhaoxia Wu, Xinyan, Yu, Erdan Gu, Zhi Kong and Wenchao Li, 2013. Characteristics Analysis of Chemical Concentration Sensor Based on Three-layer FBG. *Journal of Optics and Photonics* 3(2013), pp. 268-271.
- Jun Zhang, Wenping Cheng, and Chuan Dong. 2013. Fiber-Optic Sucrose Sensor Based on Mode-Filtered Light Detection. *Journal of Carbohydrate Chemistry*. [online] Available at: <<http://www.tandfonline.com/doi/abs/10.1080/07328303.2013.851685#.Vds0APmqqk0>> [Accessed 06 April 2015].

- Ming-Yue Fu, Hung-Ying Chang, Jin-Hone He, Chin-Chi Liu, Li-Wei Chen, Guei-Ru Lin and Weng-Fung Liu, 2014. Optical glucose sensor based on a fiber Bragg grating concatenated with a long period grating. *Journal of Applied IEEE*, [E-journal], pp. 472-473. Available through: Univerisiti Tunku Abdul Rahman Library Website <http://library.utar.edu.my> [Accessed 06 April 2015].
- Qiushun Li, Xu-lin Zhang, Yong-Sen Yu, Ying Qing, Wen-Fei Dong, Yong Li, Jianguao Shi, Juntao Yan and Hongyan Wang, 2010. Enhanced sucrose sensing sensitivity of long period fiber grating by self-assembled polyelectrolyte multilayers. *Journal of Applied UTAR Databases*, [E-journal], pp. 335-339. Available through: Univerisiti Tunku Abdul Rahman Library Website <http://library.utar.edu.my> [Accessed 06 April 2015].
- Yun-Thung Yong, Sheng-Chyan Lee and Faidz Abd Rahman, 2014. Sensitization of hybrid LPFG-FBG refractometer using double-pass configuration. *Journal of Applied UTAR Databases*, [E-journal], pp. 590-595. Available through: Univerisiti Tunku Abdul Rahman Library Website <http://library.utar.edu.my> [Accessed 06 April 2015].
- Joo Hin Chong, Ping Shun, H. Haryoon, A. Yohana, M.K. Rao, Chao Lu and Yinian Zhu, 2003. Measurements of refractive index sensitivity using long-period grating refractometer. *Journal of Applied Science Direct*, [E-journal], pp. 65-69. Available through: Univerisiti Tunku Abdul Rahman Library Website <http://library.utar.edu.my> [Accessed 06 April 2015].
- Qian Ying, Yu Yong-sen, Li Qiu-shun, Wu Si-zhu, Zhao Kai-jun, Yang Bai-liang and Zhang Yu-shu, 2009. High Sensitive Long Period Fiber Grating Sensor For Detection of Nitrite. [Online] Available at: <https://www.google.com/url?sa=t&ret=j&q=&esrc=s&source=web&cd=1&cad=rja&uact=8&ved=0CCIQFjAAahUKEwi85627jsLHAhXDC44KHb10Dzc&url=http%3A%2F%2Fwww.cjcu.jlu.edu.cn%2Fhxyj%2FEN%2Farticle%2FdownloadArticleFile.do%3FattachType%3DPDF%26id%3D12087&ei=wkLbVbz-GsPnuQS96b24Aw&usq=AFQjCNGwDdGxMTEVfTjmtWmtZqi_jDJNdg&sig2=2ATbwYQFF4RgZN_Vnzcj8g> [Accessed 17 August 2015].
- Zhao Ming-fu, Wang Nian, Luo Bing-bing, Shi Yu-jia, Cao Li-hua, 2014. Simultaneous measurement of temperature and concentration of sugar solution based on hybrid fiber grating sensor. [online] Available at: <<http://max.book118.com/html/2014/1128/10493830.shtm>> [Accessed 20 August 2015].
- Wikipedia, the free encyclopedia, 2015. Snell's law. [online] Available at: https://en.wikipedia.org/wiki/Snell%27s_law [Accessed 18 August 2015].
- Professor Benjamin J. Eggleton, 2007. Long Period Fiber Gratings. [online] Availabel at < http://photonicssociety.org/newsletters/jun07/long_period.html>

Patrick, H.J. 1998. Analysis of the response of long period fiber gratings to external index of refraction. *Journal of Applied UTAR Databases*, [E-journal], pp. 1606-1612. Available through: Univerisiti Tunku Abdul Rahman Library Website <http://library.utar.edu.my> [Accessed 06 September 2015].